Doctoral Dissertation

TAXONOMIC STUDIES OF THE GENUS *FALLACIA* (BACILLARIOPHYCEAE) AND ITS RELATED SPECIES IN JAPAN

March 2014

Graduate School of Marine Science and Technology
Tokyo University of Marine Science and Technology
Doctoral Course of Applied Marine Environmental Studies

Li Yuhang

CONTENTS

I. INTRODUCTION

Diatoms (Bacillariophyta) are unicellular, eukaryotic heterokont microalgae. Many diatoms are capable of forming colonies by secreting mucilage. The chloroplast contains chlorophyll a and chlorophyll c, appearing a golden-brown color. The remarkable feature is the highly differentiated siliceous ($Si_2O \bullet nH_2O$) cell wall (frustule). The frustule consists of two halves (valves), the larger (older) valve and associated bands (cingulum) compose a epitheca, while the smaller (newer) valves and associated bands were a hypotheca (Round et al. 1990). Diatoms inhabit most bodies of water, and are abundant in the phytoplankton and phytobenthos of marine and freshwaters. It is estimated that 40% of the earth's oxygen and carbon fixation is produced through the photosynthetic activities of diatoms. Diatoms also account for about 25–30% of the primary production in nutrient-poor waters and perhaps 75% in nutrient-rich regions (Nelson et al. 1995). Because there are many environmental sensitive species, the diatoms were ideal biological monitors. Furthermore, the diatom valves could be well preserved in the sediments of lakes and oceans, and could be used as indicator to study paloenvironment and climate change etc (Smol and Stoermer 2010).

The current widely accepted diatom taxonomic system was built by Round et al. (1990). In this system, diatoms (Bacillariophyta) were divided into three classes, namely Coscinodiscophyceae, Fragilariophyceae and Bacillariophyceae, according to the morphology of frustule observed using electron microscope (EM), the shape of chloroplast and patterns of sexual reproduction. Medlin and Kaczmarska (2004) proposed a new taxonomic system based on molecular sequence data (SSU rRNAs) and cytological features. In this taxonomic system, Bacillariophyta was divided into two new subclasses Coscinodiscophytina and Bacillariophytina. The Coscinodiscophytina consists of the amended Coscinodiscophyceae, including the Coscinodiscophycidae, Corehrophycidae, Rhizosoleniophycidae and leptocylindrales in taxonomic system of Round et al. The Bacillariophytina was divided into a new class Mediophyceae and amended

Bacillariophyceae. The Mediophyceae includes families belonged to Coscinodiscophyceae Round & Crawford (1990), such as Thalassirosirales, Triceratiales, Biddulphiales, Hemiaulales, Lithodesmiales, Cymatosirales and Chaetocerotales, and also includes two families in Fragilariophyceae, namely Ardissoneales and Toxariales. However, this taxonomic system, CMB hypothesis, was argued by Theriot et al. (2009) that this it was not robust and not a natural phylogeny both from morphological and molecular data.

The genus *Fallacia* was erected by A.J. Stickle and D.G. Mann in Round et al. (1990). The species in this genus formerly belonged to the genus *Navicula sensu lato* sect. *Lyratae* and *Bacillares* (Hustedt 1927–1966). The genus *Navicula sensu lato* was a large heterogeneous genus comprising all the symmetric raphid species without obvious distinguishable features (Round et al. 1990). Several diatomists have tried to review this genus, subdivided into a number of sections or groups. The sections *Lyratae* and *Bacillares* were first proposed by Cleve in "Synopsis of the naviculoid diatoms"(Cleve 1894). *Navicula sensu lato* was divided into sixteen sections, such as *Bacillares*, *Decipientcs*, *lineolatae*, *Lyratae*, and *Punctatae* etc. The species in the section *Bacillares* possess features such as 1. valves linear to elliptical with broad and round ends; 2. A straight raphe enclosed by siliceous thickenings, with thick terminals; 3. narrow or indistinct axial area and small central area; 4. fine transverse striae, more distant in the middle than elsewhere, slightly radiate throughout and curved, very fine punctate; and 5. simple cingulum. In the section *Bacillares* only comprised six species, including a number of species currently recognized as *Sellaphora americana* species group and *S. bacillum* species group (Cleve 1894, Mann et al. 2008) and *Fallacia subhamulata* (Cleve 1894). The species in the section *Lyratae* possess characteristics such as 1. valve elliptical to lanceolate; 2. curved raphe terminal fissures, usually in same direction; 3. indistinct axial area, lateral areas connected with a small central area; and 4. striae radiate at the ends of the valve, usually composed by distinct puncta. This section corresponds to the *Hennedyées* and *Lyrées* proposed by Van Heurck (Van Heurck 1884), including over forty

species, most of them now belong to the genus *Lyrella*, such as *L. abrupta*, *L. genifera* and *L. clavata* etc. Two species are in the genus *Fallacia*, such as *F. forcipata* and *F. pygmaea* (Cleve 1894). Cleve (1894) also pointed out that the morphology of species in this sections varied greatly, particular the shape and the size of lateral areas which is also the important characteristic of this section. In addition, he also pointed that the species in this group resemble the *Diploneis* species, especially *D. hyaline* (Donkin) Cleve 1894 and *D. hudsonis* (Grunow in Cleve) Cleve 1894. Now *D. hudsonis* has been moved to the genus *Fallacia* (Round et al. 1990) and *D. hyaline* was considered as a synonym of *Fallacia hyalinula* (De Toni) Stickle & Mann (Hustedt 1927–1966). The review of the genus *Navicula* by Cleve is totally based on the LM morphological features. Since then, numerous new species have been found, particular those in small size. Those new findings also revealed the subjective and unclear delimitations of many sections proposed by Cleve. Numerous new species could not be assigned to any of the six sections. Even in well defied sections such as *Lyratae*, the delimitations were limit to large marine species (species now belonging to *Lyrella*) (Hustedt 1927–1966). Therefore, Hustedt amended, amplified some Cleve's sections and erected many new sections (Hustedt 1927–1966). In his system, the genus *Navicula* was divided into fifteen sections. The sections *Lyratae* and *Bacillares* were kept, although many changes have been made. This amplified *Lyratae* section includes species formerly belonged to *N.* sect. *Lyratae* Cleve, *N.* sect. *nicobaricae* Cleve, *N.* subgen. *auricula* R.M. Patrick, *N.* subgen. *hennedyea* R.M. Patrick, *N.* subgen. *lyra* R.M. Patrick and many new species. The main feature of this section is also the lyra-shaped lateral areas. He also pointed out that the asymmetric and various striae between the raphe and lateral area resembles many species in the section *Bacillares* (Hustedt 1927–1966). Hustedt's section *Bacillares* includes species were in *N.* sect. *minusculae* Cleve and in *N.* sect. *mesoleiae* Cleve. The delimitations of this section have not changed so much. The main features are the distinct raphe and small valve with blunt round poles. He also suggested the chloroplasts in this section are H-shape. He also put a number of species which he believed as transitional species between *Bacillares* and

Lyratae in this section, such as *N. insociabilis*, *N. helensis*, and *N. occulta* etc. many of those species now belongs to the genus *Fallacia* or *Pseudofallacia*.

Resolution of LM is limited for studying morphology of frustules, even using most advanced light microscopy. Since1970s, the electron microscope (EM) have been used to study diatoms. Most unclear and undiscovered features with light microscopy (LM) have been revealed. The conopeum is one of those strucutures. The term conopeum was coined to a thin porous siliceous layer extending from raphe sterna, covering the surface of the primary siliceous layer (valve surface) (Sims and Paddock 1979). This feature is the major feature of the genus *Fallacia*. Mann & Stickle in Round et al. (1990) described the genus fallacia based on four major features, namely 1. cell with blunt round poles; 2. a single basically H-shaped chloroplast; 3. lateral lyre shaped sterna (appearing as hyaline area in LM); and 4. well-developed porous conopeum. This genus includes many small species in Hustedt's sect. *Lyratae* and most transitional species pointed by Hustedt (cf. Hustedt 1928–1966) in the sect. *Bacillares*.

In last two decades, the detailed morphological and systematic studies were limit to European and South American diatom flora. Sabbe et al. (1999) gave a morphological description of 10 *Fallacia* species from the Westerschelde estuary (The Netherlands) and point out that the genus *Fallacia* forms a natural monophyletic taxon, although morphological heterogeneity could not be overlook (Sabbe et al. 1999). Garcia (2003) also provided 10 species with detailed morphological observation and suggested that features such as the position of the lyre-shaped sterna, the shape of the lateral area and the conopeum, could be used to distinguish *Fallacia* species. Witkowski et al. (2000) provided micrographs of over forty species, however, none of them accompanied with ultrastructure information. In addition, Lange-Bertalot et al. (2000) proposed two combinations and a new species from central European spring. Metzeltin et al. (2005) describe two new species and a combination from Urguray. Currently, there are 103 species names (including intraspecific names), 89 species were accepted taxonomically (M.D. Guiry 2014).

However, most of the 58 species transferred by Mann & Stickle, and other new proposed species and combinations have not been well observed with EM. Several new species have been move out of the genus *Fallacia*, after detailed observing with EM. Three species, namely *F. egregia* (Hust.) D.G. Mann, *F. naumannii* (Hust.) D.G. Mann and *F. pseudomuralis* (Hust.) D.G. Mann have been transferred to the genus *Microcostatus*. *F. lucens* (Hust. ex Salah) D.G. Mann, have been transferred to the genus *Biremis*. *F. tenera* (Hust.) D.G. Mann, *F. arenaria* Sabbe *et* Vyverman, *F. losevae* Lange-Bertalot, Genkal & Vekhov, *F. monoculata* (Hust.) D.G. Mann have been transferred to the genus *Pseudofallacia*.

In sum, the taxon *Fallacia* was a confusing and problematic group of species, not only because of their small size and morphological variations, but also the complicate frustule structure and the morphological heterogeneity. Before the EM was widely used to study diatoms, the *Fallacia* species were in the sect. *Lyratae*, including many marine species have relatively large size, and in the sect. *Bacillares*, including small species could not be well observed with LM, except the distinct raphe (Cleve 1894, Hustedt 1927–1966). With the help of EM, two morphological features such as the conopeum and the lateral sterna linked the species in the two groups (Round et al. 1990). However, the varying morphology of the individual and morphological heterogeneity has not been well explained. In term of molecular phylogenetic analysis in this genus, currently, only three species have sequence data in the Genebank, namely *F. monoculata, F. pygmaea* and *F.* cf. *forcipata*. It could not help to interpret the phylogenetic relationship in this genus.

In addition, there are only 13 *Fallacia* species have been reported in Japan (Sawai et al. 2005, Fujita and Ohtsuka 2005, Watanabe 2004). This research aims is to study the morphology of *Fallacia* species in Japan, and obtain molecular data from cultural species in order to interpret the taxonomic relationship with morphological and molecular data.

II. MATERIALS AND METHODS

1. Collection and cultures

Surface sediments with benthic diatoms were collected from habits such as brackish and marine water by using a glass tube as described by Round (1953). Epipelic species were harvested on a cover slip according to Round et al.(1990). Clonal cultures of *Fallacia* species were obtained by isolated a single cell from the cover slip and transferred to F/2 medium (Watanabe 2004). Epipsammic species usually could not be isolated from sand surface directly. Enrichment culture of small amount of sandy sediments was adopted. When a number of cells of objective species was accumulated, they were isolated individually and move to F/2 medium (Watanabe 2004). However, not all epipsammic species could be isolated. Those species could not be isolated were prepared directly (cf. the section sample preparation).

For observations of sexual reproduction and auxosporulation, numerous cells of a species were isolated from natural population (the cells harvested on a cover slip), and transferred into a rough culture.

Cultures were maintained at 20–23℃, with 20–30 μmol photons • m^{-2} • S^{-1} from cool-white fluorescent tubes; The photoperiod was 14:10 light:dark (L:D).

Sediments were fixed with glutaraldehyde solution (ca. 1.0%). All cultural samples were also fixed with glutaraldehyde solution (ca. 1.0%) before sample preparation.

2. Sample preparations

For obtained clean frustule, vegetative cells need to be treated by acid to remove organic matter. All specimen from brackish and marine water were desalted before or after acidification.

Three preparation methods were used in this research as follow:

a. Bleaching method (Nagumo and Kobayasi 1990)

This method is suit for fragile frustules and perizonium with incunabula.

- Step1: Single cell or auxospore was isolated by a capillary pipette from natural population or cultural samples and transferred into a drop of distilled water on a slide glass.
- Step 2: A drop of bleaching agents or a sodium hypochlorite solution is added to this drop of distilled water. Transfer this frustule into another drop of distilled water on the slide, until the color of chloroplast nearly fades out.
- Step 3: Remove the residual chemicals by transferring this frustule to new distilled water drops, and repeat this step more than three times.
- Step 4: Each specimen is finally transferred one by one to a cover slip, and diagonally and gently pushed with the tip of a fine needle to squeeze out the contents and to loosen the frustule.
- Step 5: The specimen will be dried naturally, and coated by osmium tetroxide for SEM observation. For TEM observations, a formvar-coated copper mesh grid replaces the cover slip.

b. Nitric acids method (Mann 2009)

This method is suit for cultured samples or diatoms harvested by cover slip.

Cleaned valves or auxospores were prepared in situ by placing the cover slips on a hot plate, adding enough 70% nitric acid (SEM) to produce a domed meniscus covering the whole slip, and evaporating gently to dryness at c. 60°. Repeat the nitric acid treatment, and gently rinse by distilled water more than twice in order to remove the nitric acid and salts. Cleaned specimens were waiting for EM observations preparations.

c. Boiling method (Patrick and Reimer 1966)

Samples were boiled with concentrated sulfuric acid and potassium permanganate for 30 minutes and were washed in distilled water more than 5 times. This method has strong acidic ability than the others and could take the frustule apart.

3. Microscopy observation

Light microscopy (LM) observation

Cleaned frustules were transfer to a cover slip and dried on a hot plate. The cover slip was mounted onto a slide using pleurax (mountmedia, Wako, Osaka, Japan).

Nikon Optiphot-2 (Nikon, Tokyo, Japan) and Axio Scope A1 (Carl Zeiss, Oberkochen, Germany) light microscope with differential interference contrast (DIC) was used to observe living cells and mounted cleaned frustules.

Samples for fluorescence microscopy were fixed with 1.0 % glutaraldehyde and stained with 1μg·mL^{-1} DAPI (4', 6-diamidino-2-phenylindole) in phosphate buffer. Olympus fluorescence microscopy BX51 was used to observe fluorescence stained samples.

Scanning electron microscopy (SEM) observation

Hitachi S-4000 and S-5000 scanning electron microscopies (Hitachi, Tokyo, Japan) were used in presenting study. Two types of cover slips, 13-mm diameter and 3-mm diameter cover slips, were adopted for each SEM respectively.

For observations using S-4000 SEM, cover slips with cleaned frustules on it fixed to an aluminum stub with carbon tape and paste. Stubs were coated with osmium for a few seconds in Neoc-AN osmium coater (Meiwafosis, Tokyo, Japan). Whereas, cover slips were directly coated for observations using S-5000 SEM.

The observation using S-4000 SEM was carried out at an accelerating voltage of 5–10kv and 8 mm working distance. Whereas, 3kv and 6–8 mm working distance, when use the S-5000 SEM. All captured images were adjusted by Adobe Photoshop (Adobe Systems, Inc).

Transmission electron microscopy (TEM) observation

Cleaned frustules were drop on a formvar-coated copper mesh grid and dried naturally. JEOL-2000EX and JEM-1400 transmission electron microscopy (JEOL, Tokyo,

Japan) were used in presenting work. TEM were operated at 80 kV or 100kV accelerating voltage. All captured images were adjusted by Adobe Photoshop.

4. Molecular phylogenetic analysis

DNA extraction and purification

CTAB method was used for total DNA extraction. Samples of *c.* 500 ml of culture were filtered through 3μm pore diameter membrane filters (Millipore). Filters were immersed in 500 μL DNA extraction buffer containing 2% (w/v) CTAB, 1.4 M NaCl, 20 mM EDTA, 100 mM TrisHCl, pH 8, 0.2% (w/v) PVP, 0.01% (w/v) SDS and 0.2% β-mercaptoethanol. Immersed filters were incubated at 65℃ for 5 min, vortexed for a few seconds and then discarded. Subsequently, the buffer was cooled briefly on ice. DNA was extracted with an equal volume of chloroform–isoamyl alcohol (24:1 [v/v]) and centrifuged at maximum speed (14,000 rpm) for 10 min. The aqueous phase was collected, re-extracted with chloroform–isoamyl alcohol and centrifuged as described previously. Next, the aqueous phase was mixed thoroughly with 0.8 volumes of ice-cold 100% isopropanol, left on ice for 5 min and subsequently centrifuged in a precooled Eppendorf microfuge at maximum speed for 15 min. DNA pellets were washed in 500 μL 70% (v/v) ethanol, centrifuged for 6 min and then allowed to air-dry after decanting off the ethanol. DNA pellets were dissolved overnight in 100 mL water. The quantity and quality of DNA were examined by agarose gel electrophoresis against known standards (Sato et al. 2008c).

PCR amplification and sequencing

The sequence of the large subunit of the ribulose-bisphosphate carboxylase gene (*rbc*L), were amplified. The reaction volume was 50 μL and contained PCR buffer (67mM Tric-Cl, pH 8.8; 16mM $(NH_4)_2SO_4$; 0.01% Tween-20), 200μM dNTP, 0.3μM of each primer, 2.5 units Taq, and 2.5mM $MgCl_2$ (Takara, Biotech.). PCR were run in the Eppendorf Mastercycler gradient (Eppendorf AG, Hamburg, Germany). After

denaturation at 94℃ for 3 min, thermal cycling was carried out for 30-40 cycles of 94℃ for 1 min, 55℃ for 1 min and 72℃ for 1.5 min, with a final extension of 72℃ for 5min. The concentration was estimated by electrophoresis on a 1 % agarose gel.

Phylogenetic analyses

Four sequences of *Fallacia* and 28 diatoms were retrieved from Genbank (http://www.ncbi.nlm.nih.gov/genbank/) and aligned with six sequences of *Fallacia* in this study using Clustal X (Larkin et al. 2007). To determine which model of sequence evolution best fits the data, hierarchical likelihood ratio tests and the Akaike Information Criterion (AIC) were performed using Modeltest 3.7 (Posada and Buckley 2004, Posada and Crandall 1998).

Maximum likelihood (ML) analyses were conducted using RAxML ver. 7.0.4 (Stamatakis 2006). The ML search was carried out 25 times with 1000 bootstrap replicates each using the GTRGAMMAI model and the run with the best log likelihood score was chosen as our maximum likelihood estimate (MLE). Bayesian inference (BI) analyses were performed using MrBayes v.3.1.2 (Ronquist and Huelsenbeck 2003), using default priors and the GTR+G+I model. Posterior probabilities were assessed in two runs using four MCMC chains with trees and parameters sampled every 1000 generations. Trees were sampled after the standard deviation values of the two runs dipped below 0.01 to calculate the posterior probabilities.

The method for observation of cultured materials was mentioned by Poulíčková et al. (2007). Cleaned frustules mounted on a glass slide with Mountmedia (Wako, Osaka, Japan). Nikon Optiphot-2 light microscope, with differential interference contrast (DIC) was used in LM examination. The size range of vegetative cells, gametangia and initial cells were measured on LM photographs by using ImageJ software (Rasband, W.S. et al.1997–2012). Data set was analysised by R software (R Development Core Team 2008) graphed by the package “simba” (Jurasinski 2007).

III. MORPHOLOGY AND TERMINOLOGY

Terminology follows Anonymous (1975), Ross et al. (1979), Sims & Paddock (1979), Round et al. (1990) and Kaczmarska et al. (2013).

Valve structures

Raphe: a pair of slits through the valve wall. Each individual slit is a branch of the raphe.

- **Central ending**: the proximal ending of each raphe branch.
- **Terminal fissures (external polar raphe ending)**: a continuation of the raphe slit at an apical end as a fissure not penetrating through the valve.
- **Helictoglossa**: an inwardly projecting lipped structure terminating the raphe branch on the inner side of the valve.

Hyaline areas: areas where the basal siliceous layer is not penetrated by areolae. Hyaline areas were named by their positions on the valve face. Those terms were designed for LM observation, corresponding to different ultrastructures in SEM and are not homologous.

- **Axial area**: a hyaline field along the apical axis. In most cases, axial area corresponds to raphe sterna in SEM.
- **Central area**: an expanded or otherwise distinct portion of the axial area midway along its length.
- **Lateral areas**: apical extension of an expanded central area divides the striae. In some *Fallacia* species, more than two lateral areas exist on the surface of a valve. Thus, first, second, third lateral areas etc. were used to describe them in this study. The order of them is decided by the relative position to raphe. The first lateral area is the most closed one. In SEM observation, usually one pair of those lateral areas are sterna (canals), given rise by depression of primary valve layer: the first formed layers of valve. In many genera including the genus *Fallacia*, the valve compresses more than one layer. According to their forming order, the valve layers could be named as primary, secondary and even third valve layer etc. Ross (1979) proposed a

term “Basal siliceous layer” referring to the layer forms the basic structure of the various components of the frustule. This term was not related to the order of valve morphogenesis. In many cases, the primary valve layer and the basal siliceous layer refers to the same layer in *Fallacia*.

Conopeum: a thin siliceous layer extends from raphe sterna covering the whole or part of the primary valve layer. In *Fallacia* species, the conopeum is finely perforated.

Areola: the regularly repeated perforation through the basal siliceous layer.

Stria: a row of uniseriate areolae occluded by hymen in the genus *Fallacia*.

Valve face: a flat plan of valve.

Valve shoulder: a curved area around the valve face.

Primary side: the first formed side of valve.

Secondary side: the side of valve formed after the primary side.

Cingulum structures:

Girde: a part of the frustule between epivalve and hypovalve, composed by epicingulum and hypocingulum.

Valvocopula: an element of cingulum is adjacent to a valve.

Pleura: an element of a cingulum differs from valvocopula in structure and size.

Ligula: a projection of copula, filling the opening or curving of adjacent copula.

Auxospore structures

Auxospore: An auxospore is a specialized cell that has the capacity of expanding in a highly controlled fashion, involving the formation of unique wall elements (incunabula, perizonia) not found at any other stage of the life cycle, to regenerate the characteristic size and shape of a diatom. It is usually formed sexually, but occasionally apomictically or even vegetatively.

Auxosporulation: Auxosporulation refers to the whole process by which an auxospore is formed, develops and, following expansion, gives rise to new, enlarged initial cell(s).

Incunabula: Incunabula are the organic and inorganic components (including silicified

elements) of the auxospore wall that are produced by the zygote, prior to its expansion as an auxospore.

Perizonium: The perizonium is a part of the auxospore wall comprising siliceous bands or rings, hoops and strips that is formed underneath the incunabula as the auxospore expands, apparently to control polarity and shape of the growing auxospore and hence also the species-specific shape of the initial cell.

Initial cell: The initial cell is the first vegetative cell formed within the mature auxospore, complete with a fully formed frustule (the initial frustule composed of the initial epitheca and the initial hypotheca, each with an initial valve).

IV. DESCRIPTIONS OF THE TAXA

In this study, 15 *Fallacia* species were observed in detail, including five new species and one new combination, namely *Fallacia decussata* sp. nov., *F. florinae*, *F.* cf. *foricipata*, *F. fracta*, *F. gemmifera*, *F. hodgeana*, *F. inscriptura*, *F. litoricola*, *F. laevis* sp. nov., *F. nodulifera* sp. nov., *F. oculiformis* var. *miyajimensis* var. nov., *F. pulchella*, *F. tateyamensis* sp. nov., *F. tenera* and *F. teneroides*. According to the result of hierarchical clustering analysis of morphological characteristics, those species could be divided into four groups.

Group 1

This group includes five species, namely *F. fracta*, *F. tenera*, *F. gemmifera*, *F. litoricola* and *F. hodgeana*. They possess a combination of features such as 1. a single longitudinal line of areolae between raphe and lateral area; 2. narrow axial area. 3. two longitudinal sterna usually slightly constrict in the center; 4. internal terminal pores locate on the two terminals.

Group 2

This group includes five species, namely *F.* cf. *forcipata, F. decussata* sp. nov., *F. nodulifera* sp. nov., *F. tateyamensis* sp. nov. and *F. laevis* sp. nov.. Those species possess a combination of features such as 1. typical lyre-shaped sterna; 2. multiple lines of areolae or wide space between the raphe and sterna; 3. areolae at two terminals uncovered by conopeum.

Group 3

This group includes two species, namely *F. oculiformis* var. *miyajimensis* var. nov. and *F. florinae.* They possess the features: 1. convex lateral areas; 2. wide axial area; 3. terminal opening are holes; 4. presenting additional surface structure.

Group 4

This group includes three species, namely *F. teneroides*, *F. inscriptura* and *F. pulchella*. They possess features such as 1. multiple longitudinal lines between lateral area 2. slightly convex lateral area.

Group 1

1. *Fallacia fracta* (Hust. ex Simonsen) D.G. Mann in Round, Crawford & Mann 1990, *The Diatoms. Biology & Morphology of the genera:* 668.

(Plates 5–8)

Synonym: *Navicula fracta* Hustedt 1961, *Die Kieselalgen Deutschlands, Österreichs und der Schweiz unter Berücksichtigung der übrigen Länder Europas sowie der angrenzenden Meeresgebiete. In*: L. Rabenhorst (ed.), Kryptogamen Flora von Deutschland, Österreich und der Schweiz. Akademische Verlagsgesellschaft m.b.h. Leipzig 7 (Teil 3, Lief. 1): 127, fig. 1259.

Type locality: Pitkäjärvi Harlu, Finnland.

Distribution: Rare in intertidal area and freshwater environment. Reported from Pitkäjärvi and Fluß Vuoksi (Kupersaari), Finnland. (Hustedt 1927-1966), North America, Königswartha Germany (Krammer and Lange-Bertalot 1986), Romania (Caraus 2002), Britain (Whitton et al. 2003), Brazil (Eskinazi-Leça et al. 2010) and Okinoshima, Tateyama city, Chiba Prefecture, Japan.

LM observation

Living cells are solitary, containing a single H-shaped chloroplast. (Pl. 5, Fig. 4).

Valves are oblong or elliptical with bluntly round poles, 12.3–20.3 μm (15.4 ± 1.87 μm，mean ± *s*) long, 5.3–9.1 μm (6.65 ± 0.88 μm) wide (Pl. 5, Figs 1–3). The raphe is slightly arched, with central raphe endings close to each other. The axial area cannot be resolved in LM. The lateral area is not obvious, appearing a narrow longitudinal interruption of striae near the raphe in some specimens or missing (Pl. 5, Figs 2, 3). Central area is narrow rectangular, connecting with lateral areas. The striae are central parallel and become radical near poles, 21–27 (24 ± 1.58) in 10 μm.

EM observation

The external valve face is flat with a shallow mantle. The raphe is slightly curved.

Two terminal fissures turn towards the secondary side (Pl. 5, Fig. 6, Pl. 6, Fig. 1) on the external valve surface, whereas the internal polar raphe endings turn to the primary side, forming a small helictoglossa (Pl. 6, Fig. 6). The external central endings were straight, slightly expanded (Pl. 6, Fig. 3), whereas the internal central endings were slightly deflected in the same direction (Pl. 6, Fig. 4). The hyaline lateral areas are in fact two lateral sterna on the internal valve face, given rise by depressions of primary valve layer. Between the sternum and the raphe, there is a longitudinal line of areolae (Pl. 6, Fig. 2, 4, 6). It is asymmetric on both sides of raphe (Pl. 6, Fig. 6). In addition, there are two pores on both sides of raphe (Pl. 6, Fig. 5). And a number of areolae locate at the poles of the valve, which are external occluded hymen (Pl. 6, Fig. 5–6). The whole primary valve layer is covered by the finely porous conopeum, fused with valve mantle by several small "pegs". (Pl. 6, Fig. 5, Pl. 7, Figs 1, 3, 5). The striae are uniseriate areolae (Pl. 7, Fig. 2). There is a lumen underneath the conopeum, which connect to the exterior via the two polar pores. The cingulum consists of a valvocopula and two pleura (Pl. 8, Figs 1, 3).

2. *Fallacia tenera* (Hust.) D.G. Mann in Round, Crawford & Mann 1990, *The Diatoms. Biology & Morphology of the genera:* 668.

(Plates 9–13)

Synonym: *Navicula uniseriata* Hustedt in Schmidt et al. 1934, Atlas der Diatomaceen-kunde. Leipzig. O.R. Reisland Series VIII (Heft 97–98): pl. 392, figs 24–27. *Navicula tenera* in Schmidt et al. 1936, Atlas der Diatomaceen-kunde. Leipzig: O.R. Reisland Series VIII (Heft 101–102): pl. 405, footnote.

Type locality: Java, Ranu Klindungan.

Distribution: Cosmopolitan species, live in marine, brackish and freshwater environment. Reported from Java, Ranu Klindungan (Hustedt 1937), U.S. (Patrick R. & Reimer C.W. 1966), South Arica (Schoeman, F.R. & R.E.M. Archibald, 1976–1980), Sri Lanka (Foged, 1976), Spain (Aboal, Puig & Soler 1996), Netherlands (Sabbe, Vyverman & Muylaert 1999), Britain (Whitton et al. 2003), China (Chen C.P. 2005, Li Y. 2006), France (Méléder et al. 2007), Brazil (Eskinazi-Leça et al. 2010), Queensland (Bostock & Holland 2010), New Zealand (Harper et al. 2012). Japan (Takano 1990 as *Navicula teneroides*).

LM observation

Vegetative cells are solitary and capable of forming short straight chains under artificial cultural condition. Each cell contains one H-shaped chloroplast consisting of two plates connecting centrally (Pl. 9, Fig. 1). Valves are naviculoid to elliptical with bluntly rounded poles, 8.5–24.1 μm long and 5.4–8.6 μm wide. The raphe is slightly arched. Two curved comparatively wide lateral areas go through the valve longitudinally and connected with the slightly transapical convex central area. The striae are radiate especially towards the poles, 17–20 in 10 μm. The striae are interrupted into three longitudinal lines of areolae on one half valve face by longitudinal hyaline areas. The two longitudinal uniseriate areolae adjacent to the raphe branch were laterally asymmetric (Pl. 9, Fig. 2, arrow), and one on convex side (secondery side) of the raphe are smaller, fewer

or even missing.

EM observation

The external valve face was flat with a shallow mantle. The external raphe terminal fissures bent towards the secondary side, while the internal polar raphe endings form a small helictoglossa (Pl. 9, Figs 4, 5, arrows), curving towards the primary side. The external raphe central endings slightly curve, opening into a small spathulate groove, while the internal central endings deflected in the same direction. The distal longitudinal lines (Pl. 9, Fig. 3, arrow) of areolae in LM were in fact a circle of areolae on the valve mantle around the valve face (Pl. 10, Fig. 1). The other two longitudinal lines of areolae were on the valve face, interrupted by a depressed sternum (Pl. 10, Fig. 2), appearing as a hyaline area in LM. The striae on the valve face are covered by a finely porous conopeum that extending from the raphe sternum to the valve mantle (Pl. 10, Fig. 5, Pl. 11, Fig. 1, 2). The edge of mantle also bears a “peg” between two protrusions (Pl. 11, 1, 3) which probably could fasten the connection of the conopeum and the mantle. The conopeum and the inner edge of mantle all possess undulate margins connecting like a zipper (Pl. 10, Fig. 2). The two lateral depressed sterna (Pl.10, Fig. 2) and the finely porous conopa (Pl. 11, 1, 3) compose two longitudinal canals (Pl. 11, Figs 1, 4), which connect with the exterior via pores (Pl. 10, Fig. 5, Pl. 11, Fig. 4) on either side of terminal fissure. Around the areolae adjacent to the raphe on either side, many siliceous ribs were presented between the primary valve layer and the conopeum to support the conopeum (Pl. 11, Fig. 4). The two longitudinal lines of areolae next to the raphe are obvious lateral asymmetric (Pl. 10, Fig. 6). The areolae were occluded by a hymen with a hexagonal arrary (Pl. 11, Figs 5–6). The cingulum was composed of three none perforated bands. One open valvocopula possesses an undulate advalavar edge of the pars interior, and a curved down part of edge of pars exterior at the pole opposed to the opening (Pl. 12, Figs 1–2). Two open pleurae all have considerably large ligula and a very narrow strip that extending along the whole inner surface of the valvocopula. The two pleurae differ in their ligula

shape, the width of strips and their orientations. The ligula of pleura 1 (second band) is arc shaped (Pl. 12, Figs 5–6) and on the inner side of closed pole of valvocopula, filling the missing parts formed the curving down edge of the pars exterior of the valvocopula. The ligula of the pleura 2 (third band) is triangular (Pl. 12, Figs 5–6) and presents on the inner side of the opening of valvocopula to fill the gap. The strip of the third band is thicker than the strip of the second band (Pl. 13, Fig 3, arrowhead). The terminals of those strips were present on the poles opposed to the linguae (Pl. 13, Fig. 4).

3. *Fallacia gemmifera* (R. Simonsen) D.G. Mann *in* Round, Crawford & Mann 1990, *The Diatoms. Biology & Morphology of the genera:* 668

(Plates 14–16)

Synonym: *Navicula gemmifera* Simonsen 1960, Neue Diatomeen aus der Ostsee. II. Kieler Meeresforschungen 16 (1): p. 128; pl. 1, fig. 11–12.

Type Locality: Sandy silt, Holy harbor, Graswarder, Salztumpel.

Distribution: Marine and Brackish-waters, very widely distribute in Belt Sea, Gulf of Gdansk, Poland (Simonsen 1960, Witkowski et al. 2000), Estuary of the Yeong Stream, Korea (Joh G. 2003) and river mouth of Edogawa River in Japan.

LM observation

Living cells are solitary, containing a single typical H-shaped chloroplast. (Pl. 14, Fig. 1).

Valves are naviculoid or rhombus with relatively acute poles, 12.6–22.1 μm (16.5 ± 2.2 μm，mean ± *s*) long, 4.7–6.2 μm (5.5 ± 0.40 μm) wide (Pl. 5, Figs 2–4). The raphe is slightly arched, with central raphe endings closed to each other. Lateral areas were longitudinal and convex centrally, connecting with a narrow central area (Pl. 14, Figs 2–5). There are longitudinal uniseriate areolae between the raphe and lateral area. The striae are radical and interrupted by the lateral areas, 18–22 in 10 μm (19.6 ± 0.9).

EM observation

The valve surface is convex (Pl. 15, Fig. 1, 5). Thus, valves are usually not laying at the plain view in LM, or SEM. The raphe is slight curved (Pl. 14, Figs 7–8). The two terminal fissures bent towards the secondary side on external view (Pl. 14, Fig. 7, Pl. 15, Fig. 1). Internally, the polar raphe endings form a small helictoglossa (Pl. 14, Fig. 8, Pl. 15, Fig. 2). The external central raphe endings are slightly curved and expanded (Pl. 15, Fig. 3), whereas the internal central raphe endings are slightly deflect into the same direction (Pl. 15, Fig. 3). There were two lateral terminal slits (Pl. 15, Fig. 5) on both

sides of the raphe, through which the lumen between the conopeum and the primary valve layer can connect with the exterior. The striae are composed of uniseriate areolae and interrupted by lateral sterna which formed by depressing of the primary valve surface. The areolae between the raphe and the lateral sterna are not symmetric (Pl. 14, Fig. 8).There is a circle of areolae around the valve surface, which were occluded externally and directly connected with the exterior (Pl. 15, Figs 5–6). Those areolae are on the mantle and separated with others by a wide vimen (Pl.15, Fig. 6). The finely porous conopeum grows out of the raphe sterna. The areolae on the primary valve layer were covered by this conopeum. It fuses with valve mantle with several small “pegs” (Pl.16, Figs 1, 3). The cingulum was consisted by an open valvocopula which curved on at the unopened pole and two pleurae (Pl. 16, Fig.4). The two pleurae could be distinguished by their ligulae. One possesses a large basic triangular ligula filling the opening of valvocopula (Pl. 16, Fig. 5), the other one has a smaller ligula filling the curving down part at the opposite pole (Pl. 16, Fig. 6).

4. *Fallacia litoricola* (Hust.) D.G. Mann in Round, Crawford & Mann 1990. *The Diatoms. Biology & Morphology of the genera:* 668.

(Plates 17–19)

Synonym: *Navicula litoricola* Hustedt 1955. Marine littoral diatoms of Beaufort, North Carolina. Duke University Marine Station, Bulletin 6: p. 23; pl. 8, figs 13, 14.

Type locality: Beaufort, North Carolina, United States.

Distribution: Cosmopolitan species, widely distribute in marine coast. Beaufort, North Carolina, U.S. (Hustedt 1955, Campeau et al. 1999), Subarctic to the Mediterranean, the western Baltic Sea, South Africa (Witkowski 2000). Korea (Joh G. 2013), Japan (Ena bay, Kanagawa Prefecture; Okinoshima, Tateyama city, Chiba Prefecture; Sanbansei, Ichikawa city, Chiba Prefecture; Amamioshima, Kagoshima Prefecture; and Miyajima, Hiroshima city, Hiroshima Prefecture.).

LM observation

Living cells are solitary, containing a single typical H-shaped chloroplast usually with two volutin granules (Pl. 17, Fig. 1).

Valves are elliptical with blunt round poles (Pl. 17, Figs 2–5), 8.8–28.4 μm (14.2 ± 3.8 μm，mean ± *s*) long, 4.5–9.0 μm (5.7 ± 0.8 μm) wide. The raphe is slightly curved. Terminal fissures bent towards the primary side. Central endings are closed with each other. The slightly curved lateral areas are asymmetric and constrict centrally, connecting with a narrow central area. The areolae between the raphe and the lateral areas arrange in a single longitudinal line. The striae are parallel in the center and radical near the poles, 17–25 in 10 μm (22.8 ± 1.6).

EM observation

The valve surface was more or less flat (Pl. 18, Figs 1, 3, 5). The external central raphe endings are straight and slightly expanded, opening to a small spathulate groove (Pl. 18, Fig. 3), whereas the internal central raphe endings deflect in the same direction (Pl.

18, Fig. 4). The external raphe terminal fissures are strongly waved towards to the secondary side (Pl. 18, Fig. 5), whereas the internal polar raphe endings form a small helictoglossa, slightly curving to the primary side (Pl. 18, Fig. 6). The lateral sterna are obvious on the internal valve view (Pl. 18, Fig. 1). The areolae between raphe and lateral sterna were not exactly single longitudinal line. Many striae have two areolae transapically (Pl. 18, Fig. 2, 6). In external view, there are a number of areolae at the two terminals not covered by conopeum, arranging as one central areola on the top and a number of areolae on both sides symmetrically (Pl. 18, Figs 5–6). The striae were composed by uniseriate areolae, covered by a porous conopeum (Pl. 19, Figs 1–2). The areolae of striae are flanked by two thicked virgae, given rise a trough-like branch canal (Pl. 19, Fig. 1). Those branch canals are connecting with the main lateral canal formed by depression of lateral sterna. The lumen between primary valve layer and porous conopeum connects with the exterior via the terminal slits. The cingulum consists of an open valvocopula (Pl. 19, Figs 3–4) and two pleurae. The two pleurae could be distinguished by the shape and size of ligula. One has a large triangular ligula (Pl. 19, Fig. 5) and the other has a comparatively small semicircular ligula (Pl. 19, Fig. 6).

5. *Fallacia hodgeana* (Patrick *et* Freese) Yu H. Li *et* Hide. Suzuki 2014. Morphology and Ultrastructure of *Fallcia hodgeana* (Bacillariophyceae). *Journal of Japanese Botany* 89: 27–34.

(Plates 20–23)

Synonym: *Navicula hodgeana* Patrick & Freese 1961. Diatoms (Bacillariophyceae) from Northern Alaska. Proceedings of the Academy of Natural Sciences of Philadelphia 112(6): 189; pl. 2, fig. 2.

Type locality: Alaska, Rogers-Post Monument, Barrow. US. 15 August 1951.

Distribution: Alaska, Rogers-Post Monument, Barrow, US (Patrick & Freese 1961). And river mouth of Edogawa River, Japan.

LM observation

Vegetative cells are solitary and contain one H-shaped plastid (Pl. 20, Fig. 1). Valves are naviculoid with round poles (Pl. 20, Figs. 2–6), 11–18 μm long and 4–6 μm in wide. The raphe is slightly arched. Central endings are closed to each other. The axial area is extremely narrow and hardly resolved in LM. The longitudinal hyaline lateral areas connect with the narrow bar-like central area. The lateral areas constrict centrally, resulting in an H-shaped hyaline area. The striae are parallel, becoming radical near two poles, 19–24 in 10 μm. The striae are interrupted by the hyaline lateral area near the proximal end, giving rise to longitudinal uniseriate areolae between raphe and hyaline lateral area. The longitudinal row of areolae near the valve margin spaced from others.

SEM observation

The raphe is slightly curved. In external view, the raphe terminal fissures are strongly hooked towards the secondary side, extending on to the valve mantle (Pl. 21, Fig. 3). The central raphe endings were more or less straight and slightly expanded, opening to a spathulate groove (Pl. 21, Fig. 5). Internally, the polar raphe endings were slightly deflected and end as a small helictoglossae (Pl. 21, Fig. 4). The central raphe endings

slightly deflect in the same direction and appear slightly elevated from the general plane of valve (Pl. 21, Fig. 6). In internal view, the striae are interrupted by lateral sterna (Pl. 21, Fig. 2) at the proximal end, resulting in one longitudinal row of areolae between lateral sterna and raphe (Pl. 20, Fig. 8, Pl. 21, Fig. 2). The areolae on the margin curved up and directly connect with the exterior on the mantle (Pl. 21, Fig. 4). On the outer surface, the finely porous conopeum (Pl. 21, Figs 3, 5, Pl. 22, Figs. 1, 3, 5) extend outward from the outer edge of raphe sterna, running through the surface, and connected with proximal edge of mantle. Along the proximal edge of mantle, a number of "pegs" projections can be observed (Pl. 21, Fig. 5, Pl. 22, Figs 1,5), which are inlaid into the nonporous margin of conopeum. The porous conopeum conceal the whole canal system of valve. The depressions of longitudinal lateral sterna on the primary layer of valve give rise to two main canals on either side of raphe, which connected to each other at the central area, between two central raphe endings, composing an H-shaped space between primary layer and conopeum (Pl. 22, Figs 4, 6). This space or main canals connected with the exterior directly at slit openings (Pl. 21, Fig. 3, Pl. 22, Fig. 5) located on the both sides of terminal fissure and through the small pores of conopeum. Each stria is flanked by two thick virgae (Pl. 22, Figs 4, 6) which projected from and are perpendicular to the primary layer of valve, forming several branch canals. The branch canals were also covered by finely porous conopeum, composing an elongated chamber running from distal edge of lateral depressed canal to the proximal edge of edge of valve mantle. All of those transapical chambers connected to the main canal at the proximal end. Consequently, the protoplasm commutate with the exterior directly via the areolae on the mantle or indirectly via the canal system between conopeum and primary layer of valve. Areolae were occluded by a hymen with centric arrary (Pl. 23, Figs 3–4). The cingulum was composed of two bands, a broad valvocopula and an extremely linear pleura with a ligula (Pl. 23, Figs 1–2).

Group 2

1. *Fallacia* cf. *forcipata* (Greville) Stickle & Mann in Round, Crawford & Mann 1990. *The Diatoms. Biology & Morphology of the genera:* 668.

(Plates 24–26)

Synonym: *Navicula forcipata* Greville 1859. Descriptions of new species of British Diatomaceae, chiefly observed by the late Professor Gregory. Quarterly Journal of Microscopical Science, London p. 83; pl. 6, figs 10, 11.

Type locality: Northumberland, UK.

Distribution: Cosmopolitan species, widely distribute in marine coast. Reported from UK. Okinoshima, Uminokouen Park Yokohama, Japan. U.S. (Patrick & Reimer 1966). South America: Brazil (Eskinazi-Leça et al. 2010) Germany (Sabbe, Vyverman & Muylaert 1999), Netherlands (Sabbe, Vyverman & Muylaert 1999), Romania (Caraus 2012). Canary Islands (Gil-Rodríguez et al. 2003), New Zealand (Harper et al. 2012). Korea (Joh G. 2013).

LM observation

Vegetative cells are solitary and contain one basically H-shaped plastid with two pyrenoids (Pl. 24, Fig. 1). Valves are broad elliptical with bluntly round poles (Pl. 24, Figs. 2–4), 14.1–15.5 μm (15.0 ± 0.4 μm) long and 7.2–8.2 μm (7.8 ± 0.3 μm) wide. The raphe is straight. Central raphe endings are close to each other. Lyre-shaped lateral areas constrict centrally, connecting with a very narrow central area. The striae are parallel centrally, becoming radical near two poles, 19–21 (20.3 ± 1.0 μm) in 10 μm. The striae are interrupted by a hyaline lateral area near the proximal end, giving rise to a number of longitudinal uniseriate areolae between the raphe and the hyaline lateral area.

EM observation

The valves are convex and more or less high. The terminal fissures curve to the secondary side, while the internal polar raphe endings deflect to the primary side. The

external central raphe endings are more or less straight and expanded, opening to a small groove. Between the two central raphe endings, there is a thick siliceous block. The internal polar raphe endings, forming a small helictoglossa, deflect to the primary side. At the external terminals, two tiny pores locate laterally on both sides of the raphe. There are a number of areolae directly connecting with the exterior below the tiny pores. Internally, the virgae were thicker than vimen. There were longitudinal multiseriate areolae between the raphe and the lateral sterna. For the cingulum, only one open valvocopula and one pleura were observed in this study.

2. *Fallacia decussata* Yu H. Li sp. nov.

(Plates 27–29)

Holotype: Pl. 27, Fig. 1, Slide No. 0002, Yu H. Li collection (due to be housed in The Natural History Museum, London, U.K.).

Type material: Ena Bay, Miura Peninsula, Kanagawa Prefecture, Japan, 27 August, 2012. Material No. LYH199.

Type locality: Ena Bay, Miura Peninsula (35°08′39.34″N，139°39′49.60″E), Kanagawa Prefecture, Japan.

Etymology: the X-shaped central area, forming by crossing of lateral areas.

Description

Valves elliptical with blunt poles, 13.7–20.6 μm long and 6.1–8.4 μm wide. Raphe straight with distant central endings. Terminal fissure curved towards same direction. Lateral area thin, crossing in central area. Striae uniseriate. Striae between lateral area paralleled; Striae outside lateral area radical, 25–28 in 10 μm. Areolae occluded by hexangular hymen. Whole primary valve layer covered by finely porous conopeum. Pegs on surface of distal end of each virga around valve face. A number of pores on both side of raphe formed by dentate edge valve margin and flat edge of conopeum.

LM observation

Valves are elliptical with blunt poles, 13.7–20.6 μm (16.2 ± 2.1 μm) long and 6.1–8.4 μm (7.2 ± 0.5 μm) wide (Pl. 27, Figs 1–4). The raphe is straight with distant central endings. The thin lyre-shaped lateral areas strongly constrict centrally, appearing an X-shaped central area. The striae are slightly radical and interrupted by the lateral areas, 25–28 (26.3 ± 1.2) in 10 μm. The striae between the lateral area and the raphe are nearly parallel to each other, whereas the outer striae become comparatively radical.

EM observation

The valve surface is slightly convex (Pl. 28, Fig. 1). The raphe is straight, cured near the poles (Pl. 27, Figs 5–7). The external central endings are also straight and slightly expanded, opening to a small groove (Pl. 27, Fig 5–6, Pl. 28, Figs 3–4), whereas the internal central endings are straight (Pl. 28, Fig 2.). The polar raphe endings form helictoglossae (Pl. 28, Fig 2.), slightly deflect to the secondary side, while the internal raphe endings are straight. Axial areas are uneven on the both sides of the raphe (Pl. 27, Fig. 5, Pl. 28, Figs 4–6). Lateral sterna are thin and strongly arching, elevated from the general internal valve surface (Pl. 28, Fig. 2), forming a comparative large canal beneath the conopeum (Pl. 29, Fig. 2). Lateral sterna connect with the wide central area, which is also elevated (Pl. 28, Figs 2. 4, Pl. 29, Fig. 2). The striae are composed by uniseriate areolae (Pl. 28, Figs 2, 4, 6). The whole valve surface was covered by finely porous conopeum (Pl. 28, Figs 1, 3, 5). There are a number of areolae not covered by a conopeum at the two terminals, arranging symmetrical on both sides of the terminal fissure (Pl. 28, Fig. 5). The conopeum fused with valve mantle with pegs, which are located on one side of virgae. However, the pegs are not presents on the two terminals, thus the conopeum does not fuse with the valve mantle completely, giving rise a number of pores connecting with the canal and the exterior (Pl. 28, Fig. 5). The areolae are occluded by a hexangular hymen (Pl. 29, Fig. 4).

Ecology and distribution

This species was collected with sandy sediments from an intertidal area at the type locality. This species also were found in the sandy sediment from Kushiro city, Hokkaido (material No. LYH77). This species is epipsammic species.

Discussion

This species is characterized as the crossing lateral area, multiple areolae between the raphe and lateral area and the different orientation of striae inside and outside the lateral

areas in LM. For EM observation, the “pegs” on each virgae around the valve face and dentate valve margin giving rise a number pores on both sides of the raphe were unique to this species. The species also resembles *Fallacia clepsidroides* which also possess the similar shaped lateral area. However, there only one or two longitudinal line of areolae between the raphe and lateral area. With SEM, the external valve surface of *F. clepsidroides* resembles *F. oculiformis,* possessing the transapical ribs growth out from margin connected with conopeum. In contrast, the conopeum of *F. dencussata* covers the whole primary valve layer. In addition, the *F. clepsidroides* possess two pores on both sides of the raphe. Sabbe et al.(1999) gave a micrograph (Fig. 37) which he thought probably is probably not *F. clepsidroides* (which a question mark) from the weterschelde estuary. That specimen agrees with the above features of *F. decussate* and belongs to this species.

3. *Fallacia nodulifera* Yu H. Li sp. nov.

(Plates 30–33)

Holotype: Pl. 30, Fig. 3, Slide No. 0002, Yu H. Li collection (due to be housed in The Natural History Museum, London, U.K.).

Type material: Okinoshima, Tateyama city, Chiba Prefecture, Japan, 14 March, 2012. Material No. LYH110.

Type locality: Okinoshima (35°08′39.34″N，139°39′49.60″E), Tateyama city, Chiba Prefecture, Japan.

Etymology: Possessing a central nodule on the internal valve face.

Description

A single basic H-shaped chloroplast. Valve wide elliptical with blunt round poles, 9.3–26.7μm long, 4.9–11.3 μm wide. Raphe slightly arched, terminal fissure hooked towards same direction. Small terminal pores. Lateral area convex centrally, connected with central area. Striae uniseriate, slightly radical, 16–23 in 10μm. Longitudinal line of areolae uniseriate and asymmetric. Areolae occluded by central arrayed hymen. The edge of finely porous conopeum finger-shaped.

LM observation

Living cells are solitary, containing a basic H-shaped chloroplast with two pyrenoides (Pl. 30, Fig. 1).

Valves are elliptical with round poles (Pl. 30, Figs 2–5), 9.3–26.7 μm (12.5 ± 3.7 μm，mean ± *s*) long, and 4.9–11.3 μm (6.1 ± 1.3 μm) wide. The raphe is slightly arched. Hyalined lateral areas are very narrow, connecting with a bar-liked thin central area. The lateral areas convex at the center and constrict near the poles, giving rise a lanceolate area. The striae were radical, interrupted by lateral area at the proximal end, 16–23 (19.9 ± 2.4) in 10 μm. There are a longitudinal line of areolae between the raphe and lateral area, adjacent to the proximal side of lateral area. However, those areolae are various among

specimen. In many cases the areolae are even missing from this area, particular those small individuals.

EM observation

The valve external surface is slightly sinking at the lateral area with a shallow mantle. The external raphe terminal fissures are strongly hooked towards to the secondary side, whereas the internal polar raphe endings form a small helictoglossa (Pl. 31, Figs 1–2) and slightly deflect to the primary side. The external central endings are slightly curved and expanded, opening to a shallow cycle groove, while a remarkable central nodule is present on the internal valve face. The two internal central raphe endings are hidden in the central nodule. In addition, there also are a rectangular arched block between the two terminal ending on the external valve area, and more or less thicken layer on the external surface between the raphe and the position of lateral area (Pl. 31, Figs 3, 5) At the terminals of valve, the strongly hooked terminal fissures are flanked by two tiny pores. There are one or two areolae not covered by finely porous conopeum below them (Pl. 31, Fig. 5). The striae are uniseriate areolae (Pl. 31, Fig. 6). The whole primary valve layer is covered by a finely porous conopeum. Those pores on the conopeum are in three or four lines above the striae. In contrast, the conopeum above the vimen is no pores and connect with the vimen (Pl. 32, Figs 3–4). The valvocopula is relatively wide with a crenate margin (Pl. 32, Figs 5–6). From the TEM micrographs, the thick layer around raphe braches is obviously (Pl. 33, Figs 1–3). The areolae are occluded by a central array hymen (Pl. 33, Fig. 4).

Ecology and distribution

This species is also an epipsammic species. It was collected with sandy sediment from the intertidal area. This species is also collected from Ena-bay (Material No. LYH110), Tateyama city, Chiba Prefecture, and Miyajima (Material No. LYH209), Hiroshima Prefecture.

Discussion

Fallacia nodulifera could be easily confused with *F. florinae*. They share features such as elliptical outline, small size and lateral area convex centrally. For many small specimen, of which the striae are not resolved in LM, the identification is not easy. However, *F. nodulifera* differ from *F. florinae* in the central connected lateral area. In *F. florinae* the lateral areas are independent from each other. In SEM, the two species remarkable differ from each other in the external valve surface. The external valve surface of *F. nodulifera* is finely porous conopeum, covering the whole primary valve layer. In contrast, the *F. florinae* possesses more complicate surface, the porous conopeum only presents at the position of lateral sterna. Other surface was covering by nonporous siliceous layer. In addition, when observed using TEM, the raphe of *F. nodulifera* was surround by a thin layer. Those features could be used to well distinguish the two species.

4. *Fallacia tateyamensis* Yu H. Li sp. nov.

(Plates 34–37)

Holotype: Pl. 34, Fig. 1, Slide No. 0003, Yu H. Li collection (due to be housed in The Natural History Museum, London, U.K.).

Type material: Okinoshima, Tateyama city, Chiba Prefecture, Japan, 7 July, 2011. Material No. LYH69.

Type locality: Okinoshima (35°08′39.34″N，139°39′49.60″E), Tateyama city, Chiba Prefecture, Japan.

Etymology: The city name of the type locality.

Description

A single H-shaped chloroplast. Valves elliptical with blunt round poles, 18.6–36.1 μm long, 10.3–13.2 μm wide. Raphe straight, terminal fissures hooked towards same direction. Axial area wide. Lateral area lyre-shaped, constricted in center. A single uniseriate areolae between raphe and lateral area. Striae uniseriate, paralleled centrally, radical near poles, 20–23 in 10 μm. Whole primary valve layer covered by finely porous conopeum.

LM observation

Living cells are solitary, containing a basic H-shaped chloroplast with one pyrenoide (Pl. 30, Fig. 1). The chloroplast consists of two large slice parts appressed on the internal valve face. They are connected by a thin plate centrally (Pl. 34, Fig. 1).

Valves are elliptical with blunt round poles (Pl. 34, Figs 2–4), 18.6–36.1 μm (25.0 ± 4.5 μm，mean ± *s*) long, 10.3–13.2 μm (11.3 ± 0.8 μm) wide. The raphe is straight. The central endings are distant. The axial area is wide. The hyaline lateral areas are typical lyre-shaped and constrict at the center and near the valve poles. Between raphe and lateral area, there are longitudinal uniseriate areolae adjacent to the proximal side of lateral area. The axial area and areolae are disconnected at the center and not fuse with

the central area, forming a small groove around the central endings. The striae are parallel at the center, and become radical towards the poles, 20–23 (21.3 ± 1) in 10 μm.

EM observation

The external valve surface was flat with a very board curving down edge (Pl. 35, Fig. 1). The arched lateral sterna were very obviously on the internal view (Pl. 35, Fig. 2). The external raphe terminal fissures are strongly hooked to the secondary side, while the internal polar raphe endings slightly defect to the primary side. The external raphe central endings are slightly expanded, opening to a small shallow groove, whereas the internal central endings deflect to the primary side (Pl. 35, Fig. 3–4). The external terminal fissure was flanked by two tiny pores. Below them, there are one or two tiny pores not covered by conopeum (Pl. 35, Figs 5–6). The whole surface is covered by finely porous conopeum (Pl. 36, Fig. 1). Those pores are arranged in two or three transapical line at the distal side and brached at the proximal end (Pl. 36, Figs 3, 5). The stiae are a uniseriate areolae (Pl. 36, Figs 4, 6). There are also branch canal given rise by the thick virgae, striae and the finely porous conopeum (Pl. 37, Figs 1–2). An open valvocopula and a ligula of pleura are found in this species. The ligula is present at the inner side of valvocopula to fill the opening of the valvocopula (Pl. 37, Figs 2–4).

Ecology and distribution

This is an epipsammic species. Collected with sandy sediment from intertidal area, Okinoshima, Tateyama city.

Discussion

Fallacia tateyamensis are probably closely related to *F. forcipata.* They share features such as elliptical outline, typical lyre-shaped lateral areas and the shape of central area. The key feature distinguish the two species is the striae between the raphe and the lateral areas. In *F. forcipata*, there are longitudinal multistriate areolae, whereas

the *F. tateyamensis* only has longitudinal uniseriate areolae with wide axial area instead. *F. litoricola* also possess uniseriate longitudinal areolae, but without the wide axial area. In addition, *F. litoricola* also differ from *F. tateyamensis* in the valve outline.

5. *Fallacia laevis* Yu H. Li sp. nov.

(Plates 38–40)

Holotype: Pl. 38, Fig. 2, Slide No. 0004, Yu H. Li collection (due to be housed in The Natural History Museum, London, U.K.).

Type material: A cultural material from octopus aquarium.

Type locality: Cultural sample.

Etymology: The smooth surface of the valve in LM.

Description

A single H-shaped chloroplast. Valves elliptical with blunt round poles, 7.4–18.3 μm long, 4.16–7.4 μm wide. Raphe slightly arched, central ending distant, terminal fissure curved towards the same direction. Lateral area longitudinal constrict near poles and slightly constrict centrally, connected with bar-liked central area. Striae not resloved in LM. Multiple line of areolae between raphe and lateral sterna. Whole primary valve layer covered by porous conopeum. A number of pores located on valve mantle.

LM observation

Living cells are solitary, containing a basic H-shaped chloroplast (Pl. 30, Fig. 1).

The valves are elliptical with round poles, 7.4–18.3 μm (12.6 ± 3.2 μm，mean ± *s*) long, 4.16–7.4 μm (5.5 ± 0.8 μm) wide. The raphe is slightly arched. The central endings are distant. The hyaline lateral areas are thin and lyre-shaped, constrict at the center and near the two poles. The thin-bar liked the central area connected with the lateral area. The area between the central area and central raphe endings were sinking in. The striae are not resolved in LM. The whole valve appears hyaline.

EM observation

The raphe is slightly curved. External terminal fissures hook into the secondary side. (Pl. 38, Fig 6, Pl. 39, Fig. 1), while the internal polar raphe endings form a small

helictoglossa usually deflected towards the primary side (Pl. 39, Figs 2, 6). The external central endings are slightly curved and expanded, forming a relatively large round circle groove (Pl. 39, Fig. 3). The internal central raphe endings slightly defect to the primary side and are more or less arched (Pl. 39, Fig. 4). The striae are uniseriate areolae. There were a number of small pores at the terminal and at the valve mantle around the valve face (Pl. 39, Fig. 5). The nonporous layer around the external raphe endings fuse with each other, forming a rectangular central area (Pl. 40, Fig. 2). The whole valve surface is covered by a finely porous conopeum. Those tiny pores are arranged in triseriate line above striae and segregated by the nonporous area which fused with the virgae (Pl. 40, Figs 1–4). From the valve with broken conopeum, the canal system beneath the conopeum is present. The main lateral canals connect with each branch canals. The whole system was connect with the exterior via the fine pores of conopeum.

Discussion

Fallacia laevis was isolated from an aquarium of octopus culturing. Currently it has not been found in other locations. Thus, the living environment and habit of natural population were still unknown. Morphologically, *F. laevis* is very unique in the genus *Fallacia* and possesses a number of features found in *Diploneis* species. The conopeum is well fused with the primary valve layer. The connections between conopeum and valve margin (“pegs” or the margin of conopeum) are invisible in this species. The small pores on the valve mantle differ from the areolae uncovered by conopeum in other species, which usually external occluded by hymen. And those pores are usually found in *Diploneis* species. At the beginning, I questioned whether this species should belong to *Fallacia*. However, the result of molecular phylogenetic analysis and a number of morphological features such as H-shaped chloroplast, lateral depressed sterna, and two layer simple composition of valve suggested this species should belong to the genus *Fallacia*. Since the high striation density and small areolae, the striae could not be resolved in LM, it needs observed with SEM for accurate identification.

Group 3

1. *Fallacia oculiformis* var. *miyajimensis* Yu H. Li var. nov.

(Plates 41–43)

Holotype: Pl. 41, Fig. 1, Slide No. 0005, Yu H. Li collection (due to be housed in The Natural History Museum, London, U.K.).

Type material: Miyajima, Hiroshima Prefecture, Japan, 4 November, 2011. Material No. LYH209.

Type locality: Miyajima (34°14′30.12″N，132°16′15.37″E), Hiroshima Prefecture, Japan.

Etymology: The name of type locality.

Description

Valves oblong to elliptic with blunt round poles, 8.6–13.9 μm long, 5.1–7.0 μm wide. Raphe straight, terminal fissures waved towards secondary side, central endings distant. Lateral areas wide, independent, projected inwards centrally. Striae uniseriate, parallel centrally, radical near poles, 29–33 in 10 μm. Finely porous conopeum above lateral sterna and striae, edge finger-shaped. Thick siliceous layer around raphe branches with pores on it.

LM observation

The valves are oblong to elliptic with blunt round poles, 8.6–13.9 μm (11.1 ± 1.4 μm，mean ± *s*) long, 5.1–7.0 μm (6.1 ± 0.5 μm) wide. The raphe is straight. The raphe central ending are distant with each other. The out lateral areas are relatively wide. The inner edge of lateral areas arched inwards. The two lateral areas are independent from each other, not connecting with the central area. The areolae between the lateral areas and raphe are not interrupted at central area, forming a longitudinal area between the two independent lateral areas. The lateral areas were relatively wider than other *Fallacia* species. The striae are parallel at the center and become radical towards the poles, 29–33 (30 ± 1.5) in 10 μm.

EM observation

The valve possesses unique margin ribs around the external valve face (Pl. 41, Figs 6–7, Pl. 42, Fig. 1). The external central endings slightly expanded and deflect to the primary side, surrounding with a relatively large and a shallow round groove (Pl. 42, Figs 1, 3). The two central endings are distant. The two internal central endings slightly curved and deflect into the primary side (Pl. 42, Figs 2, 4). The external raphe terminal fissures are waved, and curved to the secondary side (Pl. 42, Figs 1, 5). The axial area is wide. There are longitudinal uniseriate or biseriate areolae between the raphe and the lateral area (Pl. 42, Figs 2, 6). The lateral sterna are wide and connect with the central area (Pl. 42, Figs 2). The finely porous conopeum grow out from the raphe sterna with finger-liked edge which possess uniseriate small pores filling the gap between the margin ribs (Pl. 42, Figs 3, 5, Pl. 43, 1–2). In addition, the conopeum was depressed form the general external valve surface (Pl. 42, Figs 3, 5). The remarkable feature of this species is that the thicken siliceous structure between the lateral areas and the raphe above the conopeum, appearing longitudinal uniseriate pores (Pl.43, Fig. 3). The TEM micrograph shows the transapical ribs in this area (Pl.43, Figs 4, 6). The terminal fissures are flanked by two round comparative large terminal pores which also connected with the lumen between the conopeum and the primary valve layer (Pl. 42, Fig. 5, Pl. 43, 1–2). Below the two pores, there are biseriate pores (Pl. 42, Fig. 5, Pl. 43, 1–2). The areolae are occlude by hexagonal hymen (Pl. 43, Fig. 5).

Ecology and distribution

This species was collect with sandy sediment at intertidal area, near a small river mouth. It is an epipsammic speices. Currently, only found in the type locality.

Discussion

Fallacia oculiformis var. miyajimensis differs from *F. oculiformis* in the shape and width of lateral area, and higher striation density. In *F. oculiformis,* the outer edge of

lateral area convex centrally, whereas the inner edge projects to the central area. The striation density is 25–28 in 10 μm in *F. oculiformis* whereas 29–33 in 10μm.

2. *Fallacia floriane* (Møller) Witkowski 1993. *Fallacia florinae* (Moeller) comb. nov., a marine, epipsammic diatom. *Diatom Research* 8(1) p. 215; figs 1–18.

(Plates 44–45)

Synonym: *Navicula florinae* Møller 1950. The Diatoms of Praesto Fiord. (Investigations of the Geography and Natural History of the Praesto Fiord, Zealand). *Folia Geographica Danica* 3(7) p. 204; fig. 9.

Type Locality: Præstø Fjord, Demark.

Distribution: Præstø Fjord, Demark (Møller, M 1950). Puck Bay, Polankd (Witkowski 1993), Netherlands (Sabbe, Vyverman & Muylaert 1999), Portugal (Ribeiro et al. 2013). New Zealand (Harper et al. 2012). Brazil (Garcia 2003), Korea (Joh G. 2013) and Japan (Ena bay, Kanagawa Prefecture; Okinoshima, Tateyama city, Chiba Prefecture; Sanbansei, Ichikawa city, Chiba Prefecture; and Miyajima, Hiroshima city, Hiroshima Prefecture.).

LM observation

Valves are short elliptic to circle, with round poles, 7.8–13.7 μm (10.0 ± 1.5 μm, mean ± *s*) long, 4.7–7.6 μm (5.7 ± 0.8 μm) wide. The Raphe is slightly arched. The raphe central endings are distant from each other. The lateral areas are very thin and independent form each other. The two lateral areas were convex centrally and constrict at the two terminals. The axial area fused with the central area, forming an elevated H-shaped none perforated hyaline area. Because of the small size, the striae are barely resolved in LM.

EM observation

The external valve surface is convex (Pl. 45, Fig. 1), and possesses well developed and complicated siliceous structures (Pl. 45, Figs 1–3). The external raphe endings are slightly expanded and curved to the primary side. The terminal fissures are waved towards the secondary side. The raphe branches are surrounded by a siliceous layer, which grows outwards at the two terminals, along the out edge of finely porous

conopeum. This none performed layer possesses finger shaped margin, fusing with the transapical margin ribs (Pl. 45, Figs 3–4). Internally the central endings were arched with the small central noddle (Pl. 45, Fig. 2). The polar raphe endings terminate by a small helictoglossa (Pl. 45, Fig. 2), deflect to the primary side. The finely porous conopeum was only limit to the area above the lateral sterna. The layer around the two raphe branches possesses two longitudinal slits on the primary side. At the two poles, there are flower-like opening composed by 7 short radical arranged slits. Internally, there is a large round pore there (Pl.45, Figs 5–6).

Group 4

1. *Fallacia teneroides* (Hustedt) D.G. Mann in Round, Crawford & Mann 1990. *The Diatoms. Biology & Morphology of the genera*: 669.

(Plates 46–47)

Synonym: *Navicula teneroides* Hustedt 1956: Diatomeen aus dem Lago de Maracaibo in Venezuela. In: *Ergebnisse der deutschen limnologischen Venezuela-Expedition 1952 (F. Gessner & V. Vareschi). Deutscher Verlag der Wissenschaften, Berlin 1:93–140, Figs 42, 43.*

Type Locality: Lago Maracaibo, Venezuela.

Distribution: Rare, widely distribute in marine coast. Reported from Netherlands (Sabbe et al. 1999), Portugal (Ribeiro et al. 2013). Brazil (Eskinazi-Leça et al. 2010). Japan (Okinoshima, Tateyama city, Chiba Prefecture; Sanbansei, Ichikawa city, Chiba Prefecture; Shirahama, Shimoda city, Shizuoka Prefecture; and Uminokouen Park, Yokohama city, Kanagawa Prefecture.).

LM observation

Valves are naviculoid, oblong or elliptic with blunt round poles, 7.2–17.2 μm long and 3.8–5.1 μm wide. The raphe is arched. The central endings are distant or closed to each other. There are two hyaline lateral areas on both side of the raphe. The secondary lateral areas are comparatively larger and take about one third to one half size of the valve face. The first hyaline lateral are is barely resolved in LM. In contrast, it usually apears arched or elevate from the valve surface. The central area is thin bar-liked. The striae are interrupted into three longitudinal parts, such as the one around the valve margin, the longitudinal uni- or biseriate striae between the two lateral areas and longitudinal unisriate striae between raphe and the first lateral areas. And those two lines between large hyaline area and raphe were variable among specimens. The striae were parallel at center and radical at subpole area, 22–24 in 10μm.

EM observation

The valve is arched, curving down slowly from the raphe sterna (Pl. 47, Fig. 1, 3, 5). The raphe is curved. The external central endings are slightly curved to the primary side. The terminal fissures hooked to the secondary side (Pl. 46, Figs 6–7, Pl. 47, Fig. 5). Internally, the polar raphe endings terminate by a small helictoglossa (Pl. 47, Fig. 6), slightly deflect to the primary side. The central endings are straight and very close to each other (Pl. 47, Fig. 4). The comparatively larger hyaline lateral areas (the secondary lateral are) in LM, in fact they are areas without areolae, rather than depression of lateral sterna, whereas the first hyaline lateral areas are clearly depression sterna in the internal valve view (Pl. 47, Figs 3–6). The striae between the lateral sterna and the raphe are asymmetric, usually are longitudinal uni- or biseriate areolae (Pl. 47, Figs 4, 6). In addition, the areolae on the margin are elongate areolae extending to the valve mantle. Other areolae are small round areolae (Pl. 47, Figs 4, 6). The finely porous conopea grow out from raphe sterna, covering about one third to half valve surface. The edge of the conpeum is strength by several small pegs (Pl. 47, Fig. 3). The terminal edge of the conopeum does not connect with proximal edge of the non-areolae lateral area, forming a expend slits communicate with the exterior (Pl. 47, Fig. 5).

2. *Fallacia inscriptura* (Hendey) Witkowski, Lange-Bertalot & Metzeltin 2000.

Diatom Flora of Marine Coasts I. In: Lange-Bertalot, H. (ed.), Iconographia Diatomologica. Annotated Diatom Micrographs. Vol. 7. Diversity Taxonomy Identification. Koeltz Scientific Books, Königstein, Germany: 206.

(Plates 48–49)

Synonym: *Navicula inscriptura* Hendey 1977. The species diversity index of some in-shore diatom communities and its use in assessing the degree of pollution insult on parts of the north coast of Cornwall. *Beihefte zur Nova Hedwigia* 374; fig. 9.

Type Locality: North Cornwall, UK.

Distribution: Very rare, live in inter intertidal sandy sediments. Reported from North Cornwall, UK (Hendey 1977), New Zealand (Harper et al. 2012) and Japan (Okinoshima, Tateyama city, Chiba Prefecture and Nigata Prefecture).

LM observation

Valves are elliptic with round poles, 7.9–16.8 μm (11.8 ± 2.5 μm, mean ± *s*) long, 4.4–9.5 μm (5.9 ± 1.2 μm) wide. The raphe is arched. The raphe central endings are distant. The hyaline lateral areas are very thin and constrict at center and near the poles of valve. The position of lateral areas are asymmetric, on the primary side, it is at the middle of the valve width, whereas on the secondary side, it is at the one third the valve width. As the result, the length of striae between the lateral area and the raphe are correspond to the position of lateral area. The striae are parallel at the center and radical near the poles, 23–28 (25.9 ± 1.4) in 10μm.

EM observation

The external surface of valve could not be observed in this study. On the internal valve face, the thin lateral sterna are noticeable (Pl. 48, Fig. 5, Pl. 49, Fig. 1). The internal polar raphe ending form a small helictoglossa (Pl. 49, Figs 2, 4). The central raphe endings were closed and flatten to the secondary side. Around the apical margin and the

whole valve, there were several tiny pores differ from other areolae (Pl. 49, Figs 2, 4). Those areolae probably directly connect with the exterior and were not covered by porous conopuem.

3. *Fallacia pulchella* Sabbe *et* Muylaert in Sabbe, Vyverman *et* Muylaert 1999.

New and little-known *Fallacia* species (Bacillariophyta) from brackish and marine intertidal sandy sediments in Northwest Europe and North America. *Phycologia* 38(1):17; figs 46, 47, 66–68, 72, 74.

Type Locality: Sandy intertial sediments in the mouth of the Westerschelde estuary, the Netherlands.

Distribution: widely distribute in Sandy intertial sediments. Westerschelde estuary, the Netherlands, Belgian coast. and Japan (Ena bay, Kanagawa Prefecture; Okinoshima, Tateyama city, Chiba Prefecture; Sanbansei, Ichikawa city, Chiba Prefecture; and Uminokouen Park, Yokohama city, Prefecture.).

(Plate 50)

LM observation

Valve were oblong with round poles, 8.0–14.5 (11.8 ± 1.8, mean ± *s*) μm in length, 3.7–5.1 (4.6 ± 0.6) μm in width. The raphe branch ribs were invisible with LM. The terminal fissures were turn to same direction. The central ending were expand pores and closed to each other. There were two very thin hyaline lateral areas, the one near the valve margin could be observed with high focus (Pl. 50, Fig 1), whereas the one near the raphe only could be observed with deep focus (Pl. 50, Figs 2–4). The lateral sterna also could be visible with LM (Pl. 50, Fig. 5). The striae were parallel, slightly radical at the terminal area, 23–28 (25.5 ± 1.5) in 10μm.

EM observation

The valve surface was flat with a shallow mantle (Pl. 50, Fig. 1). The raphe was slightly curved, with straight central endings and strongly hooked terminal fissure. The finely porous conoepum outgrowth from the raphe sterna, covering about two third of valve face (Pl. 50, Figs 1, 3, 5). The margin of conopeum was not fused nor connect with the valve margin, but connect with vimen of primary valve layer beneath itself (Pl. 50, Fig. 4). The thin hyaline longitudinal lines were in fact the gap betweent the margin of conopeum and elevated primary valve layer margin.

***Sellaphora* species**

1. ***Sellaphora pupula* (Kützing) Mereschkowsky 1902.** On *Sellaphora*, a new genus of Diatoms. *Annals and Magazine of Natural History, series 7, 9* :187; pl. 4, figs 1–5.

(Plates 51–52)

Synonym: *Navicula pupula* Kützing 1844. Die Kieselschaligen. Bacillarien oder Diatomeen. Nordhausen. p. 93; pl. 30, fig. 40.

Type locality: Fresh water near Nordhausen, Germany.

Distribution: Cosmopolitan, distribute word widely.

Europe: Britain (Ettl & Gärtner 1995, Mann et al. 2008), Germany (Mann et al. 2004), Poland (Zelazna-Wieczorek 2011), Romania (Caraus 2002, Caraus 2012), Scotland (Evans & Mann 2009).Spain (Álvarez Cobelas & Estévez García 1982), Turkey (Ersanli & Gönülol 2006).

Asia: China (Y.L. Li 2010), Korea (Joh G. 2013), Singapore (Pham et al. 2011), Japan.

South America: Argentina (Rodriguez et al. 2006), Brazil (Eskinazi-Leça et al. 2010).

Australia and New Zealand: Queensland (Bostock & Holland 2010).

Pacific Islands: Hawaiian Islands (Sherwood 2004).

(Partly from algaebase 2014)

LM observation

The valves are narrowly elliptical with narrowly rostrate ends, 10.3–24.9 (18.9 ± 3.5, mean ± *s*) μm long, 5.0–7.0 (6.1 ± 0.6) wide (Pl. 51, Figs 1–3). The axial area is narrow and straight. The central area is a rectangular or slightly bow-tie-shaped subfascia. The central striae are of alternate long and short one. The polar bars appear perpendicular to the apical axis. The striae are radiate centrally, becaming parallel or slightly convergent near the poles. The striation density is 21–25 (22.7 ± 1.0) in 10μm.

EM observation

The external valve face is nearly plain (Pl. 52, Fig. 1). The external terminal fissures turn in the same direction (Pl. 51, Fig. 1). External central endings are straight and expanded (Pl. 51, Fig. 1, Pl. 52, Fig. 3). Internally, the raphe end with a narrow and elongate helictoglossa (Pl. 51, Fig. 2, Pl. 52, Fig. 6). Central raphe endings are expanded and deflected towards the primary side (Pl. 52, Fig. 4). The striae are uniseriate areolae, which are internal occluded hymen (Pl. 52, Figs 4, 6). The raphe sterna was elevated from the general external valve surface, whereas the adjacent areolae were slight curving down (Pl. 52, Fig. 3). One open valvocopula and a ligula of pleura are found. The valvocopula possess a line of pores on lateral sides (Pl. 52, Figs 4, 6).

2. *Sellaphora seminulum* (Grunow) D.G. Mann 1989, The Diatom genus *Sellaphora*: Separation from *Navicula*, *British Phycological Journal*, 24: 2.

(Plates 53–54)

Synonym: *Navicula seminulum* Grunow, A. 1860. Ueber neue oder ungenügend gekannte Algen. Erste Folge, Diatomeen, Familie Naviculaceen. Verhandlungen der Kaiserlich-Königlichen Zoologisch-Botanischen Gesellschaft in Wien 10:503–582, Tabs III–VII.

Distribution: Freshwater species. Cosmopolitan. Reported word widely.

Europe: Britain (Ettl & Gärtner 1995), Czech Republic and/or Slovakia (Ettl & Gärtner 1995), Germany (Ettl & Gärtner 1995), Romania (Caraus 2002), Spain (Álvarez Cobelas & Estévez García 1982).

Atlantic Islands: Iceland (Ettl & Gärtner 1995).

North America: United States of America (Patrick & Reimer 1966).

Australia and New Zealand: Victoria (Day et al. 1995).

Europe: Britain (Whitton et al. 2003), Poland (Zelazna-Wieczorek 2011), Romania (Caraus 2012).

North America: Arkansas (Smith 2010).

South America: Brazil (Eskinazi-Leça et al. 2010).

Australia and New Zealand: New Zealand (Harper et al. 2012), Queensland (Bostock & Holland 2010).

Pacific Islands: Hawaiian Islands (Sherwood 2004).

(From algaebase 2014)

LM observation

Valves are from linear, lanceolate or elliptical, 10.7–17.3 (14.2 ± 1.6, mean ± *s*) μm long, 3.2–3.9 (3.6 ± 0.2) wide (Pl. 53, Figs 1–7). . There are no polar bars. The axial area is narrow, and the central area is rectangular. Raphe straight, central raphe ending are distant. The striae are radiate centrally, becoming parallel or slightly convergent near the poles. The striation density is 20–25 (22.3 ± 1.3) in 10 μm.

EM observation

The external valve face are plain (Pl. 54, Fig. 1). The external terminal fissures turn towards the same direction (Pl. 53, Fig. 8, Pl. 54, Fig. 1). External central endings are slightly expanded and curving to the primary side (Pl. 53, Fig. 8, Pl. 54, Figs 3). Internally, the raphe ends with a small and elongate helictoglossa (Pl. 53, Fig. 9, Pl. 54, and Fig. 6). Central raphe endings are slightly deflected towards the primary side (Pl. 54, Fig. 4). The striae are uniseriate or biseriate areolae, which are internal occluded hymen (Pl. 54, Figs 4, 6).

V. THE SEXUAL REPRODUCTION AND AUXOSPORULATION OF *FALLACIA TENERA*

1. Results

Morphology of vegetative and initial cell

Vegetative cells are solitary or could form short straight chains under the artificial cultural condition, which are not found in natural populations. Valves are naviculoid to elliptical with bluntly rounded poles, 8.5–24.1 μm long and 5.4–8.6 μm wide. The raphe is straight and slightly arched near the apices. Terminal fissures curved toward the same side. Two hyaline curved narrow lateral areas went through the valve longitudinally and connected with the slightly transapical convex central area. The striae are radiate especially at subpolar areas, 17–20 in 10μm. The striae are interrupted into three longitudinal lines of areolae on half valve face. The two lines of areolae which adjacent to the raphe branch on both sides are laterally asymmetric, and areolae in the line on convex side of the raphe are smaller, fewer or even missing. In initial cells, the centre of outline and middle parts of lateral area are more convex than normal vegetative cells (Pl. 5, Fig. 1). Size diminution resulted in smaller valves becoming elliptic or even circular (Pl. 55, Figs 1–5).

Auxosporulation

Auxosporulation occurred in the rough cultures after introduction of fresh medium. The size range of vegetative cells, gametangia and initial cells was measured and illustrated in Plate 55. Two cells engaged in sexual reproduction. Usually of different sizes, were paired parallel with the girdle (Pl. 56, Fig. 1). Each gametangium formed two gametes (Pl. 56, Fig. 2, arrowheads). After a trans physiological anisogamy (Pl. 56, Fig. 3), two zygotes are formed in the frustules of the two gametangia respectively (Pl. 56, Fig. 4), and released (Pl. 56, Fig. 5). Then the two zygotes elongate into two auxospores. In young auxospores, the convex primary transverse perizonial band (Pl. 56, Fig. 6, arrow)

and two chloroplasts in each auxospore are present. Unfortunately, we did not know the exact number of chloroplasts in the zygote, since it is really hard to observe. In mature auxospores, the two chloroplasts begin to appressed to the wall of the auxospore (Pl. 56, Fig. 7, arrow). The longitudinal perizonial bands could be observed in the auxospores (Pl. 56, Fig. 7, arrowhead). Each auxospore could produce one initial cell. While the initial cell is forming in auxospore, the two chloroplasts contracted and appressed to one side of auxospore, lying one towards each pole of auxospore (Pl. 57, Figs 1–2, arrows). The newly formed theca of the initial cell (Pl. 57, Figs 1–2, arrowheads) could be seen clearly in some auxospores. After the formation of the initial cell frustule, the two chloroplasts rotate to transapical axis, elongate and appress to both sides of the frustule. At this time, the two chloroplasts still keep their identity except the hyaline connection (Pl. 57, Figs 2–5). One of the two chloroplasts appears to extend along the hyaline connection towards another one (Pl. 57, Figs 2–3). Finally, an H-shaped chloroplast is formed before the initial cell emerged from the wall of the auxospore. The initial cell break the incunabular cap and escaped via the end of the auxospore (Pl. 57, Figs 6–7). The incunabular cap (Pl. 57, Fig. 6, arrow), transverse perizonial bands (Pl. 57, Figs 6–7, arrowheads) and longitudinal perizonial bands (Pl. 57, Fig. 6, double arrows) could be observed in this moment. The mucilage capsule around the auxospore was not found in several auxosporulation. In addition, the expansion is more or less parallel to the gametangia. The frustules were not always present on a terminal of auxospore. Some could be seen near the primary perizonial transverse band (Pl. 57, Fig. 6) or two theca are at two terminal of the auxospore separately (Pl. 57, Fig. 4, left auxospore).

The ultrastructure of perizonium and incunabula

The perizonium of *F. tenera* consists of a set of transverse and longitudinal bands. The transverse bands comprise a moderately broader primary band that is about twice the width than secondary bands (Pl. 58, Figs 2, 4, arrow), and a series of narrow secondary bands on both sides of primary band, overlapping each other (Pl. 58, Figs 2, 4). The

primary band is a closed band (Pl. 58, Fig. 3, double arrows). The secondary bands are open bands. All the secondary bands have splits that formed a suture longitudinally (Pl. 58, Fig. 3, arrow).

The longitudinal bands are immediately beneath a series of transverse bands, and consists of five bands including one primary band (Pl. 58, Fig. 6, double arrows) and four semilanceolate secondary bands. Two are on one side of the primary band (Pl. 58, Fig. 5). The primary longitudinal band is bifacial and lanceolate with fimbriate margin. The secondary longitudinal bands are unifacial and possess fimbriate margin at one side (Pl. 58, Fig. 5). The distal lateral edges of secondary bands are more or less convex (Pl. 58, Fig. 5, arrowhead).

Concentric normal scales (incunabular scales) are detected on the two terminals and the surface of transverse primary band (Pl. 58, Figs 7–8).

2. Discussions

Sexual reproduction and Auxosporulation

Fallacia tenera became capable of sexual reproduction when it reached cardinal point that in this study is 15.33 μm of the apical length. It is about 63.5% of the upper boarder of initial cells size range. The average length of gametangia (mean ± s = 11.62 ± 1.84) is 53% of average length of initial cells (21.92 ± 1.19). The length of the two pairing cells (gametangia) usually is in different size, including a longer cell measured 11.39–15.33 μm (13.02 ± 0.94) and a shorter cell measured 8.84–13.59 μm (10.22 ± 1.40). Kaczmarska et al. (2013) described four types of cardinal points. In this study, the length of initial cell and upper sexual size threshold were measured. The minimum size of gametangia is also provided here. Those data measured directly from the pairing gametangia in a rough culture, not from separated monoclonal culture. Thus we could not identify those cells under 8.84μm were not paring is due to size or they were sexual incompatible.

The auxosporulation of *F. tenera* belongs to type IA1a of Geitler's classification

(Geitler 1973). It shows several features the agree with *Fallacia pygmaea*, such as two auxospores per pair of gametangia, presence of a perizonium, expansion more or less parallel to the gametangia, contraction during formation of the initial cells (Karsten 1899). The mucilage capsule around the auxospore illustrated by Karsten (1899), however, was not observed in this study. Because of lacking the mucilage, we also could not determine the presence of several single auxospores surrounded by four thecae is type II auxosporulation or caused by our preparation of a slide.

Unfortunately, the detailed process of meiosis and unequal cytokinesis could not been observed in this study, since the cells laid in the valve faces in most cases. Although a few individual cells seem like undergo unequal cytokinesis, we could not know after that it will die or produce gametes (the separation from another cell caused by the preparation of a slide). The change of chloroplasts during auxosporulation is another interesting point. In every case thus far, the chloroplast inherited from the gametes either survive and retain their identity or undergo controlled senescence and death (anonymous reviewer, pers. Comm.). Based on our observation, the two chloroplasts inherited from the gametes seems fused after the formation of initial cells forming an H-shaped chloroplast, although we could not continually focus on one pair of auxospore to observe the whole process. From Plate 57, figs 4–5, the tendency of projection and fusion of chloroplasts was present. In addition, the left initial cell in figure 5 Plate 57, shows a completely formed H-shaped chloroplast. They are all at the last stage of initial cell forming. Based on these observations it seems unlikely that one of the chloroplasts will undergo the controlled senescence and death.

Ultrastructure of incunabula and perizonium

All of the auxospore envelop and wall components were review in recent proposal for terminology of sexual reproduction and auxospore and resting spore by Kaczmarska et al. (2013). In this study, only scales (incunabular scales) and perizonial bands including a set of longitudinal bands and transverse bands were detected. In the proposal from

kaczmarska et al. (2013), five types of scales were mainly introduced, namely simple scales, distorted scales, slit scales, dendroid scales and spinescent scales. In recent study, two types of scales, the simple scales and the distorted scales, were reported in *Diploneis papula* (Idei et al. 2013). For *F. tenera* only the simple scales were found. Similar scales also were reported in *Sellaphora marvanii* (Mann et al. 2011), *Nitzschia inconspicua* Grunow (Mann et al. 2013) and *Caloneis linearis* (Ishii et al. 2012).

In pennate diatoms, incunabular scales have been reported in araphid diatoms, *Rhabdonema* (Stosch 1982); *Gephyria media* (Sato et al. 2004); *Grammatophora marina* (Sato et al. 2008b); *Pseudostriatella oceanica* (Sato et al. 2008c) and *Tabularia parva* (Sato et al. 2008a), and in the biraphid diatom, *S. marvanii*, *D. papula*, *C. linearis* and *F. tenera* (this study). In monoraphid diatoms *Achnanthes crenulata* (Toyoda et al. 2006) and *Achnanthes yaquinensis* (Toyoda et al. 2005), however, scales were not present. Also, the transverse perizonial bands were not present in the two monoraphid species. Toyoda et al. (2005) suggested they were lost during the evolution from biraphid to monoraphid diatoms. Since those siliceous scales also were present in centric diatoms, which were believed to be the ancestor of pennate diatoms, those isodiametric scales may be the primitive form of incunabula. *Navicula cryptocephala* Kütz. (Poulíčková and Mann 2006) bear “organic caps” instead of caps consists of isodiametric scales. Although it has similar perizonium with *S. marvanii* and *F. tenera* which was formerly belonged to *Navicula*, they seem to belong to different lineages.

The set of transverse perizonial bands that are comprised of an open primary band and seven to nine bands on both sides of the primary transverse band. The primary transverse band is nearly two times wider than the secondary transverse band, whereas the primary band in *Rhoicosphenia curvata* (Mann 1982) and *Neidium* cf. *ampliatum* (Mann 2009) are less than twice wider. In contrast, *S. marvanii* has primary band much wider than in *F. tenera* shared with *Caloneis silicula* (Mann 1989) and *Navicula cryptocephala* (Poulíčková and Mann 2006), *Pinnularia* cf. *gibba* (Poulíčková *et al.* 2007) has the widest primary band than above. In addition, the prominent suture between

primary and secondary band found in *S. marvanii* was also not detected in *F. tenera*.

The longitudinal bands are composed of five bands. A similar arrangement has been reported from *Rh. curvata*, *D. papula* and *N. inconspicua*. The longitudinal bands in *D. papula* have a primary band in the middle flanked on each side by two unifacial bands of different structure (Idei et al. 2013). The two bands are the secondary and tertiary longitudinal bands. Their shaped highly differ from *F. tenera*. The shape of complete longitudinal perizonium contracts in the middle, which correspond with the outline of the initial cells. Similarly, the outline of complete longitudinal perizonium convexing in the centre also corresponds with the outline of the initial cells of *F. tenera*. Moreover, just like the lateral symmetric vegetative cells the longitudinal perizonal bands also arranged lateral symmetricly in *D. papula* and *F. tenera*. In contrast, the longtitudinal perizonal bands in *N. inconspicua* are not laterally symmetric like its vegetative cells. It suggests the longitudinal perizonium closely related to or even determine the shape of initial cells.

VI. CLUSTERING ANALYSIS OF MORPHOLOGICAL CHARACTERISTICS

The fifteen *Fallacia* species were grouping using morphological clustering analysis. Based on the morphology of those species in Section IV, 15 morphological features were chosen and codes according to different types for clustering analysis. Those features are present below:

1) Shape of apices: 0-lanceolate; 1- blunt board.
2) Terminal fissure of raphe: 0-hooked; 1-waved.
3) Shape of sterna: 0-central constrict; 1-almost parallel slightly constrict in center; 2-convex.
4) Longitudinal lines of areolae between raphe and sterna: 0-single; 1-multiple lines.
5) Axial area: 0-wide; 1-narrow.
6) Terminal holes on both sides of raphe: 0- absent; 1-small holes; 2-holes; 3-slit; 4-open.
7) Location of conopeum uncovered areolae: 0- terminal; 1-around valve face; 2-with siliceous layer not conopeum; 3- on the valve face.
8) Peg: 0-absent; 1-present.
9) Finger shaped edge of conopeum: 0-absent; 1-present.
10) Structure on axial area: 0-absent; 1-holes; 2-slit opening.
11) External central raphe endings: 0-normal; 1- distant.
12) Shape of chloroplast: 0-H-shaped chloroplast consisted of two ribs; 1- Basically H-shaped chloroplast consisted of two plates; 2- Basically H-shaped chloroplast consisted of two triangular pieces connected centrally; ?-unobserved.
13) Shape of external central raphe endings: 0-straight: 1-expaned, water-drop liked.
14) Siliceous block between external central endings: 0-absent; 1-present.
15) Internal central area: 0-flat; 1-arched.

The morphological features matrix is present on table 1. The dendrogram of result shows in Plate 55.

From the result of clustering analysis derived from morphological features, the fifteen *Fallacia* species in this study could be divided into four groups. The group1 including *F. fracta, F. tenera, F. gemmifera, F. litoricola* and *F. hodgeana* possess a combination of features such as 1. a single longitudinal line of areolae between raphe and lateral area; 2. narrow axial area. 3. two longitudinal sterna slightly constrict in the center; and 4. internal terminal pore locate on the two terminal. Group 2 including *F.* cf. *forcipata*, *F. tateyamensis*, *F. nodulifera*, *F. decussate* and *F. laevis.* Those species possess a combination of features such as 1. typical lyre-shaped sterna; 2. multiple lines of areolae or wide space between raphe and sterna; 3. areolae uncovered by conopeum only present at two terminals. Group 3 including *F. oculiformis* var. *miyajimensis* and *F. florinae* possess the features: 1. convex lateral area; 2. wide axial area; 3. terminal opening are holes; and 4. presenting dedicated surface structure. And Group 4. includes *F. teneroides*, *F. inscriptura* and one new species. They possess features such as 1. multiple longitudinal lines between lateral area and 2. slightly convex lateral area etc.

VII. MOLECULAR PHYLOGENETIC ANALYSIS

This study determined the *rbc*L sequences of 6 cultured *Fallacia* species in this study, namely *Fallacia tateyamensis, F. fracta, F. litoricola, F. laevis, F. tenera* and *F. hodgeana,* with 28 taxa from Genbank including three *Fallacia species* (there only three *Fallacia* species have *rbc*L gene sequence), such as *Fallacia pygmaea, F. cf. forcipata* and *F. monoculata*. The informations of those 28 taxa are list in Table 3. Most of those species are in the genus *Pinnularia, Sellaphora, Fallacia* and *Mayamea,* which have been suggest to in a large clade (Sato et al. 2013, Bruder 2006). The *Amphora montana* was chosen to be outgroup.

The *Fallacia* taxa are form a monophyletic clade with slightly slightly weak bootstrap support (BS) = 72. The sister group is *Rossia*. The monophyletic group comprises three robustly supported clades, such as Clade 1 comprising *F. tenera, F. fracta, F. litoricola* and *F. hodgeana* with a high bootstrap support (BS = 95); Clade 2 including *F.* cf. *focipata* and *F. laevis*, also with a high bootstrap support (BS = 98); Clade 3 including *F. tateyamensis* and *F. monoculata* with the bootstrap valve are 86. The *F. pygmaea* was not group with any species. Thus, it form a monophyletic group.

Compare with the groups derived from morphological features in section VII, the clade 1 is correspond to the morphological groups 1, which includes five species, such as *F. fracta, F. tenera, F. gemmifera, F. litoricola* and *F. hodgeana.* Thus, those species have been well proved to be a groups both from morphological and molecular data. However, other monophyletic groups were a little misleading, although the robustly supported clade do share a number of morphological traits. The *F. tateyamensis* and *F. monoculata* in clade 4 both possess a single longitudinal line of areolae between the raphe and lateral area. In contrast, the *F. laevis and F.*cf. *forcipata* both have multiple longitudinal lines of areolae in the same position. In addition, the freshwater species *F. pygmaea* and *F. monoculata* also did not merge with other marine species with over 90 bootstrap.

VIII. GENERAL DISCUSSION

1. Morphology

Fallacia species do share a number of morphological features such as basic H-shaped chloroplast, two longitudinal lateral sterna, valves formed by two layers (a primary valve layer and a conopeum) and canal system beneath the finely porous conopeum etc. The morphological features and their variations among species are discussed as follow:

Chloroplast

A basic H-shaped chloroplast varies greatly. It could consisted of two plates or lobs connected by an isthmus or a connecting point. The isthmus is a wide band. In a number of species possess an elongate rib projected from the isthmus.

Lateral sterna

Possessing lateral sterna may be the most important feature of *Fallacia* species with LM. Species transferred from *Navicula* sect. *Lyratae* possess noticeable lateral areas. Whereas the lateral area in small species placed in *Navicula* sect. *Bacillares* are very difficult to find with LM. The lateral hyaline areas with LM, usually correspond to lateral sterna in *Fallacia* species. In many cases, however, the hyaline lateral areas are also flat area of valve without perforation. Thus it is necessary to observe those small species with lateral hyaline areas using EM to ensure that those species are *Fallacia* species. Furthermore, its shape is mainly of two forms, such as typical Lyre-shaped, and longitudinal nearly straight. The shape and position of lateral areas also correspond to the pattern of primary valve layer, particular the arrangement of areolae. As a result, this feature is very important for identifying species.

The structure of valve and its variation

As mentioned in the terminology section, the valve of *Fallacia* species was composed by two layers, a primary valve layer and secondary valve layer consisted of the

conopeum and many structures associate with the conopeum formed after the primary valve layer. The pattern of the lumen (canal system) between the two layers is also an important features of this genus. *Pseudofallacia* species do not possess the transapical canals. *Diploneis* species has more complicate lumen that does not connect with the exterior via the terminal openings as in *Fallacia*. Movever, Species in Group 1(Clade 1) possess larger terminal openings and more areolae not covered by conopeum. It makes the lumen and cytoplasm connect with the exterior more easily. Most species in this group are epipelic. Whereas the species in other groups are epipsammic and possess smaller terminal openings and fewer areolae uncovered by conopeum. Taylor (2010) suggested that the conopeum could help diatom to keep the water or reduce evaporation. It probably could explain those epipelic species with movability in group 1 possess less area of valve surface covered by conopeum, whereas the surface of those epipsammic species with limit movability possess more area of valve surface covered by conopeum. Because the epipelic species could move up and down rapidly according to the rhythm of tide. In contrast, those epipsammic species with limit movability have to enhance the ability of prevent dehydration.

Outline of valves

Stickle & Mann in Round (1990) gave the description "Valves naviculoid, linear lanceolate to elliptical usually with bluntly round poles." Based on my observations, the epipelic species usually possess the naviculoid or linear lanceolate cell shape, such as *F. litoricola, F. hodgeana, F. gemmifera* and *F. tenera*. In contrast, the epipsammic species usually possess elliptical valve. The naviculoid shape could reduce the water resistance, enhance the movability of epipelic species. Whereas the elliptical shape could expand the attached surface, enhance the adhesion force.

Symmetric of valves

Pennate diatoms were not symmetric by the apical axial (Round et al. 1990). In the genus *Fallacia*, this asymmetric of valve is even more significant. The asymmetric line of

areolae between raphe and lateral area may be the most problematic feature, particular those species only have one longitudinal line of areolae there. In some cases, the areolae on one side will be missing, even in monoclonal culture. Thus this feature could not be used for distinguish species.

External siliceous layer

The slits on axial area in *F. florinae,* the block between two external central raphe endings in *F. tateyamensis* and the pores on the axial area in *F. oculiformis* var. *miyajimensis* are stable morphological characteristics. Species from different locations all possess those features could be used for identification.

The result of molecular phylogenetic analysis is not totally corresponding to the result of morphological clustering analysis. However, the Group 1 was well support by both of them, and also proved by habits. Thus based on both results, the morphological features are important for taxonomy in this genus were list the following:

a. shape, size and arrangement of lateral sterna.
b. outline of the valve face.
c. striae arrangement and striation density.
d. shape of terminal fissures and central endings.
e. shape and size of conopeum.
f. pegs, axial slits and central block.

2. Ecology and distribution

All the fifteen *Fallacia* species, except *Fallacia laevis,* were collected from intertidal area. Species in Group 1 and *Fallacia* cf. *foricpata* are epipelic species. *Fallacia fracta* was collected from sandy sediments. *Fallacia tenera*, *Fallacia litoricola* and *F*. cf. *forcipata* could be collected from sandy sediment and mudflat of river mouth. *Fallacia gemmifera* and *Fallacia hodgeana* only have been isolated from mudflat of river mouth. Other species were collected from intertidal sandy beach, and were epipsammic species. *Fallacia litoricola* and *Fallacia tenera* are cosmopolitan species and widely distribute in

intertidal area.

3. Taxonomy and phylogeny

Since the earlier diatom research, diatomists wish to establish the taxonomic system and reconstructing the evolutionary history of diatoms. The relatively complete taxonomic system and evolutionary hypotheses have not been proposed until the 1980. As the result of new ultrastructure information of small diatom, a number of genera have been resurrected or erected such as *Sellaphora*, *Diadesmis*, *Chamaepinnularia*, *Microcostatus*, *Mayamaea*, *Pseudofallacia* and *Eolimna*. The genus *Fallacia* is also the same. Stickle and Mann used H-shaped chloroplast, longitudinal sterna and finely porous conopeum to delimit this genus. In this study, more common ultrastructures have been found within the genus (mentioned in front sections), particular the canal system beneath the conopuem. Other genera also possess canals, such as *Diploneis*, *Scoliotropis*, *Biremis*, *Muelleria* and *Neidium*. However, the canals in most of them are closed by valve layer, whereas in *Fallacia* species the canal system could connected with the exterior via terminal pores. *Muelleria* also possesses those terminal pores. However, the variations of conopeum differs them. Thus from the current morphological observations, the genus *Fallacia* forms a monophyletic taxon. In the result of preliminary phylogenetic analysis, the *Fallacia* species also forms one clade, although without high bootstrap support.

In this study, the fifteen *Fallacia* species could be divided into four morphological groups. The group1 includes *F. litoricola* liked epipelic species. The group2 includes *F. forcipata* liked epipelic and epipsammic species. The group 3 includes relatively small and rare epipsammic species. The group 4 includes *F. florinae* liked epipsammic speices. The group 1 and 2 have been well supported by morphological features, molecular phylogenetic analysis, and inhabit environments. However, because of the difficulty of isolation, there is no sequence data to analysis molecular phylogenetic relationship of the group 3 and 4.

According to the taxonomic system of Round et al. (1990) the Sellaphoraceae

includes four genera, namely *Sellaphora*, *Fallacia*, *Rossia* and *Caponea*. Liu et al. (2012) also placed the genus *Pseudofallacia* in Sellaphoraceae. The morphological differences between *Pseudofallacia* and *Fallacia* have been discussed. *Rossia* resembles *Fallacia* in possession of lateral sterna and porous conopeum. It differs from *Fallacia* in "extra nodules" of raphe (Voigt 1959). Currently, *Rossia* species have been reported in typical location. Sabbe (1999) also found a broken valve in the material from Beaufort (USA). The ultrastructures of *Rossia* species have not been studied. From the result of molecular phylogenetic analysis, the *Rossia* branch cannot been divided from *Fallacia* with high Bootstrap support. In addition, the peculiar "extra nodule" structure associated with raphe is very rare in diatom. Interestingly, similar nodule structure could be found in long time culturing deformed individuals of *Fallacia* species in this study. Thus, it is need to study the morphology of *Rossia* in detail to review the relationship of the two genera. *Sellaphora* resembles *Fallacia* in possessing on basic H-shaped chloroplast. In term of the valve structure, it seems not easy to connect those two genera. *Sellaphora* species possess none perforated conopeum limited to axial area rather than fine porous conopeum fully or partly covering the whole primary valve layer. A number of *Sellaphora* species even possess biserate striae rather than uniserate striae in *Fallacia*. However, the longitudinal lateral depressions (canals) appear some similarity between those two genera. Many *Sellaphora* species particular the "americana" group possesses a relatively wide longitudinal lateral depressions (canals) covered by conopeum at axial area. Other groups such "laevissima", "pupula" and "bacillum" also possess this feature, although not wide as the "americana" group species. Similarly, *Pseudofallacia* species also possess longitudinal lateral canals adjacent to the raphe. In addition, the *Fallacia* species live in marine, to freshwater. The genus *Pseudofallacia* is a freshwater diatom genus. The genus *Sellaphora* is in freshwater and extending to brackish. Furthermore, Taylor et al.(2010) suggested the conopeum (the canal system beneath) could prevent the desiccation when diatoms encounter dry environment. Thus the marine and brachish *Fallacia* speices, particular those live in intertidal area, possess developed conopeum and canal system to

prevent desiccation. In contrast, in freshwater water environment, this morphological feature became unnecessary, and reduced the canal area and space between conopeum and primary valve layer like in *Pseudofallacia* and *Sellaphora americana* group etc. Finely it perhaps will be lost during evolution, only lest a wider raphe sterna and the single primary valve layer, perhaps *Mayameae*, *Eolimna.* On the contrary, those species facing long time dry condition have to enhance the capability of conoepum and canal system to get water in short period of time and keep them for a comparative long time. The genus *Microcostatus* may be this case.

The hyaline lateral areas in LM are not all the depressed lateral canals (sterna) on the primary valve layer in SEM. It could be relatively wide vimen (in *Fallacia tenera*, *Fallacia hodgeana* and *Fallacia gemmifera*) or area without perforation (in *Fallacia teneroides*). Sabbe et al. (1999) reported a number of *Fallacia* species possessing longitudinal ribs instead of lateral depressed lateral canals (sterna), including *F. tenera*, which in this study clear possessing the lateral depressed lateral canals (sterna). Thus it is necessary to study those species to figure out the ultrastructure of those hyaline lateral areas, since this is the key delimitation of the genus *Fallacia*.

In this study, fifteen *Fallacia* species and two *Sellaphora* species were observed in detail, including five new species and one new combination. The ultrastructures of most species are the first time to be reported. It is also the first time to report the complete sexual reproduction, auxosporulation and structure of auxospore in the genus *Fallacia*. This study also offered six new molecular sequences data of *Fallaica* and is the also the first time to interpret the phylogenetic relationship of the genus *Fallacia* using molecular data. In future study, the morphology of other *Fallacia* species needs to be study in detail. The molecular phylogenetic relationship should be analyzed using multi-molecular markers and with larger dataset.

ACKNOWLEDGEMENTS

I wish to express my sincere thanks to Professor Jiro Tanaka (Tokyo University of Marine Science & Technology), Associate Professor Hidekazu Suzuki (Tokyo University of Marine Science & Technology) and Professor Tamotsu Nagumo (Nippon Dental University), for their valuable advices and encouragements. I also wish to thanks Associate Professor Kotara Tsuchiya (Tokyo University of Marine Science & Technology) for reviewing the present study.

I would like to express my thanks to Professor Jiahai Ma (Shanghai Ocean University), for supporting and suggestion for my study. Associate Research Fellow Zhongmin Sun (Institute of Oceanology, Chinese Academy of Sciences), for his help and suggestions with molecular phylogenetic analysis. I am grateful to Dr. Matsuoka and Dr. Mitsuhashi (Nippon Dental University) for their help for using SEM and TEM. I am also wish to thanks Dr. Shinya Sato and Dr. Oriha Ishii for valuable advices and suggestions for this research.

I owe special thanks to Dr. Monika Zofia Graczyk-Raczynska, Mr. Hiroshi Suzuki, Ms. Yurika Mikame, Mr. Youichi Maeda, Ms. Marikko Sakai, Mr. Nozomi yoshida and other student members of the phycological Laboratory in Tokyo University of Marine Science and Technology, for great encouragement and supporting my work in collecting samples.

Finally, I wish to express great thanks to my family and Ms. Nan Si for supporting and encouraging my study and research, during the three and half years in Japan.

REFERENCES

ABOAL, M., PUIG, M.A. & SOLER, G. 1996. Diatom assemblages in some Mediterranean temporary streams in southeastern Spain. *Arch. Hydrobiol.* 136: 509–527.

ÁLVAREZ COBELAS, M. & ESTÉVEZ GARCÍA, A. 1982. *Catálogo de las algas continentales españolas. I. Diatomophyceae Rabenhorst 1864.* Lazaroa 4: 269–285.

ALVERSON, A.J., JANSEN, R.K. & THERIOT, E.C. 2007. Bridging the Rubicon: Phylogenetic analysis reveals repeated colonizations of marine and fresh waters by thalassiosiroid diatoms. *Molecular Phylogenetics and Evolution* 45: 193–210.

BOSTOCK, P.D. & HOLLAND, A.E. 2010. *Census of the Queensland Flora*. pp. 1–320. Brisbane: Queensland Herbarium Biodiversity and Ecosystem Sciences, Department of Environment and Resource Management.

BRUDER, K. 2006. Taxonomic revision of diatoms belonging to the family Naviculaceae based on morphological and molecular data. Universität Bremen.

CAMPEAU, S., PIENITZ, R. & HÉQUETTE, A. 1999. *Diatoms from the Beaufort Sea coast, southern Arctic Ocean (Canada): modern analogues for reconstructing Late Quaternary environments and relative sea levels*: J. Cramer.

CARAUS, I. 2002. The algae of Romania. *Studii si Cercetari, Universitatea Bacau, Biologie* 7: 1–694.

CHEN C. P., GAO Y.H., LIN P. 2005. Four newly recorded species of Bacillariophyta from the mangroves in China. *Acta Phytotaxonomica Sinica* 44: 95–99.

CLEVE, P.T. 1894. *Synopsis of the naviculoid diatoms.* PA Norstedt & söner.

DAY, S.A., WICKHAM, R.P., ENTWISLE, T.J. & TYLER, P.A. 1995. Bibliographic check-list of non-marine algae in Australia. *Flora of Australia Supplementary Series* 4: i–vii, 1–276.

ESKINAZI-LEÇA, E., GONÇALVES DA SILVA CUNHA, M. DA G., SANTIAGO, M.F., PALMEIRA BORGES, G.C., CABRAL DE LIMA, J.M., DA SILVA, M.H., DE PAULA LIMA, J. & MENEZES, M. 2010. *Bacillariophyceae. In*: Catálogo de plantas e fungos do Brasil.

Vol. 1. (Forzza, R.C. Eds), pp. 262–309. Rio de Janeiro: Andrea Jakobsson Estúdio; Instituto de Pesquisas Jardim Botânico do Rio de Janeiro.

ETTL, H. & GÄRTNER, G. 1995. *Syllabus der Boden-, Luft- und Flechtenalgen*. pp. i–vii, 1–721. Stuttgart: Gustav Fischer.

FOGED N. 1976. Freshwater diatoms in Sri Lanka (Ceylon). *Bibliotheca Phycologica* 23: 1–112.

FUJITA, Y. & OHTSUKA, T. 2005. Diatoms from paddy fields in northern Laos. *Diatom* 21: 71–89.

GARCIA, M. 2003. Observations on the diatom genus *Fallacia* (Bacillariophyta) from southern Brazilian sandy beaches. *Nova hedwigia* 77: 3–4.

GEITLER, L. 1973. Auxosporenbildung und Systematik bei pennaten Diatomeen und die Cytologie vonCocconeis-Sippen. *Österreichische botanische Zeitschrift* 122: 299–321.

GIL–RODRÍGUEZ, M.C., HAROUN, R., OJEDA RODRÍGUEZ, A., BERECIBAR ZUGASTI, E., DOMÍNGUEZ SANTANA, P. & HERRERA MORÁN, B. 2003. *Proctoctista. In*: Lista de especies marinas de Canarias (algas, hongos, plantas y animales). (Moro, L., Martín, J.L., Garrido, M.J. & Izquierdo, I. Eds), pp. 5–30. Las Palmas: Consejería de Política Territorial y Medio Ambiente del Gobierno de Canarias.

HENDEY, N.I. 1974. The species diversity index of some in-shore diatom communities and its use in assessing the degree of pollution insult on parts of the north coast of Cornwall. *Beihefte zur Nova Hedwigia* 54: 355–378.

HARPER, M.A., CASSIE COOPER, V., CHANG, F.H., NELSON, W.A. & BROADY, P.A. 2012. *Phylum Ochrophyta: brown and golden-brown algae, diatoms, silicioflagellates, and kin. In*: New Zealand inventory of biodiversity. Volume Three. Kingdoms Bacteria, Protozoa, Chromista, Plantae, Fungi. (Gordon, D.P. Eds), pp. 114–163. Christchurch: Canterbury University Press.

HUSTEDT, F. 1927–1966. Die Kieselalgen Deutschlands, Österreichs und der Schweiz. *Dr. L. Rabenhorst's Kryptogamen-Flora von Deutschland, Österreich und der*

Schweiz. Akademische Verlagsgesellschaft, Leipzig.

HUSTEDT, F. 1955. Marine littoral diatoms of Beaufort, North Carolina. *Bulletin Duke University Marine Station* 6: 1–67.

IDEI, M., SATO, S., WATANABE, T., NAGUMO, T. & MANN, D.G. 2013. Sexual reproduction and auxospore structure in *Diploneis papula* (Bacillariophyta). *Phycologia* 52: 295–308.

ISHII, O., IDEI, M., SUZUKI, H., NAGUMO, T. & TANAKA, J. 2012. Sexual reproduction and fine structure of auxospore in *Caloneis linearis* (Bacillariophyceae). *Journal of Japanese Botany* 87: 96–107.

JOH, G. 2013. Species diversity of the old genus *Navicula* Bory (Bacillariophyta) on intertidal san-flats in the Nakdong River estuary, Korea. *Journal of ecology and environment* 36: 371–390.

KACZMARSKA, I., POULÍČKOVÁ, A., SATO, S., EDLUND, M.B., IDEI, M., WATANABE, T. & MANN, D.G. 2013. Proposals for a terminology for diatom sexual reproduction, auxospores and resting stages. *Diatom Research* 28: 1–32.

KARSTEN, G. 1899. Die Diatomeen der Kieler Bucht. *Wissenschaftliche Meeresuntersuchungen, herausgegeben von der Kommission zur Untersuchung der deutschen Meere in Kiel und der Biologischen AnstaU auf Helgoland. AUg. Kiel. Neue Folge, B* 4.

KRAMMER, K. & LANGE-BERTALOT, H. 1986. *Bacillariophyceae 1. Teil: Naviculaceae, in* Süsswasserflora von Mittleuropa Band 2/1, Gustav Fischer Verlag, Stuttgart.

LARKIN, M., BLACKSHIELDS, G., BROWN, N., CHENNA, R., MCGETTIGAN, P.A., MCWILLIAM, H., VALENTIN, F., WALLACE, I.M., WILM, A. & LOPEZ, R. 2007. Clustal W and Clustal X version 2.0. *Bioinformatics* 23: 2947–2948.

LI Y. 2006. Ecological characteristics and taxonomic studies on nano-diatoms in coastal water of China. Doctor Dissertation. Xiamen University.

LIU, Y., KOCIOLEK, J.P., FAN, Y. & WANG, Q. 2012. *Pseudofallacia* gen. nov., a new freshwater diatom (Bacillariophyceae) genus based on *Navicula occulta* Krasske.

Phycologia 51: 620–626.

MANN, D.G. 1989. On auxospore formation in *Caloneis* and the nature of *Amphiraphia* (Bacillariophyta). *Plant Systematics and Evolution* 163: 43–52.

MANN, D.G. 1982. Structure, life history and systematics of *Rhoicosphenia* (Bacillariophyta). II. Auxospore formation and perizonium structure of *Rh. curvata*. *Journal of Phycology* 18: 264–274.

MANN, D.G., THOMAS, S.J. & EVANS, K.M. 2008. Revision of the diatom genus *Sellaphora*: a first account of the larger species in the British Isles. *Fottea* 8: 15–78.

MANN, D.G., POULÍČKOVÁ, A., SATO, S. & EVANS, K.M. 2011. Scaly incunabula, auxospore development, and girdle polymorphism in *Sellaphora Marvanii* sp. nov. (Bacillariophyceae). *Journal of Phycology* 47: 1368–1378.

MANN, D.G., SATO, S., ROVIRA, L. & TROBAJO, R. 2013. Paedogamy and auxosporulation in *Nitzschia* sect. *Lanceolatae* (Bacillariophyta). *Phycologia* 52: 204–220.

MANN, D.G. POULÍČKOVÁ, A. 2009. Incunabula and perizonium of *Neidium* (Bacillariophyta). *Fottea* 9: 211–222.

MEDLIN, L.K. & KACZMARSKA, I. 2004. Evolution of the diatoms: V. Morphological and cytological support for the major clades and a taxonomic revision. *Phycologia* 43: 245–270.

NAGUMO, T. & KOBAYASI, H. 1990. The bleaching method for gently loosening and cleaning a single duatom frustule. *Diatoms* 5: 45–50.

NELSON, D.M., TRÉGUER, P., BRZEZINSKI, M.A., LEYNAERT, A. & QUÉGUINER, B. 1995. Production and dissolution of biogenic silica in the ocean: Revised global estimates, comparison with regional data and relationship to biogenic sedimentation. *Global Biogeochemical Cycles* 9: 359–372.

MØLLER, M. 1950. The Diatoms of Praesto Fiord. (Investigations of the Geography and Natural History of the Praesto Fiord, Zealand). *Folia Geographica Danica* 3: 187–237.

PATRICK, R.M. & FREESE, L.R. 1961. Diatoms (Bacillariophyceae) from Northern Alaska. *Proceedings of the Academy of Natural Sciences of Philadelphia* 112: 129–293.

PATRICK, R.M. & REIMER, C.W. 1966. *The diatoms of the United States, exclusive of Alaska and Hawaii.* Philadelphia.

POSADA, D. & CRANDALL, K.A. 1998. MODELTEST: testing the model of DNA substitution. *Bioinformatics* 14: 817–818.

POSADA, D. & BUCKLEY, T.R. 2004. Model Selection and Model Averaging in Phylogenetics: Advantages of Akaike Information Criterion and Bayesian Approaches Over Likelihood Ratio Tests. *Systematic Biology* 53: 793–808.

POULÍČKOVÁ, A. & MANN, D.G. 2006. Sexual reproduction in *Navicula cryptocephala* (Bacillariophyceae). *Journal of Phycology* 42: 872–886.

POULÍČKOVÁ, A., MAYAMA, S., CHEPURNOV, V.A. & MANN, D.G. 2007. Heterothallic auxosporulation, incunabula and perizonium in *Pinnularia* (Bacillariophyceae). *European Journal of Phycology* 42: 367–390.

RIBEIRO, L., BROTAS, V., BROTAS, V., RINCÉ,Y. & JESUS, B. 2013. Structure and diversity of intertidal benthic diatom assemblages in contrasting shores: a case study from the Tagus estuary. *Journal of Phycology* 49: 258–270.

RONQUIST, F. & HUELSENBECK, J.P. 2003. MrBayes 3: Bayesian phylogenetic inference under mixed models. *Bioinformatics* 19: 1572–1574.

ROSS, R., COX, E.J., KARAYEVA, N.I., MANN, D.G., PADDOCK, T.B.B, SIMONSEN, R. & SIMS, P.A. . 1979. An amended terminology for the siliceous components of the diatom cell. *Nova Hedwigia Beiheft* 64: 513–533.

ROUND, F.E. 1953. An investigation of two benthic algal communities in Malham Tarn, Yorkshire. *The Journal of Ecology* 41: 174–197.

ROUND, F.E., CRAWFORD, R.M. & MANN, D.G. 1990. *Diatoms: biology and morphology of the genera.* Cambridge University Press.

RUCK, E.C. & THERIOT, E.C. 2011. Origin and Evolution of the Canal Raphe System in Diatoms. *Protist* 162: 723–737.

SABBE, K., VYVERMAN, W. & MUYLAERT, K. 1999. New and little-known *Fallacia* species (Bacillariophyta) from brackish and marine intertidal sandy sediments in Northwest Europe and North America. *Phycologia* 38: 8–22.

SATO, S., NAGUMO, T. & TANAKA, J. 2004. Auxospore formation and the morphology of the initial cell of the marine araphid diaotm *Gephyria media* (Bacillariophyceae). *Journal of Phycology* 40: 684–691.

SATO, S., KURIYAMA, K., TADANO, T. & MEDLIN, L.K. 2008a. Auxospore fine structure in a marine araphid diatom *Tabularia parva*. *Diatom Research* 23: 423–433.

SATO, S., MANN, D.G., NAGUMO, T., TANAKA, J., TADANO, T. & MEDLIN, L.K. 2008b. Auxospore Fine Structure and Variation in Modes of Cell Size Changes in *Grammatophora marina* (Bacillariophyta). *Phycologia* 47: 12–27.

SATO, S., MANN, D.G., MATSUMOTO, S. & MEDLIN, L.K. 2008c. *Pseudostriatella* (Bacillariophyta): a description of a new araphid diatom genus based on observations of frustule and auxospore structure and 18S rDNA phylogeny. *Phycologia* 47: 371–391.

SATO, S., TAMOTSU, N. & MANN, D.G. 2013. Morphology and life history of *Amphora commutata* (Bacillariophyta) I: the vegetative cell and phylogenetic position. *Phycologia* 52: 225–238.

SAWAI, Y., NAGUMO, T. & TOYODA, K. 2005. Three extant species of *Paralia* (Bacillariophyceae) along the coast of Japan. *Phycologia* 44: 517–529.

SCHOEMAN, F.R. & ARCHIBALD, R.E.M. 1976–1980. *The diatom flora of southern Africa* Nos. 1–6. CSIR Special Report WAT 50.

SIMONSEN, R. 1960. Neue Diatomeen aus der Ostsee. II. *Kieler Meeresforschungen* 16: 126–160.

SIMS, P.A. & PADDOCK, T.B.B. 1979. Observations and comments on some prominent morphological features of naviculoid genera. *Nova Hedwigia, Beiheft* 64: 169–175.

Sherwood, A.R. 2004. Bibliographic checklist of the nonmarine algae of the Hawaiian

Islands. *Records of the Hawaii Biological Survey for 2003*. Bishop Museum Occasional Papers 80: 1–26.

SMITH, T.E. 2010. Revised list of algae from Arkansas, U.S.A. and new additions. *International Journal on Algae* 12: 230–256.

SMOL, J.P. & STOERMER, E.F. 2010. *The Diatoms: Applications for the Environmental and Earth Sciences.* Cambridge University Press.

STOSCH, H.A. 1982. On auxospore envelopes in diatoms. *Bacillaria* 5: 127–156.

TAKANO, H. 1990. Semiconical covers in valves of *Navicula teneroides* Hustedt. *Diatom* 5: 5–7.

TAYLOR, J.C., LEVANETS, A., BLANCO, S. & ECTOR, L. 2010. *Microcostatus schoemanii* sp. nov., *M. cholnokyi* sp. nov. and *M. angloensis* sp. nov. three new terrestrial diatoms (Bacillariophyceae) from South Africa. *Phycological Research* 58: 177–187.

THERIOT, E.C., CANNONE, J.J., GUTELL, R.R. & ALVERSON, A.J. 2009. The limits of nuclear-encoded SSU rDNA for resolving the diatom phylogeny. *European Journal of Phycology* 44: 277–290.

TOYODA, K., IDEI, M., NAGUMO, T. & TANAKA, J. 2005. Fine-structure of the vegetative frustule, perizonium and initial valve of *Achnanthes yaquinensis* (Bacillariophyta). *European Journal of Phycology* 40: 269–279.

TOYODA, K., WILLIAMS, D.M., TANAKA, J. & NAGUMO, T. 2006. Morphological investigations of the frustule, perizonium and initial valves of the freshwater diatom *Achnanthes crenulata* Grunow (Bacillariophyceae). *Phycological Research* 54: 173–182.

VAN HEURCK, H. 1884. *Synopsis des diatomées de Belgique.* L'auteur.

VOIGT, M. 1959. A new diatom genus from east asia. *Journal of the Royal Microscopical Society* 79: 95–96.

WATANABE, T. 2004. Diatom flora of intertidal mudflat in Japan, Master Degree Thesis Tokyo Gakugei University.

WHITTON, B.A., JOHN, D.M., KELLY, M.G. & HAWORTH, E.Y. 2003. *A coded list of freshwater algae of the British Isles. Second Edition*. World-wide Web electronic publication.

WITKOWSKI, A. 1993. *Fallacia florinae* (moeller) comb. nov. A marine epipsammic diatom. *Diatom Research* 8: 215–219.

WITKOWSKI, A., LANGE-BERTALOT, H. & METZELTIN, D. 2000. *Iconographia Diatomologica: Annotated Diatom Micrographs*. Koeltz Scientific Books.

ZELAZNA-WIECZOREK, J. 2011. *Diatom flora in springs of Lódz Hills (Central Poland). Biodiversity, taxonomy and temporal changes of epipsammic diatom assemblages in springs affected by human impact*. pp. 419, 124 pl.: A.R.G. Gantner Verlag K.G.

Table 1. The Matrix of Morphological characteristics code.

ID	Species	Morphological characteristics														
		1-5					6-10					11-15				
1	*F. decussata*	1	1	0	1	1	0	0	1	0	0	1	?	1	0	0
2	*F. florinae*	1	1	2	0	0	2	2	0	0	2	1	?	1	0	1
3	*F.* cf. *forcipata*	1	0	0	1	1	1	0	0	0	0	0	1	1	1	0
4	*F. fracta*	1	0	1	0	1	2	0	1	0	0	0	0	0	0	0
5	*F. gemmifera*	0	1	2	0	1	3	1	1	0	0	0	0	1	0	0
6	*F. hodgeana*	0	1	1	0	1	3	1	1	0	0	0	0	1	0	0
7	*F. inscriputa*	1	1	0	2	1	3	0	0	0	0	0	?	1	0	0
8	*F. laevis*	1	0	1	1	1	0	0	0	0	0	0	2	1	0	0
9	*F. litoricola*	0	1	1	0	1	3	0	0	0	0	0	0	1	0	0
10	*F. nodulifera*	1	0	2	0	0	1	0	0	0	0	0	1	1	1	1
11	*F. oculiformis* var. *miyajimensis*	1	1	1	1	0	2	2	0	1	1	1	0	1	0	0
12	*F. puchella*	1	0	1	?	1	4	1	0	0	0	0	?	0	0	0
13	*F. tateyamensis*	1	0	0	0	0	1	0	0	0	0	0	1	1	1	0
14	*F. tenera*	1	0	1	0	1	2	1	0	0	0	0	0	1	0	0
15	*F. teneroides*	1	1	1	1	1	3	3	1	0	0	0	?	0	0	0

Table 4. The four groups of *Fallacia* species in this study based on the morphological characters and molecular phylogenetic analysis.

	Group 1	**Group 2**	**Group 3**	**Group 4**
Cell shape	Basicly naviculoids cells	Elliptic cells	Elliptic cells with round poles	Elliptic cells
Sterna	Longitudinal, slightly constrict centrally	Lyre-shaped sterna	Convex	Convex
Axial area	Narrow	Narrow or wide	Wide	Wide
Areolae between raphe and sterna	Longitudinal uniseriate	Longitudinal Multiseriate or uniseriate with wide axial area	Longitudinal Uniseriate with wide axial area	Longitudinal Uniseriate or multiseriate
Habits	Epipelic & epipsammic	Epipsammic	Epipsammic	Epipsammic
Species	*F. fracta*, *F. litoricola*, *F. tenera*, *F. gemmifera*, *F. hodgeana.*	*F. tateyamensis*, *F.* cf. *forcipata*, *F. laevis*, *F. decussate*, *F. nodulifera*.	*F. teneroides*, *F. pulchella*, *F. inscriptura*.	*F. oculiformis* var. *miyajimensis*, *F. florinae*.

Table 2. Primer sequences used for the amplification and sequencing of *rbc*L gene.

Primer	**sequence**	**Refernce**
66F	TTA AGG AGA AAT AAA TGT CTC AAT CTG	Alverson *et al.* 2007
40F	GGA CTC GAA TYA AAA GTG ACC G	Ruck *et al.* 2011
404F	GCT TTA CGT TTA GAA GAT ATG	Ruck *et al.* 2011
587R	GTC TAA ACC ACC TTT TAA MCC TTC	Alverson *et al.* 2007
1255R	TTG GTG CAT TTG ACC ACA GT	Alverson *et al.* 2007
1444R	GCG AAA TCA GCT GTA TCT GTW G	Alverson *et al.* 2007

Table 3. List of taxon and Genbank accession number used in this study.

Accession No.	Taxon
KC309549.1	*Amphipleura pellucida*
KC736590.1	*Amphora montana*
HQ912444.1	*Caloneis lewisii*
JN418663.1	*Caloneis silicula*
HQ912508.1	*Climaconeis riddleae*
HQ912445.1	*Craticula cuspidata*
HQ912461.1	*Diploneis subovalis*
AM710427.1	*Eolimna minima*
EF143289.1	*Fallacia* cf. *forcipata*
HQ912460.1	*Fallacia monoculata*
HQ912469.1	*Fallacia pygmaea*
HF563527.1	*Haslea ostrearia*
HE978356.1	*Haslea pseudostrearia*
KC736600.1	*Mayamaea permitis*
KC309554.1	*Meuniera membranacea*
HQ912467.1	*Navicula cryptocephala*
AY604699.1	*Navicula salinicola*
HQ912455.1	*Neidium bisulcatum*
HQ912446.1	*Neidium productum*
JN418662.1	*Pinnularia borealis*
HQ912468.1	*Pinnularia brebissonii*
HQ912465.1	*Pinnularia termitina*
EF143281.1	*Rossia* sp.
HQ912473.1	*Scoliopleura peisonis*
KC911805.1	*Sellaphora auldreekie*
KC911816.1	*Sellaphora pupula*
KC736613.1	*Sellaphora seminulum*
HQ912443.1	*Stauroneis acuta*

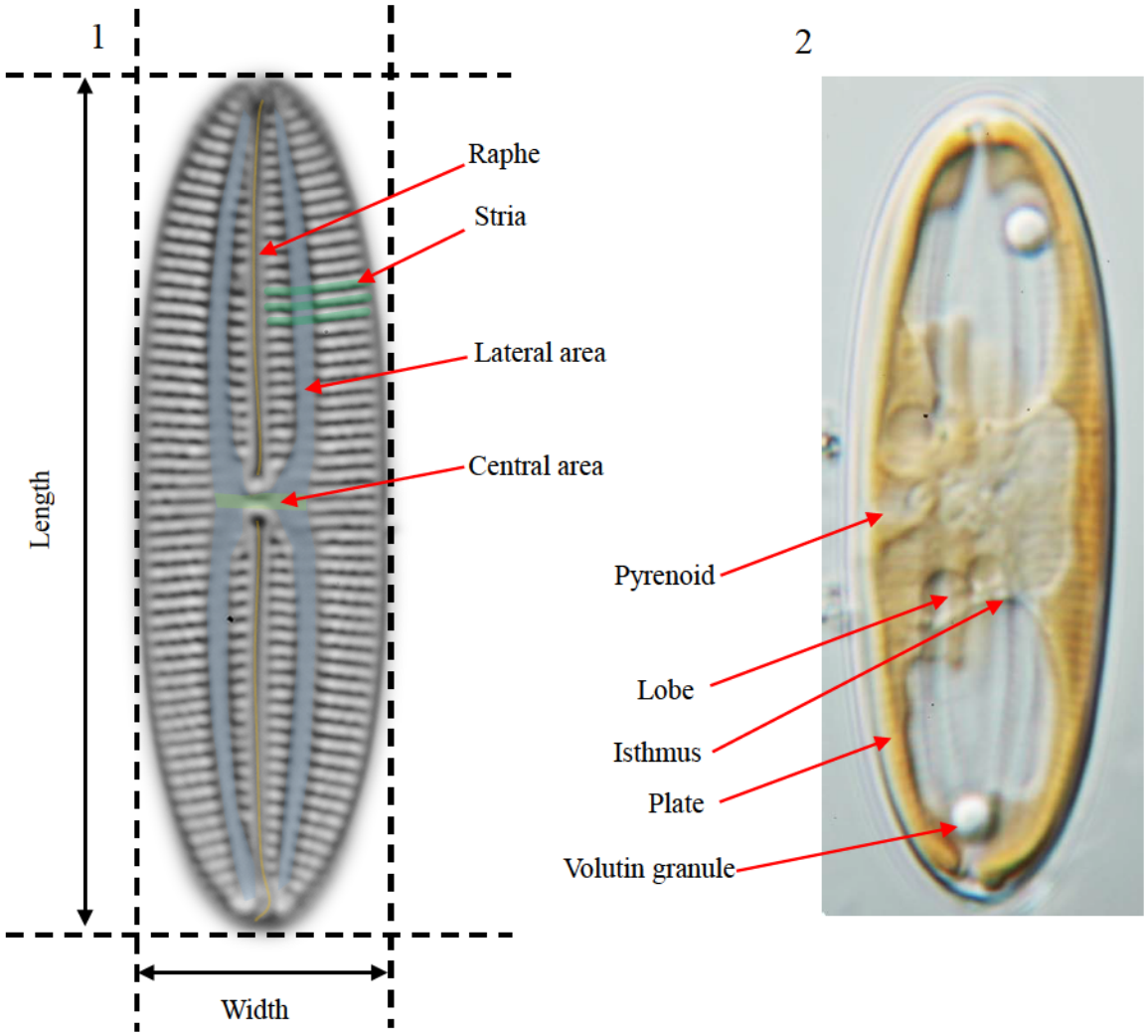

Plate 1. Descriptive terms of frustule and chloroplast in LM.

Fig. 1. Valve view.

Fig. 2. H-shaped chloroplast.

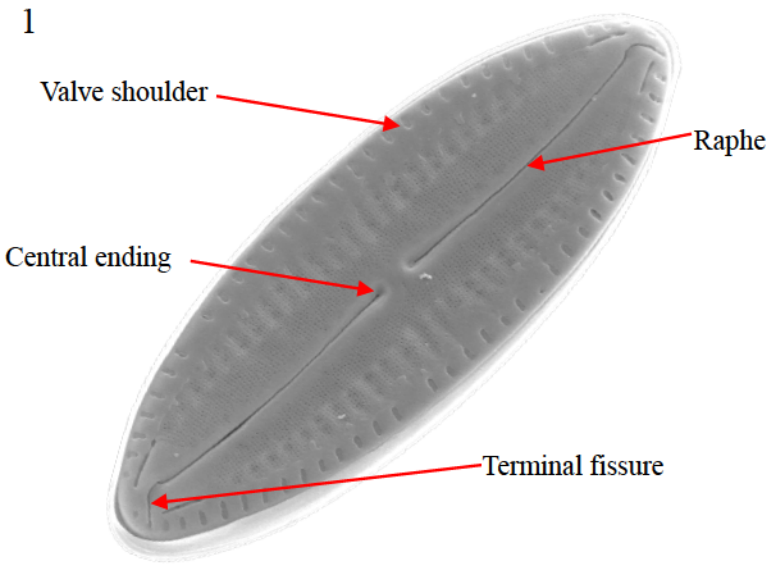

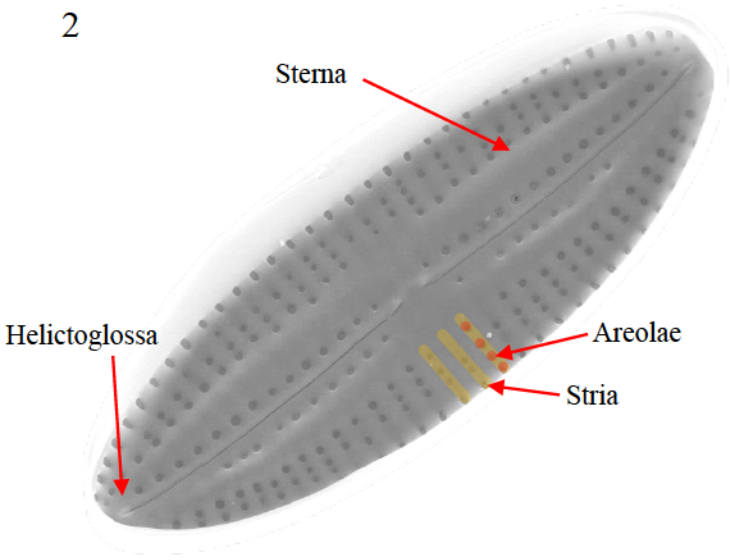

Plate 2. Descriptive terms of valve in SEM.

Fig. 1. External view of valve.

Fig. 2. Internal view of valve.

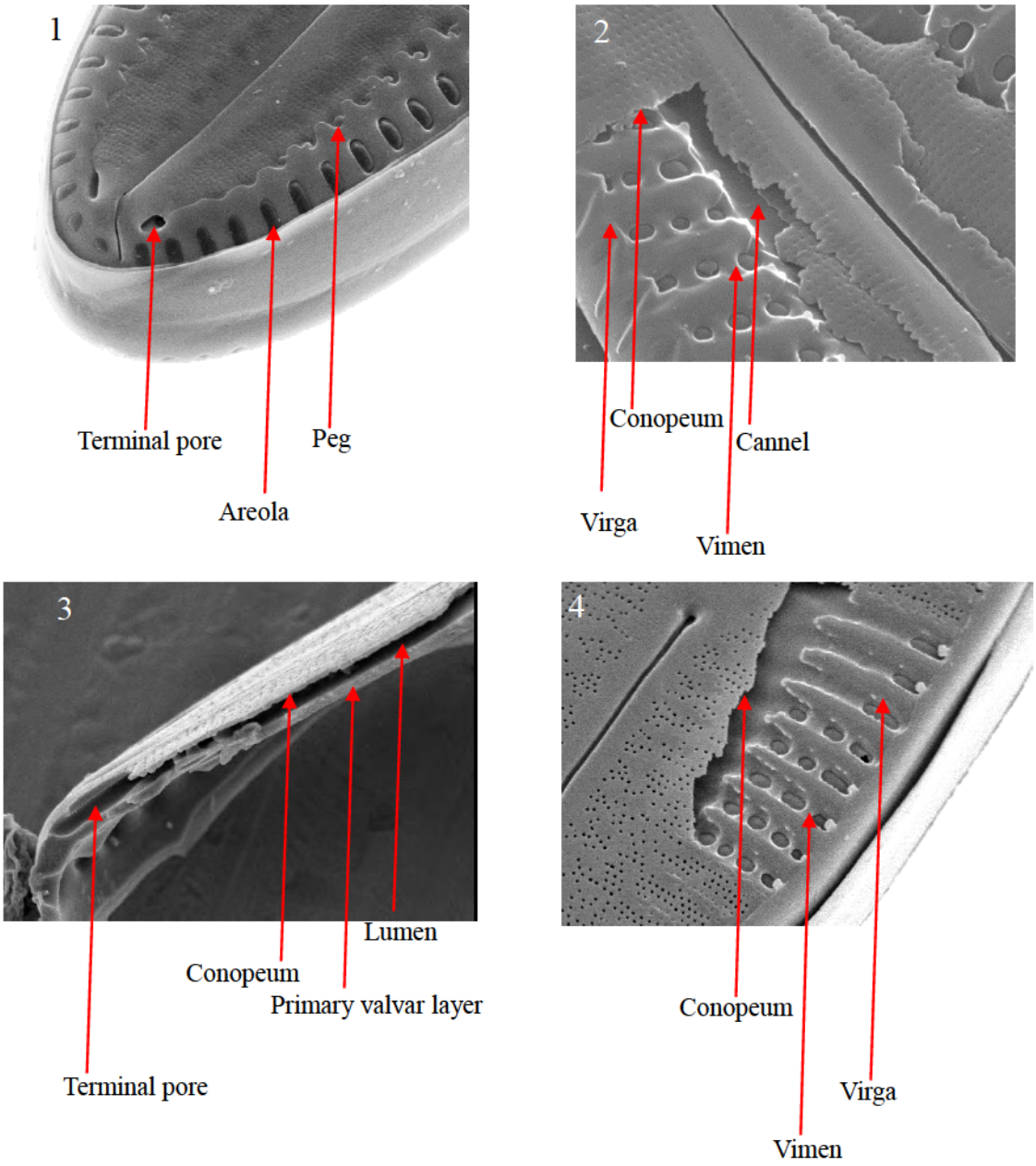

Plate 3. Descriptive terms of valve in SEM.

Fig. 1. External view of a terminal.

Figs 2, 4. External view of valve faces.

Fig. 3. Sectional view of a valve.

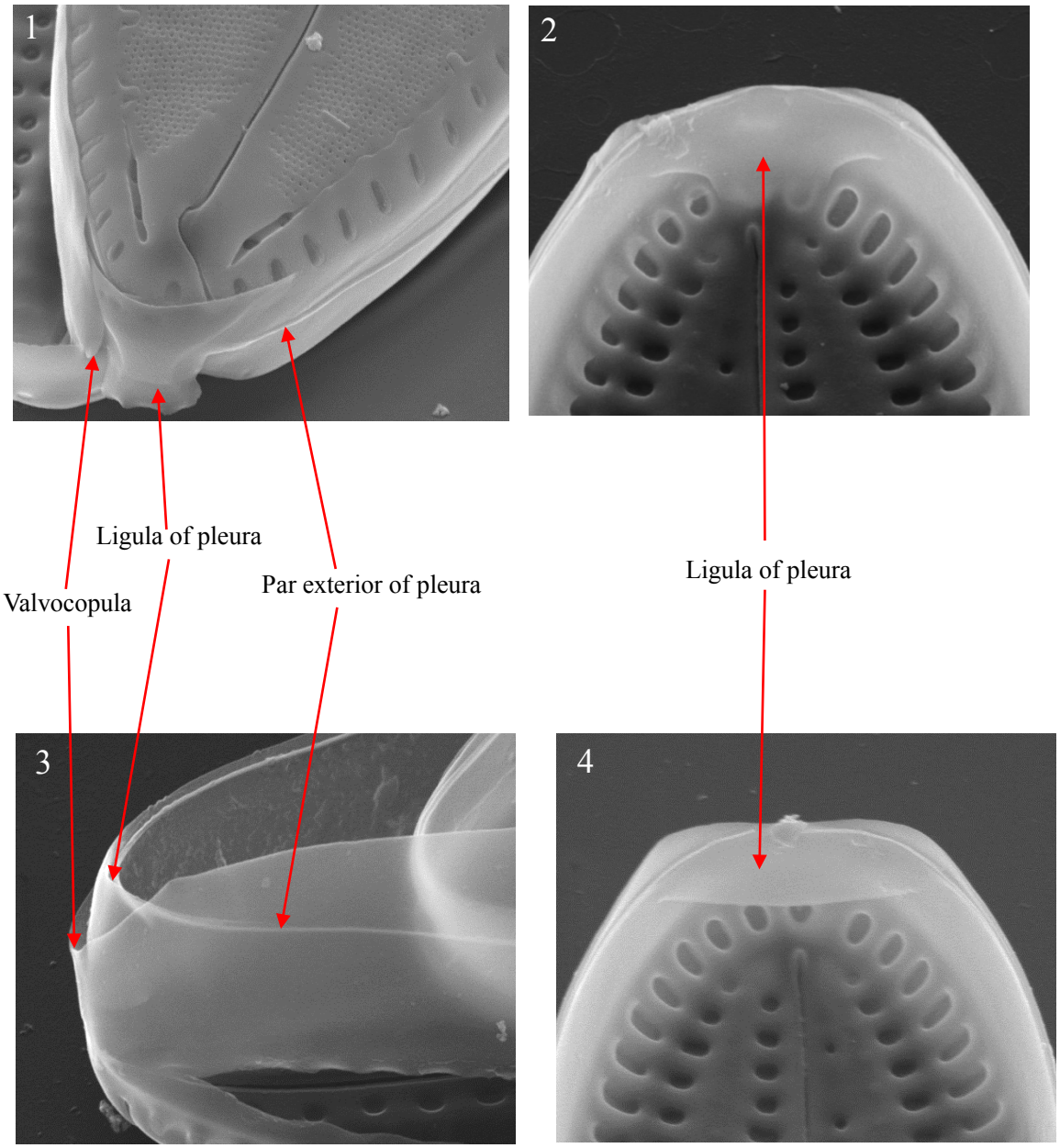

Plate 4. Descriptive terms of a cingulum.

Fig. 1. External view of the opening of the valvocopula.

Fig. 2. Internal view of the ligula at the opening side of valvocopula.

Fig. 3. External view of the unopening terminal.

Fig. 4. Internal view of the ligula at the unopening side of valvocopula.

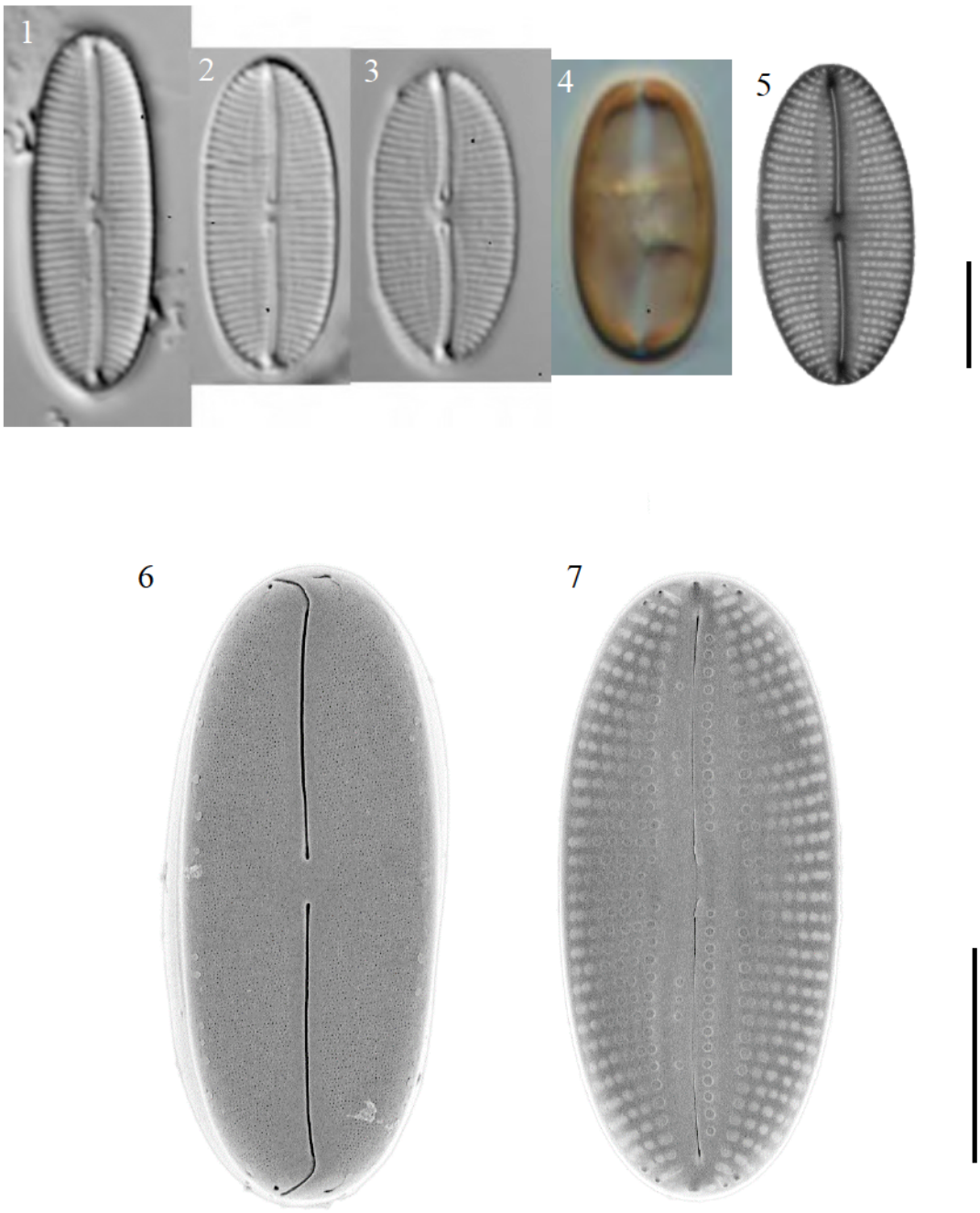

Plate 5. *Fallacia fracta* with LM (Figs 1–4), TEM (Fig. 5) and SEM (Figs 6, 7). Scale bars = 5 µm.

Figs 1–3, 5. Plain view of Valves.

Fig. 4. Chloroplast.

Figs 6, 7. External and internal view of valve face in plain view.

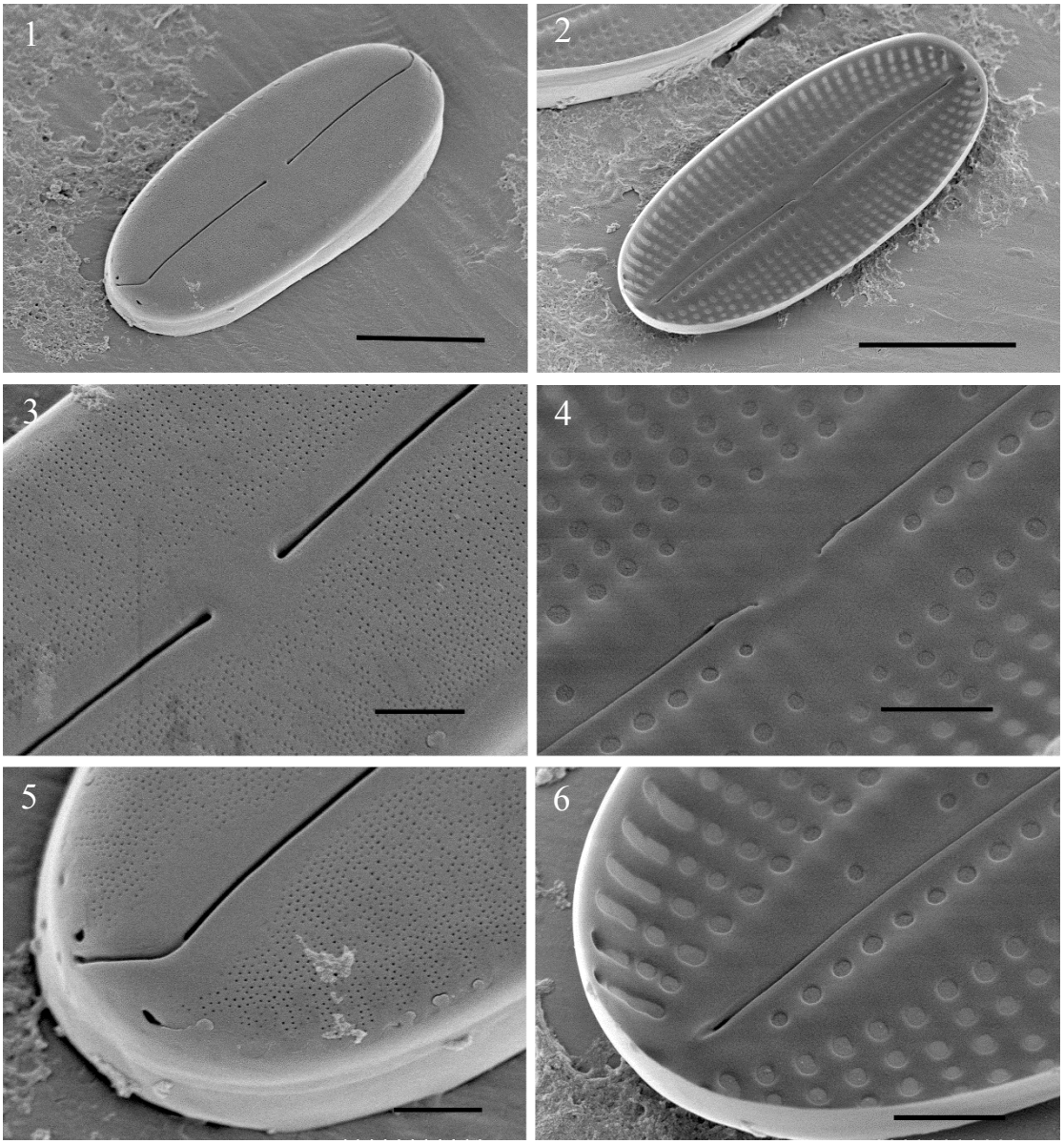

Plate 6. External (Figs 1, 3, 5) and internal (Figs 2, 4, 6) views of valve of *Fallacia fracta* with SEM (tilt 30°). Scale Bars = 5 μm (Figs 1, 2), 1 μm (Figs 3–6).

Figs 1, 2. Whole valves.

Figs 3, 4. Central endings of raphe.

Figs 5, 6. Terminals of valve.

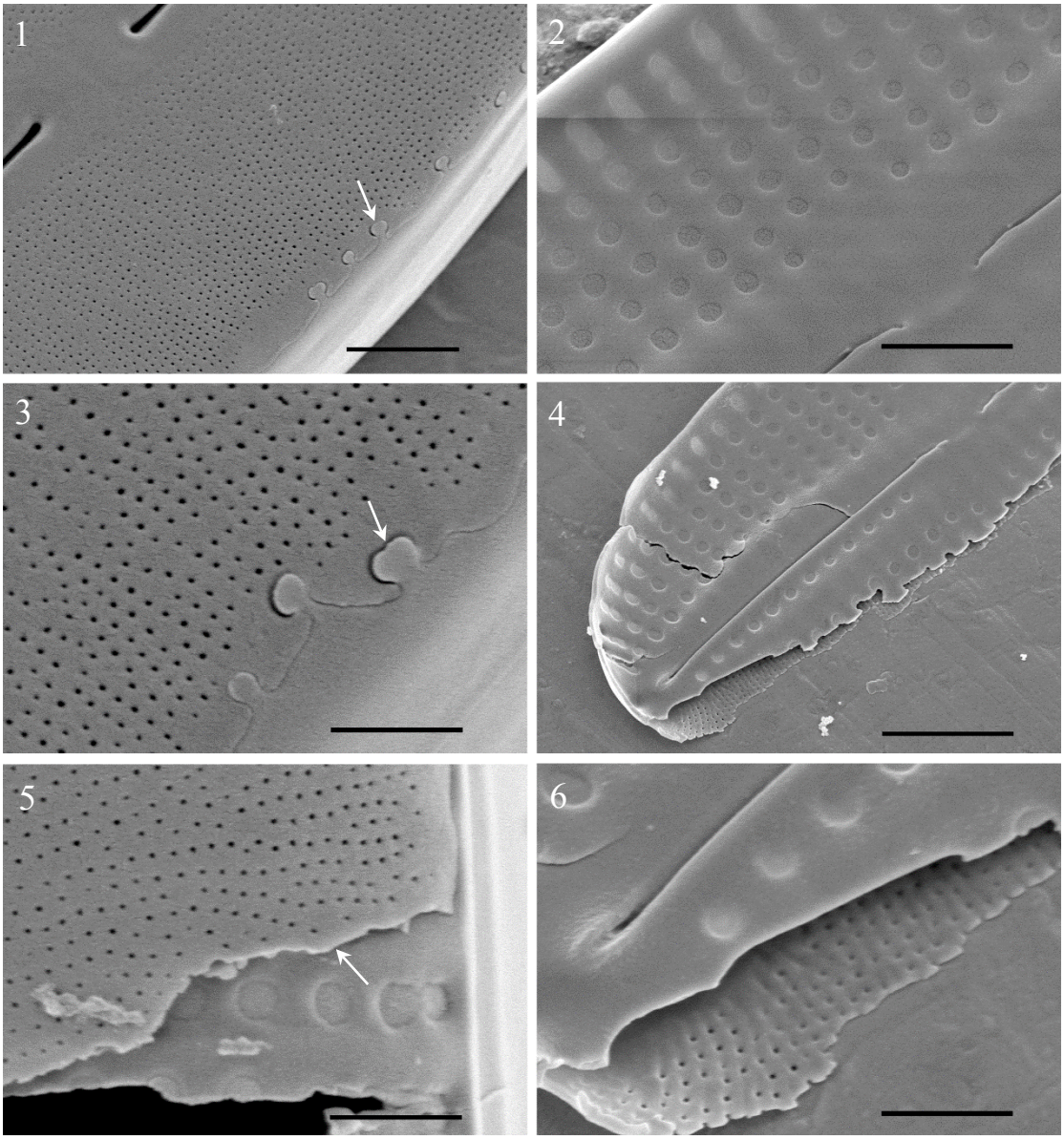

Plate 7. Structure of a valve of *Fallacia fracta* SEM. Scale bars = 500nm (Figs 3, 5, 6), 1 μm (Figs 1, 2), 2 μm (Fig. 4).

Fig. 1. External view of whole primary valve layer covered by finely porous conopeum, which connecting with valve shoulder by a series of pegs (arrow).

Fig. 2. Internal striae comprise a uniseries of areolae.

Fig. 3. Detail of the pegs (arrow), external view.

Figs 4, 6. Lumen between the primary valve layer and the conopeum (arrow), external view.

Fig. 5. Striae beneath conopeum.

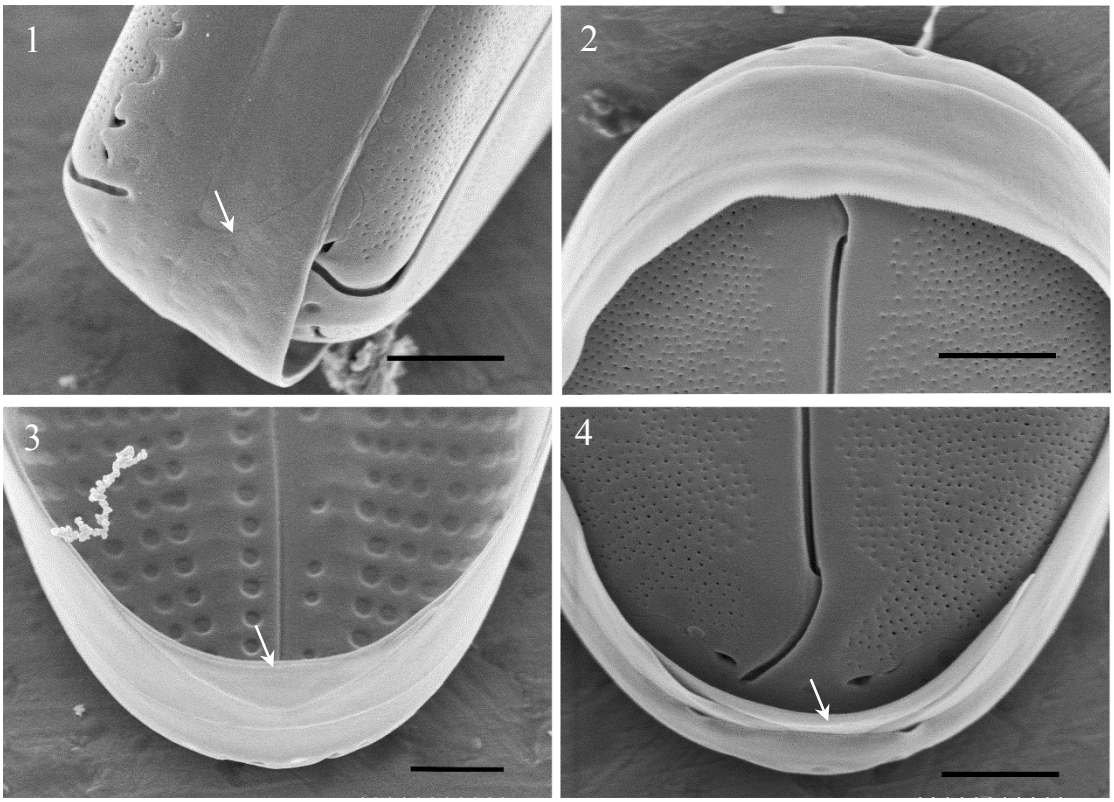

Plate 8. Cingulum of *Fallacia fracta* SEM, Scale Bars = 1 µm.

Fig. 1. Opening pole of valvocopula filled by a large ligula (arrow) of pleura.

Fig. 2. Unopening pole of valvocopula.

Fig. 3. Unopeing pole of valvocopula filled with a small ligula (arrow) of pleura.

Fig. 4. Opening pole of valvocopula with a ligula (arrow), opposite pole of Fig. 2.

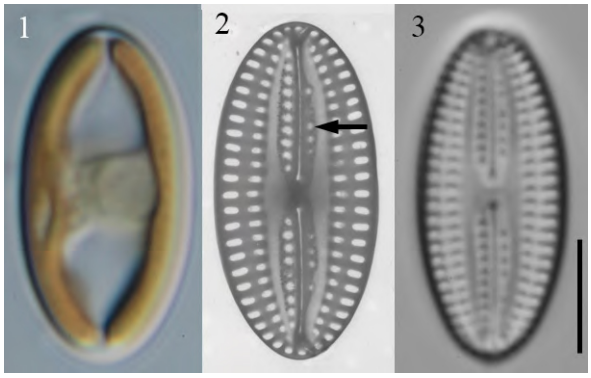

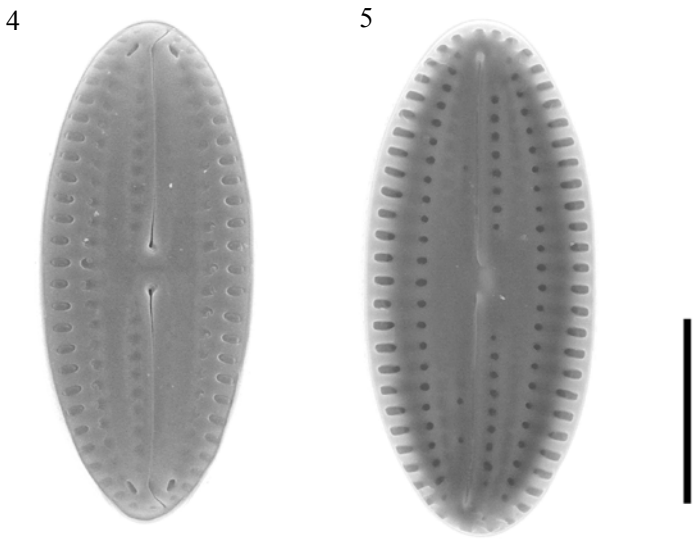

Plate 9. Plain view of vegetative cells and valve of *Fallacia tenera* with LM (Figs 1, 3), TEM (Fig 2) and SEM (Figs 4, 5), Scale bars = 5 µm.

Fig. 1. H-shaped chloroplast.

Figs 2, 3. Valve, showing the asymmetric areolae adjacent to the raphe (arrow).

Fig. 4, 5. External and internal views of valve.

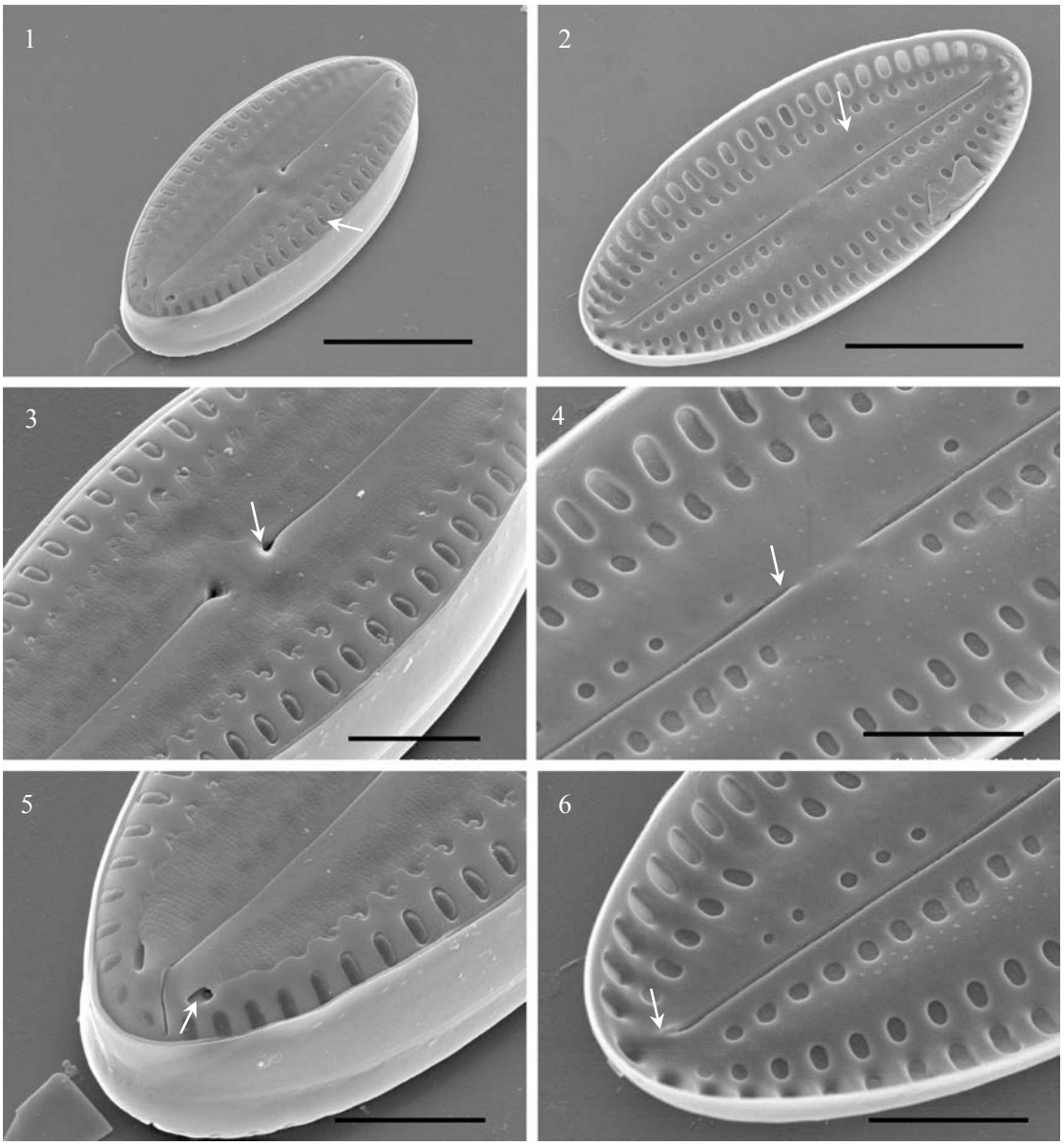

Plate 10. External (Figs 1, 3, 5) and internal (Figs 2, 4, 6) views of valve of *Fallacia tenera*. Scale bars = 5 µm (Figs 1, 2), 2 µm (Figs 1–6).

Figs 1, 2. Valve in tilt 30°, showing the areolae (arrow, fig. 1) on the valve shoulder and the lateral sterna (arrow, fig. 2) on both sides of the raphe.

Figs 3, 4. Central raphe ending, showing the expanded, water drop liked central pores on external face and slit on internal face.

Figs 5, 6. Poles of valve, showing two pores locates on both sides of raphe (arrow, fig. 5) and small helictoglossa (arrow, fig. 6) on polar raphe endings.

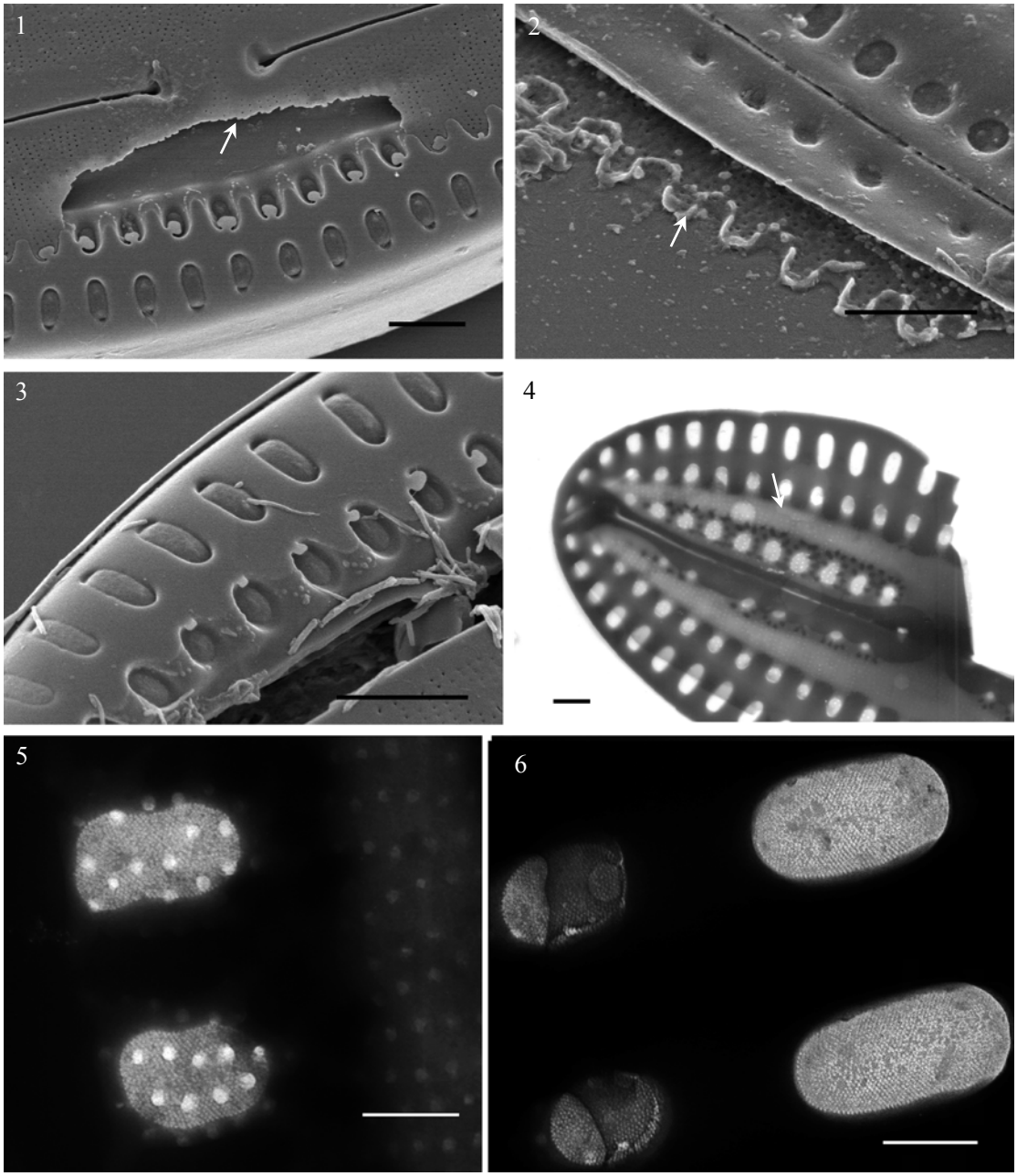

Plate 11. Valve structure of *Fallacia tenera*, Scale bars = 1 µm (figs 1–3), 500 nm (Fig. 4) and 200 nm (Figs 5, 6).

Figs 1, 3. External view of a valve with a broken conopeum (arrow).

Fig. 2. Internal view of waved edge of conopeum (arrow).

Fig. 4. Valve with TEM, showing the hyaline canal (arrow) through the valve.

Figs 5, 6. Areolae occlusion: hymens with hexagonal array perforation.

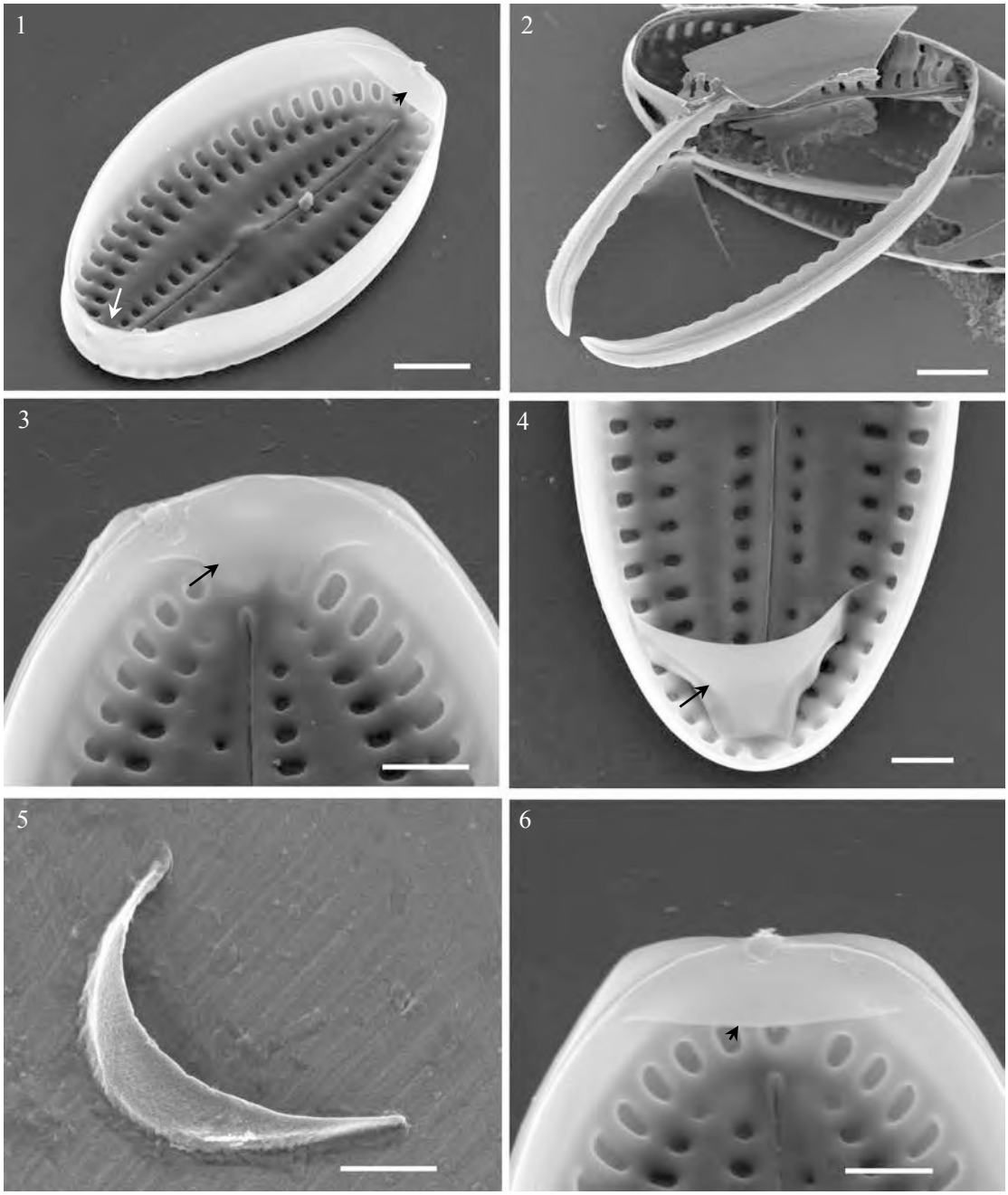

Plate 12. Fine structure of a complete cingulum. Scale bars = 2 μm (Figs 1, 2), =1 μm (Figs 3–6).

Fig. 1. A complete theca, two ligulae (arrow and arrowhead) of pleurae.

Fig. 2. An open valvocopula with undulate margin.

Fig. 3. Internal view of a ligula (arrow) of the pleura 2 (the third band).

Fig. 4. External view of the ligula (arrow) of the pleura 2 (the third band).

Fig. 5. External view of a ligula of the pleura 1 (the second band).

Fig. 6. Internal view of the ligula (arrowhead) of the pleura 1 (the second band).

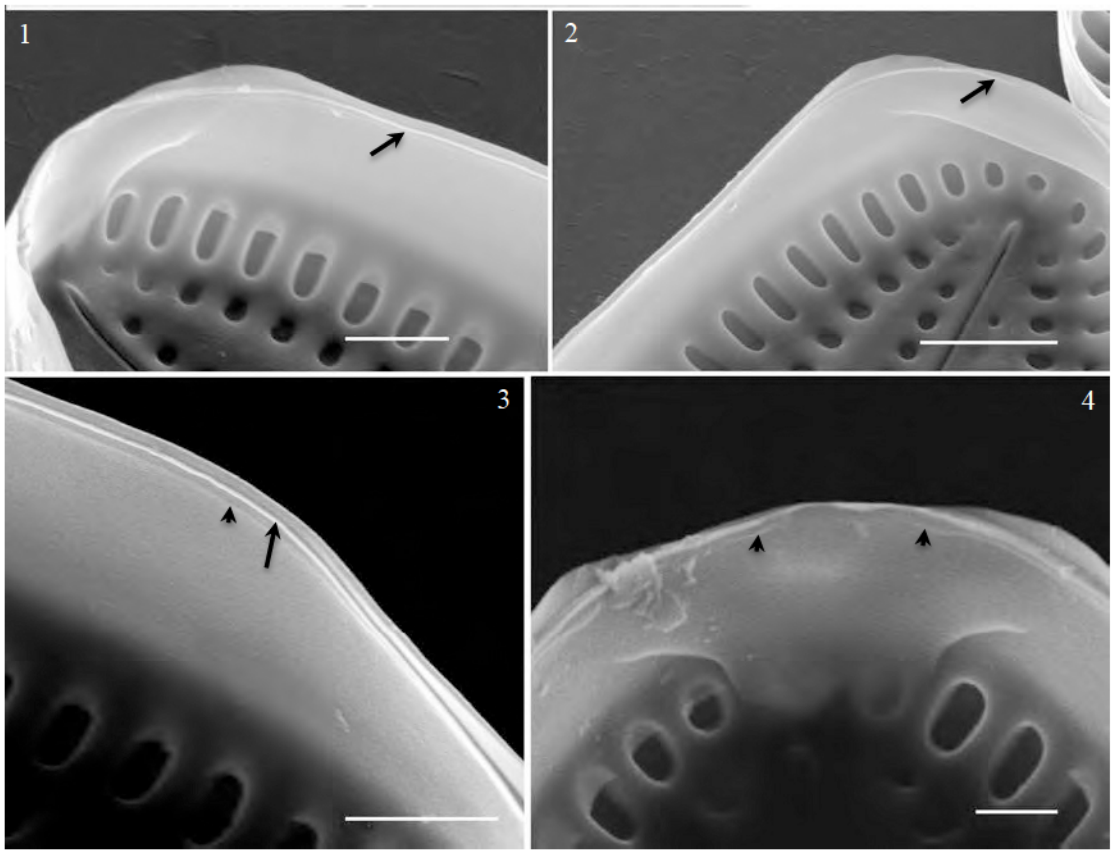

Plate 13. Fine structure of a complete cingulum. Scale bars = 1 μm (Figs 1–3) and 500nm (Fig. 4).

Fig. 1. Linear strip (arrow) of the pleura 2 (the third band).

Fig. 2. Two terminals of the linear strips (arrow) of the pleura 2 (the third band).

Fig. 3. Linear strip (arrow) of pleura 2 (the third band) and the linear strip (arrowhead) of pleura 1 (the second band).

Fig. 4. Two terminals (arrowhead) of pleura 1 (the second band).

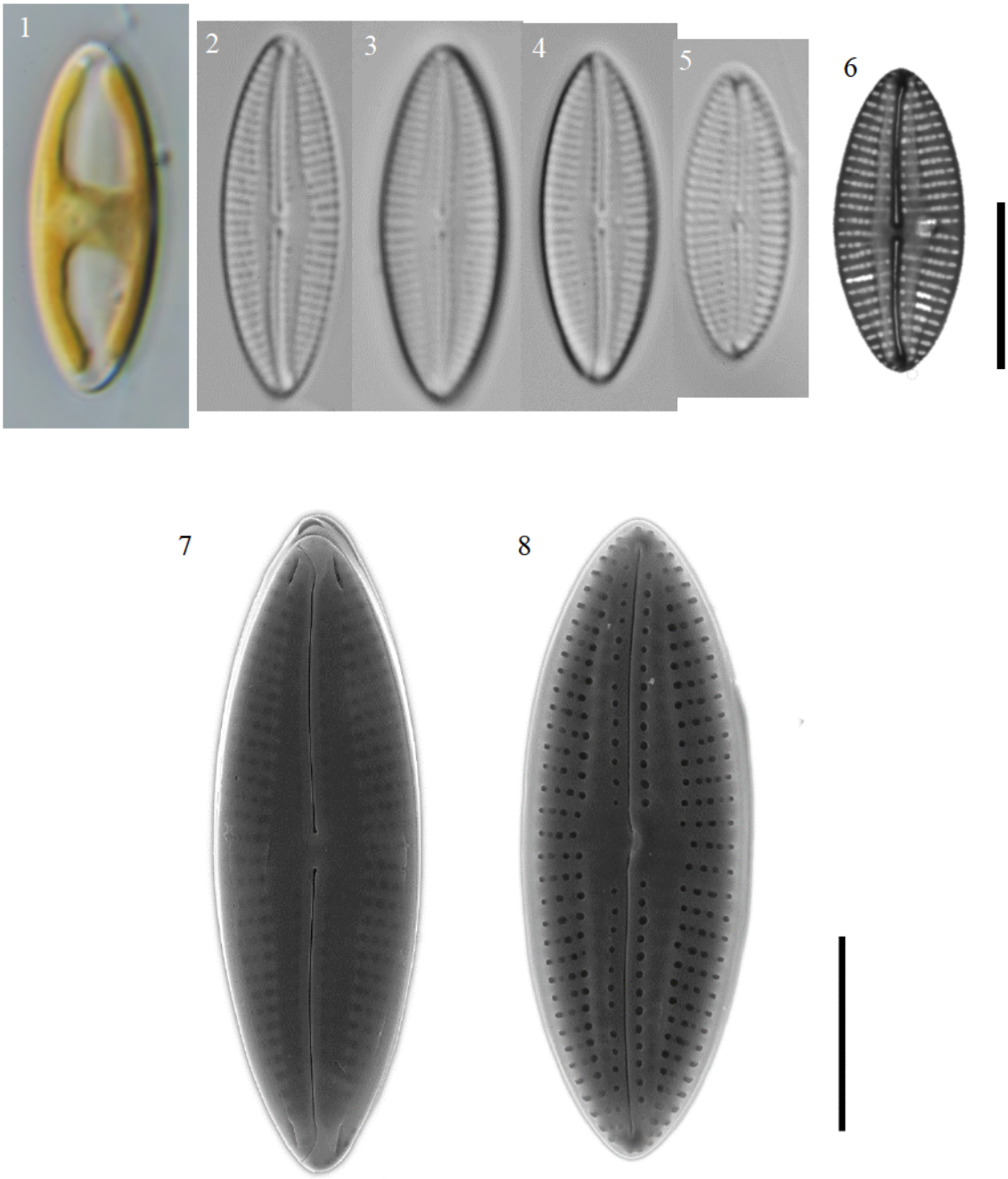

Plate 14. Plain views of vegetative cells and valve of *Fallacia gemmifera* with LM (Figs 1–5), TEM (Fig. 6) and SEM (Figs 7, 8), Scale bars = 5 µm.

Fig. 1. H-shaped chloroplast.

Figs 2–5. Cleaned Valves.

Fig. 6. Valve with TEM.

Fig. 7, 8. External and internal views of valve.

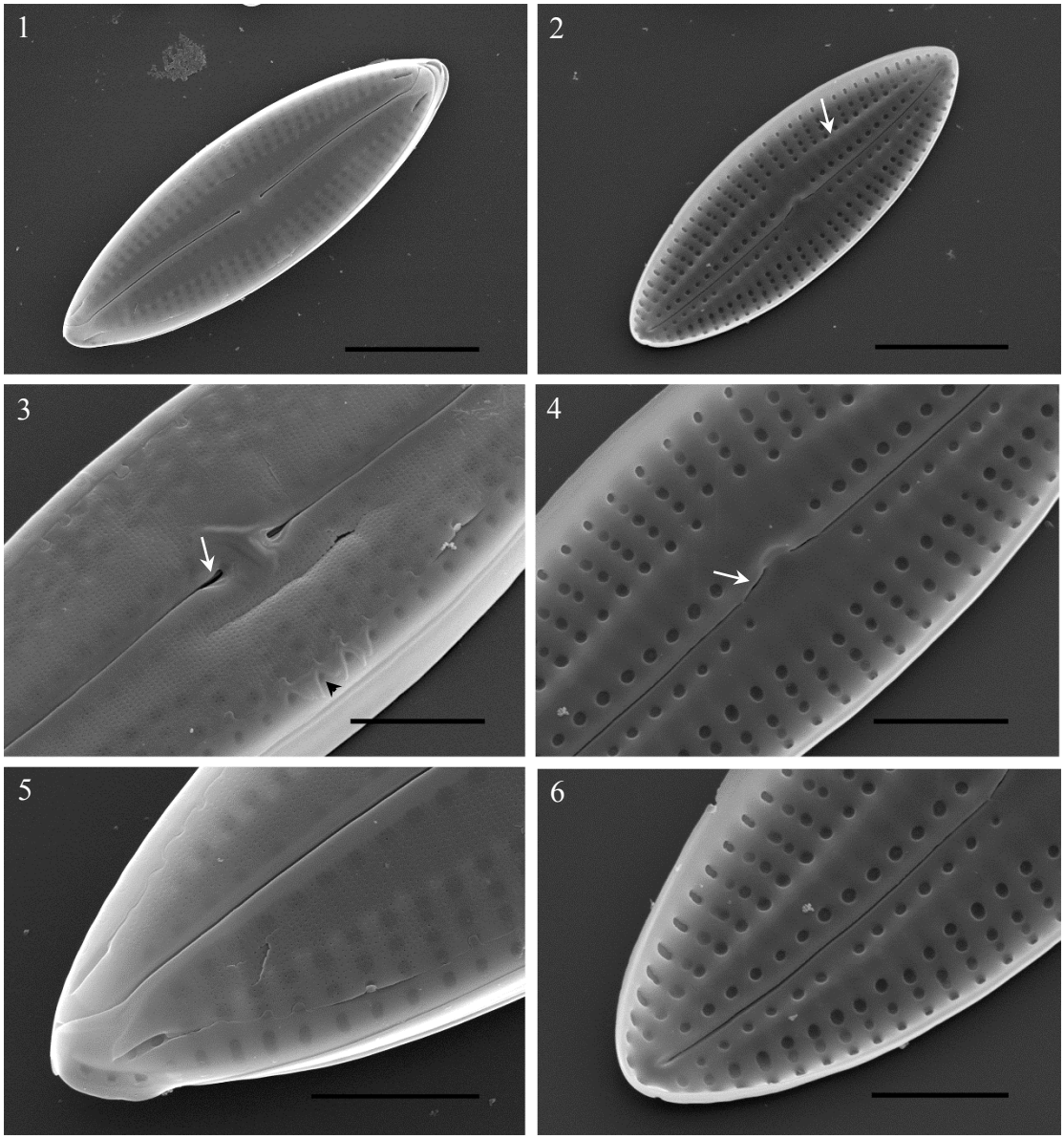

Plate 15. External (Figs 1, 3, 5) and internal (Figs 2, 4, 6) views of valve of *Fallacia gemmifera*. Scale bars = 5 μm (Figs 1, 2), 2 μm (Figs 3–6).

Figs 1, 2. Valves in tilt 30°, showing the lateral sterna (arrow) on both sides of the raphe.

Figs 3, 4. Central raphe endings, showing the slightly curved and expanded water drop liked central raphe endings (arrow, Fig. 3) on external face and slightly curved slit (arrow, Fig. 4) on internal face.

Figs 5, 6. Poles of valve, showing two opening slits locates on both sides (arrow, Fig. 5) of raphe and small helictoglossa on pole raphe ending (arrow, Fig. 6).

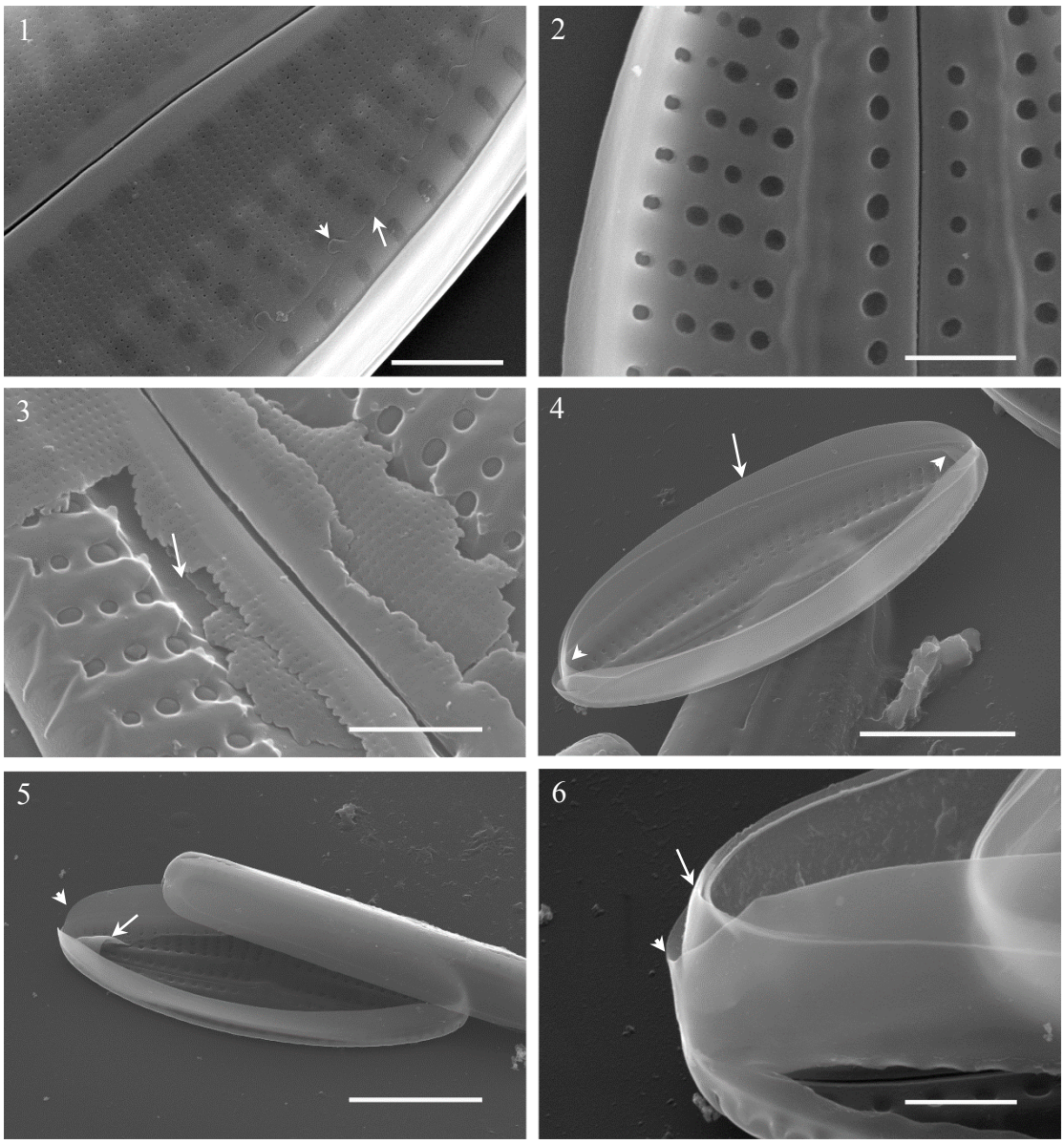

Plate 16. Structure of a valve and cingulum of *Fallacia gemmifera.* Scale bars = 1 μm (Figs 1–3, 6), 5 μm (Figs 4, 5).

Fig. 1. Valve covered by a finely porous conopeum (arrow), connecting with the valve shoulder by pegs (arrowhead).

Fig. 2. Stria consisted of uniseriate areolae.

Fig. 3. A valve with broken finely porous conopeum, showing the depressed canal (arrow).

Fig. 4. Cingulum consisted of an open valvocopula (arrow), two pleurae (arrowheads).

Fig. 5. The ligula (arrow) of pleura is present at the opening pole (arrowhead) of valvocopula.

Fig. 6. Ligula (arrow) of a pleura locates on the unopened pole of valvocopula.

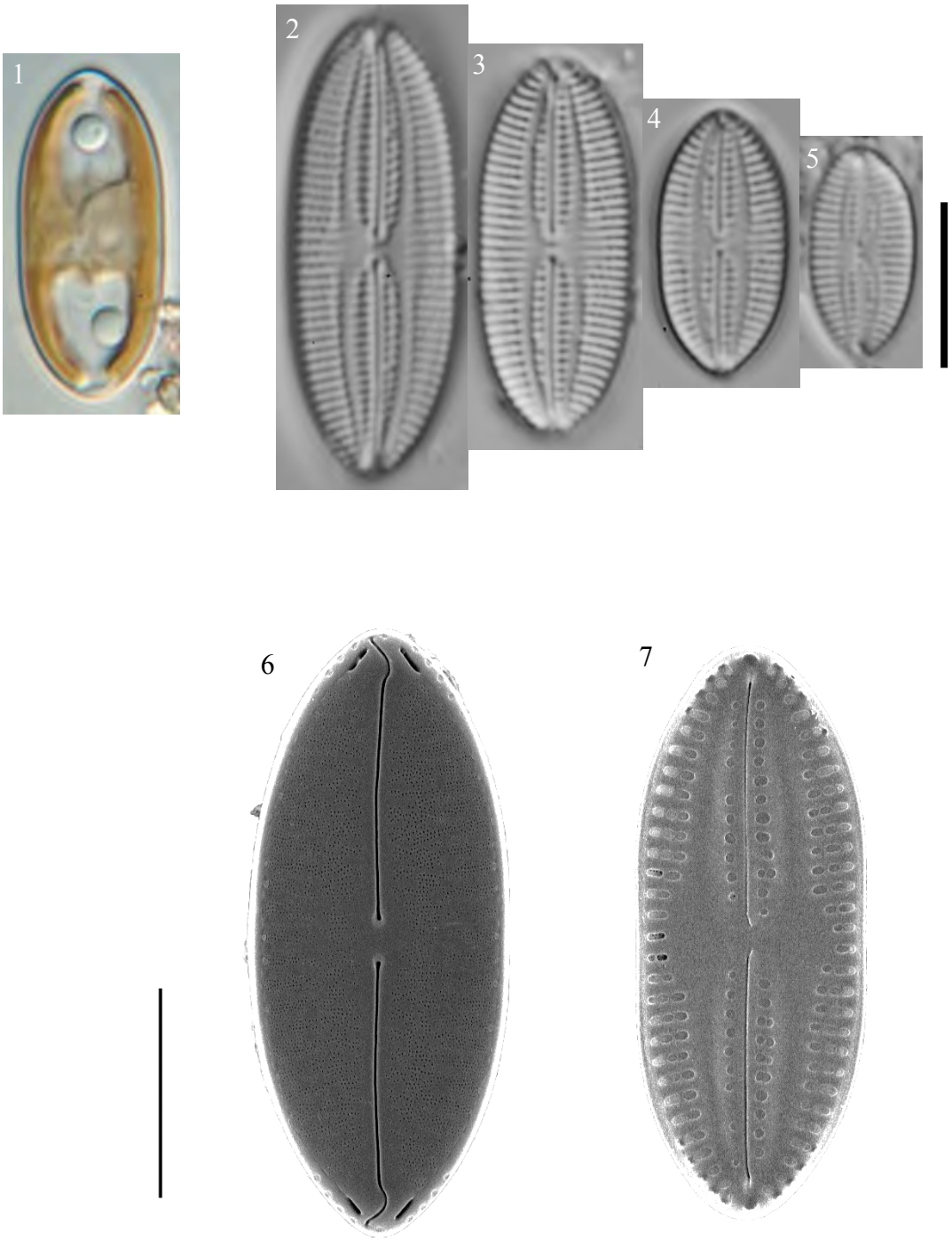

Plate 17. Plain views of vegetative cells and valves of *Fallacia litoricola* with LM (Figs 1–5) and SEM (Figs 6, 7), Scale bars = 10 µm (Figs 1–5) and5 µm (Figs 6, 7).

Fig. 1. H-shaped chloroplast.

Figs 2–5. Cleaned valves.

Figs 6, 7. External and internal view of valves.

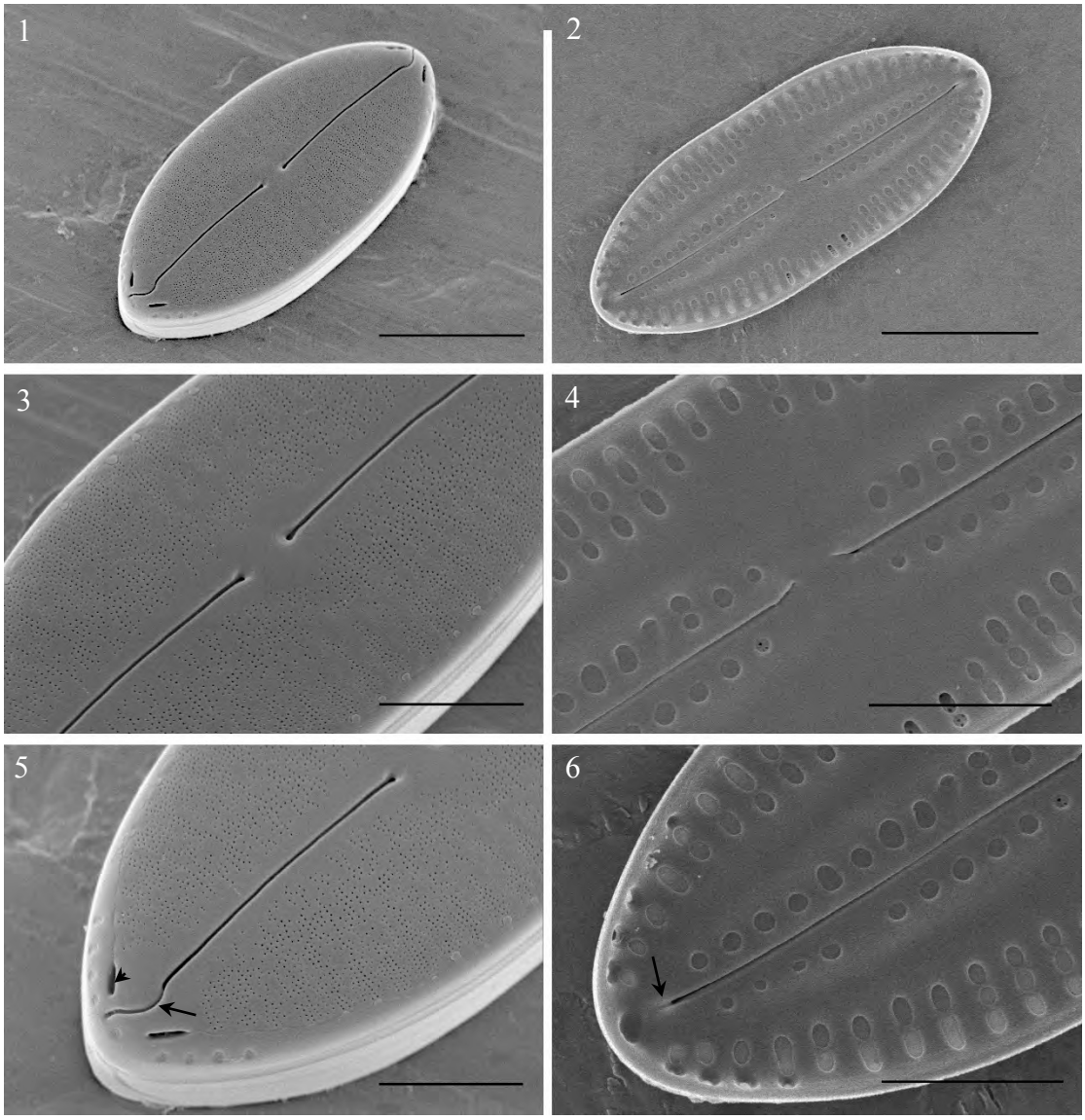

Plate 18. External (Figs1, 3, 5) and internal (Figs 2, 4, 6) views of valve of *Fallacia litoricola*, Scale bars = 5 μm (Figs 1, 2), and 2 μm (Figs 3–6).

Figs 1, 2. Whole valves.

Fig. 3. External central raphe endings expand, water drop like.

Fig. 4. Internal central raphe endings, deflate to primary side of valve.

Fig. 5. Poles of valve, note the waved terminal fissure of raphe (arrow), one openings slits (arrowhead) on both sides of raphe and a number of areolae uncovered by conopeum (double arrows).

Fig. 6. Internal view of terminal of a valve, showing a small helictoglossa (arrow).

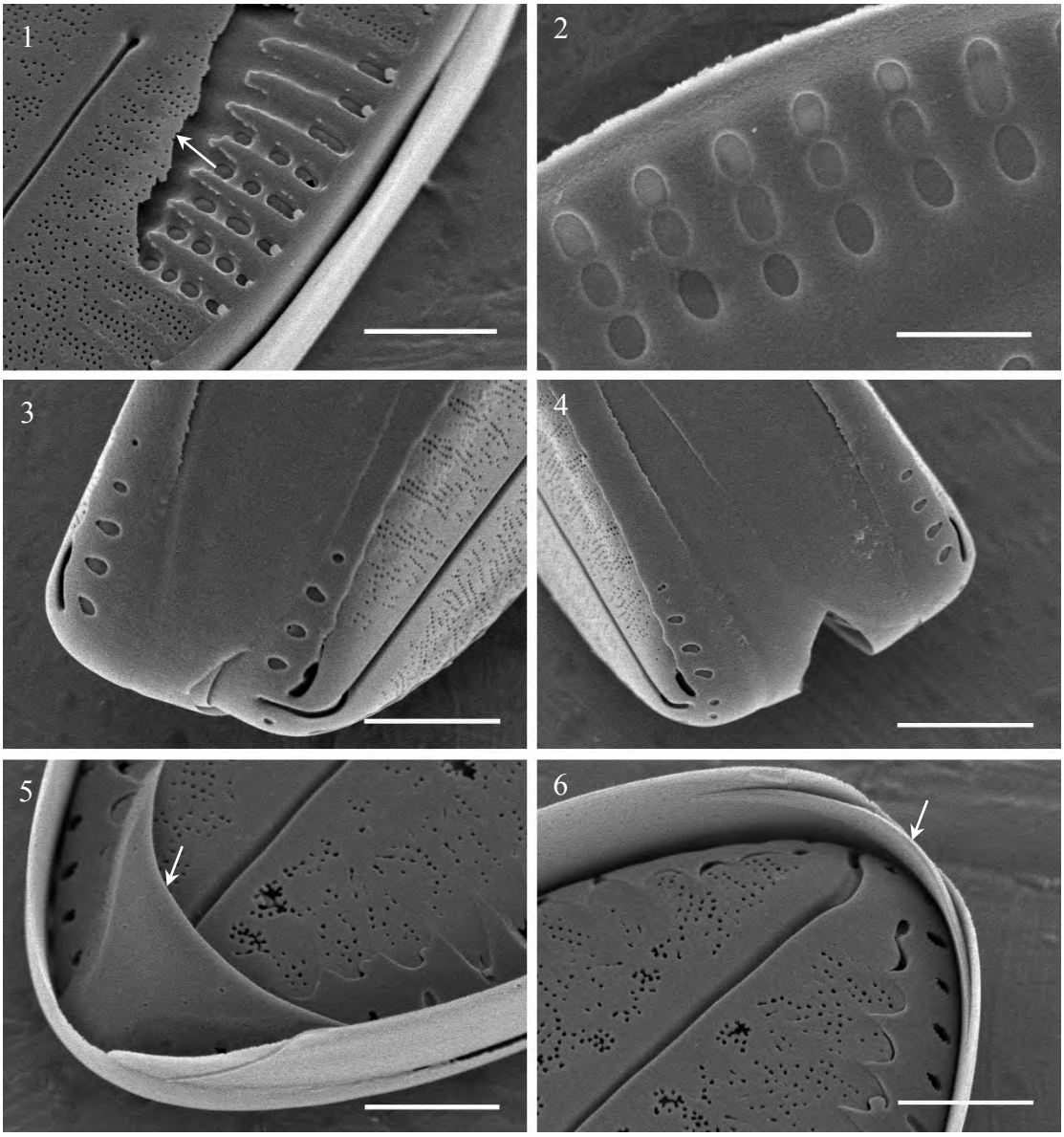

Plate 19. Fine structure of a valve and cingulum of *Fallacia litoricola*, Scale bars = 1.5 μm (Figs 1, 3), 750 nm (Fig. 2), 2 μm (Fig. 4) and 1.2 μm (Figs 5, 6).

Fig. 1. Valve with broken conopeum, showing striae covered by conopeum (arrow).

Fig. 2. Striae composed of uniseriate areoale.

Fig. 3. Valve pole where valvocopula unopened (arrow).

Fig. 4. Valve pole showing the opening of valvocopula (arrow).

Fig. 5. A large ligula of pleura (arrow).

Fig. 6. A small ligula of pleura (arrow).

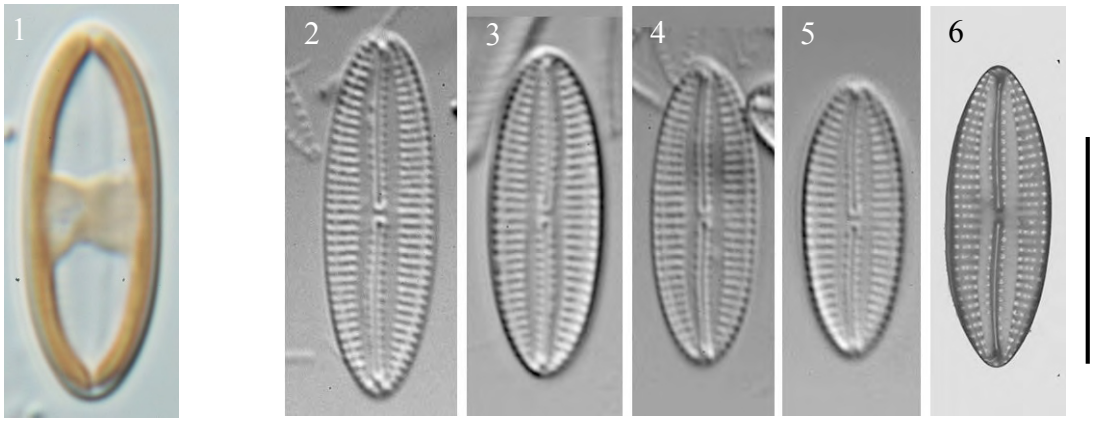

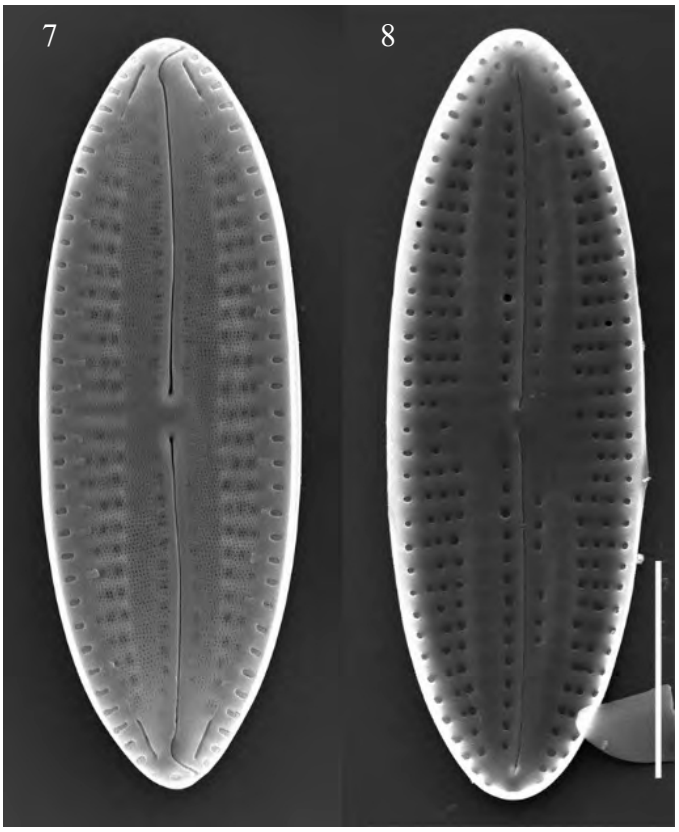

Plate 20. Plain view of vegetative cells and valves with LM (Figs 1–5), TEM (Fig. 6) and SEM (Figs 7, 8) of *Fallacia hodgeana*, Scale bars = 10 µm (Figs 1–5) and 5 µm (Figs 7, 8).

Fig. 1. H-shaped chloroplast.

Figs 2–5. Cleaned valves.

Fig. 6. Valve with TEM.

Figs 7, 8. External and internal view of a valve.

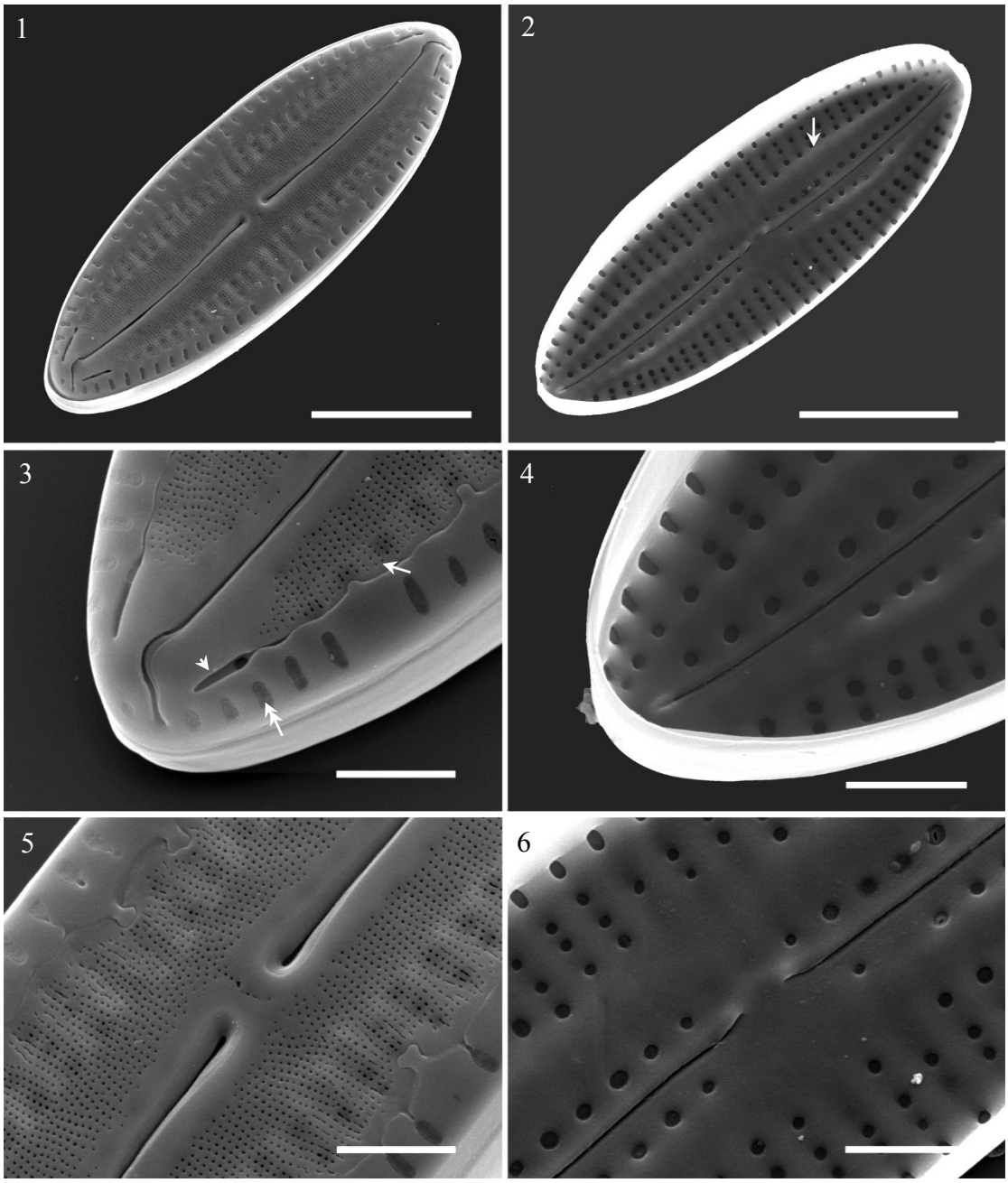

Plate 21. External (Figs 1, 3, 5) and internal (Figs 2, 4, 6) views of valve of *Fallacia hodgeana* with SEM. Scale bars = 1µm, except Figs 1, 2 (5µm).

Figs 1, 2. Views of external and internal valve faces at 20˚ tilt, showing the lateral sterna (arrow) in internal view.

Fig. 3. Pole of valve showing the finely porous conopeum (arrow), opening slit (arrowhead) and elongate areola (doublearrows) on the shoulder of valve.

Fig. 4. Internal view of pole, showing the small helictoglossa at the distal end of raphe.

Fig. 5. External central raphe endings slightly expanding, opening to a groove.

Fig. 6. Internal raphe central endings slightly deflected.

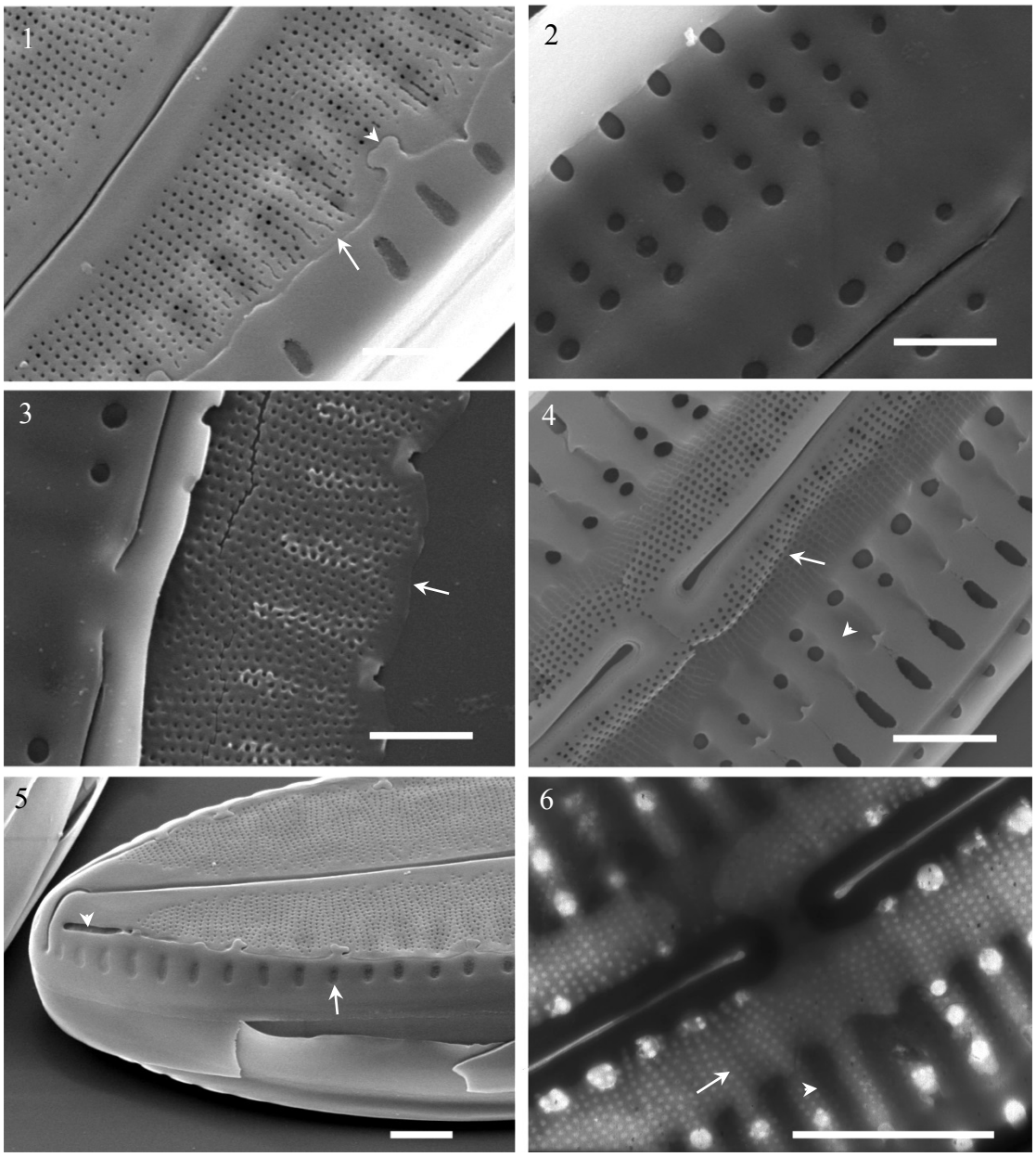

Plate 22. The structure of valve of *Fallacia hodgeana* in detail.

Fig. 1. External view of valve face. Note the finely porous conopeum (arrow) and "peg" structure (arrowhead).

Fig. 2. Internal view of valve face. The striae were interrupted into three parts.

Fig. 3. Internal view of finely porous conopeum (arrow).

Fig. 4. A developing valve, showing the formation of conopeum (arrow) and lateral strengthened transapical virgae of striae (arrowhead).

Fig. 5. Side view of valve, showing the areolae on the valve mantle (arrow) and the opening slit (arrowhead).

Fig. 6. Central area with TEM. Note the longitudinal canals (arrow) and lateral transapical virgae (arrowhead).

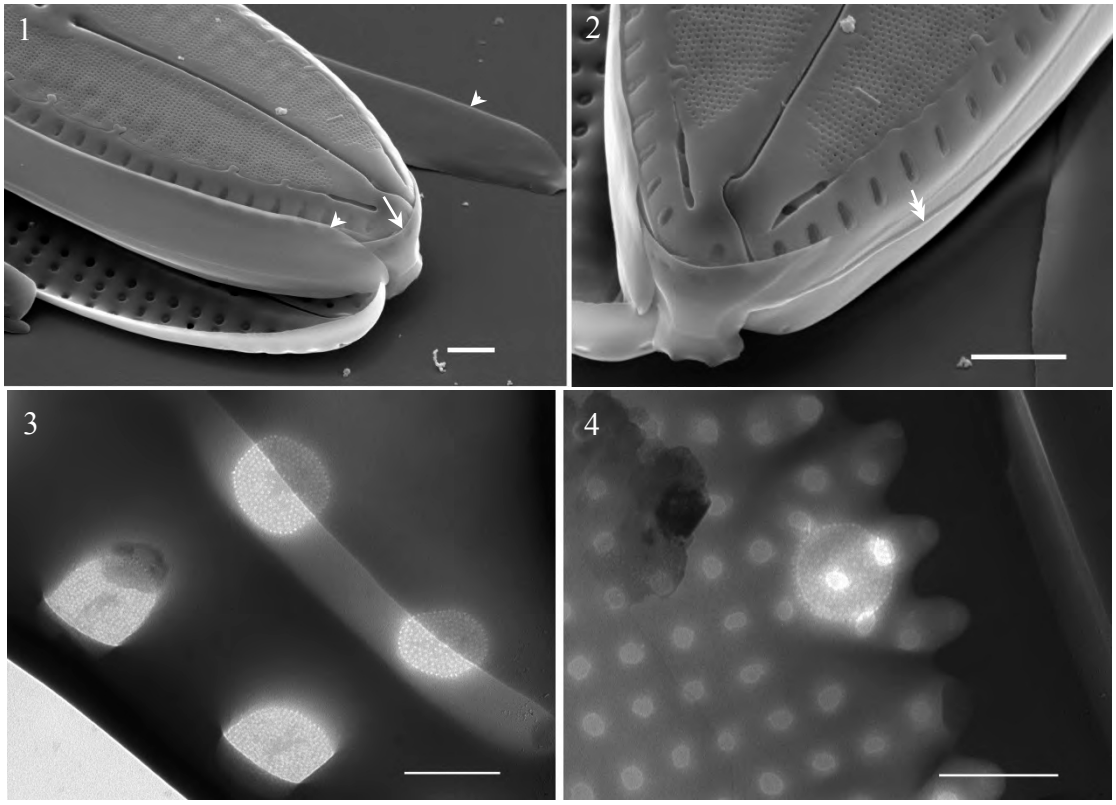

Plate 23. Cingulum and areolae pattern of *Fallacia hodgeana*. Scale bars=1µm.
Fig. 1. Cingulum consists of an open valvocopula (arrow heads) and a pleura (arrow).
Fig. 2. Pars exterior (double arrows) and a large lingula (arrow).
Figs 3, 4. Areolae occlusion: Hymens with linear perforations in a centric array.

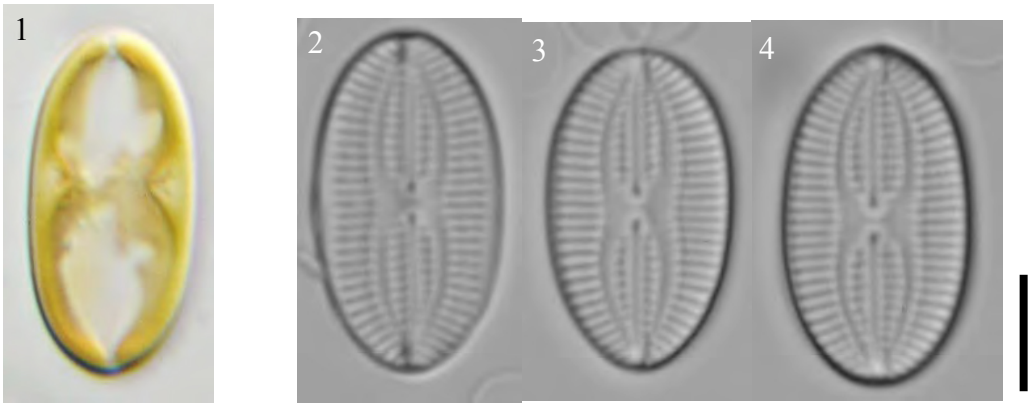

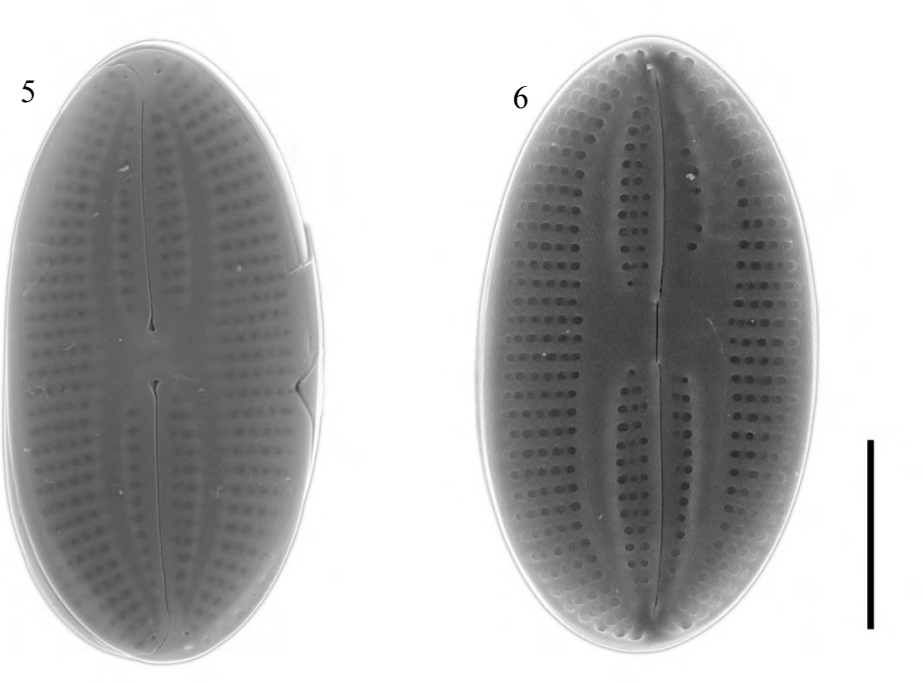

Plate 24. Plain views of vegetative cells and valve of *Fallacia* cf. *forcipata* with LM (Figs 1–4), and SEM (Figs5, 6). Scale bars = 5 µm.

Fig. 1. A basically H-shaped chloroplast, showing two pyrenoides.

Figs 2–4. Cleaned Valves.

Figs 5–6. External and internal view of valve with SEM.

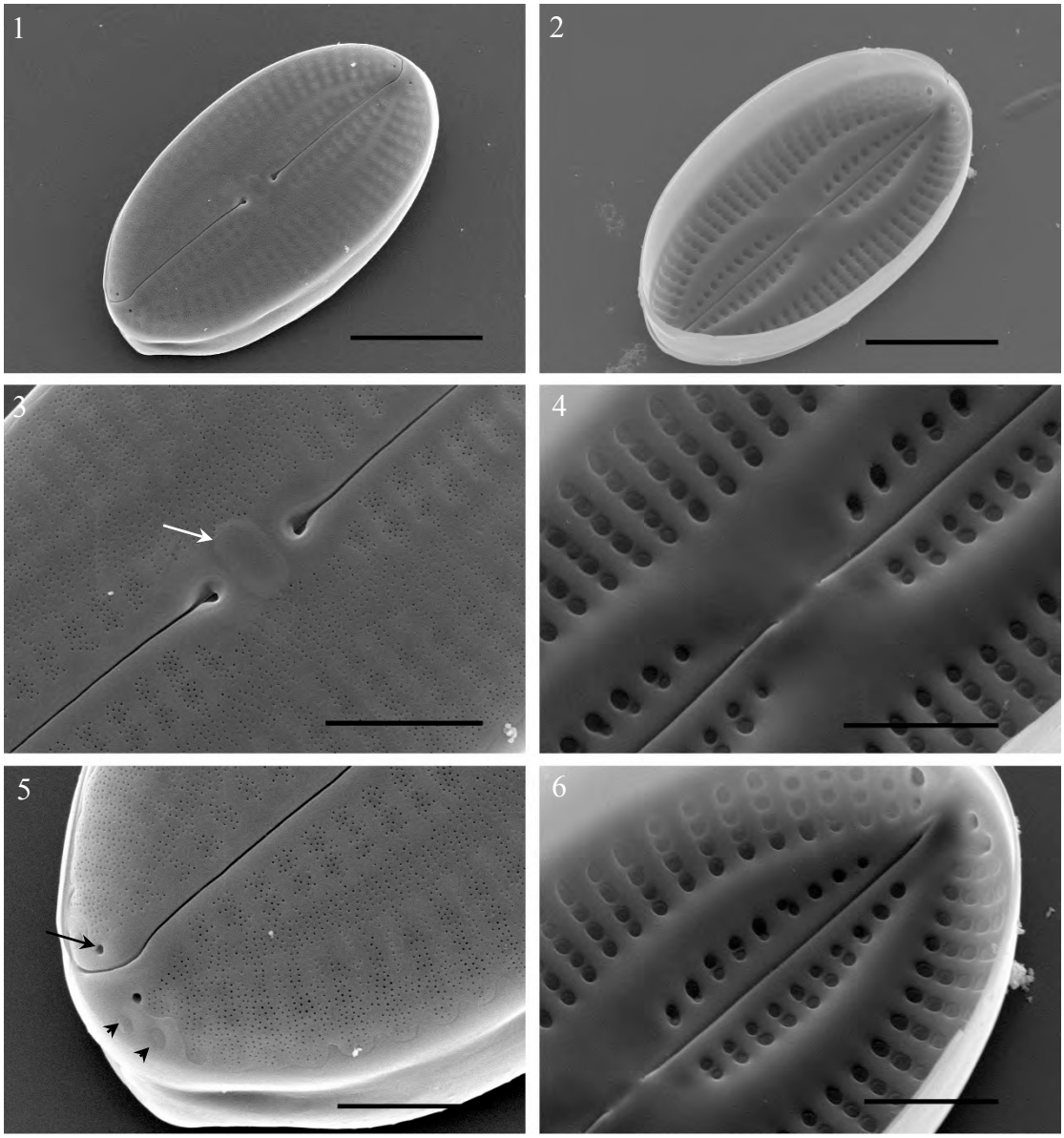

Plate 25. External (Figs 1, 3, 5) and internal (Figs 2, 4, 6) valve view of *Fallacia* cf. *forcipata*. Scale bars = 5 μm (Figs 1, 2) and 2 μm (Figs 3–6).

Figs 1, 2. Whole valves.

Figs 3, 4. Central raphe endings. Note the siliceous block (arrow) between central raphe endings.

Fig. 5. Pole of valve, showing the two small pores (arrow) on both sides of raphe and two areolae (arrowheads) on each side below the pores.

Fig. 6. Internal valve view, showing a small helictoglossa at the distal ending of raphe.

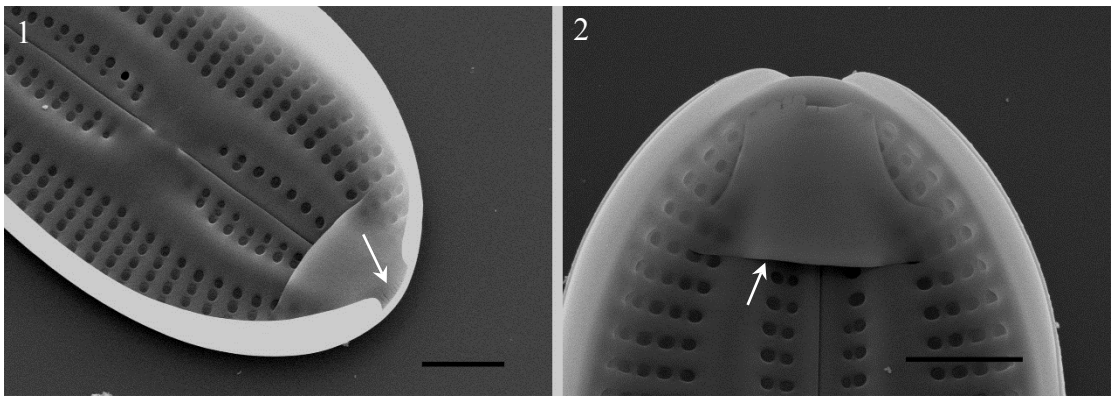

Plate 26. Structure of a cingulum of *Fallacia* cf. *forcipata*. Scale bars = 2 μm.
Fig. 1. Opening (arrow) of the valvocopula.
Fig. 2. A ligula (arrow) of pleura lying on the internal valve surface.

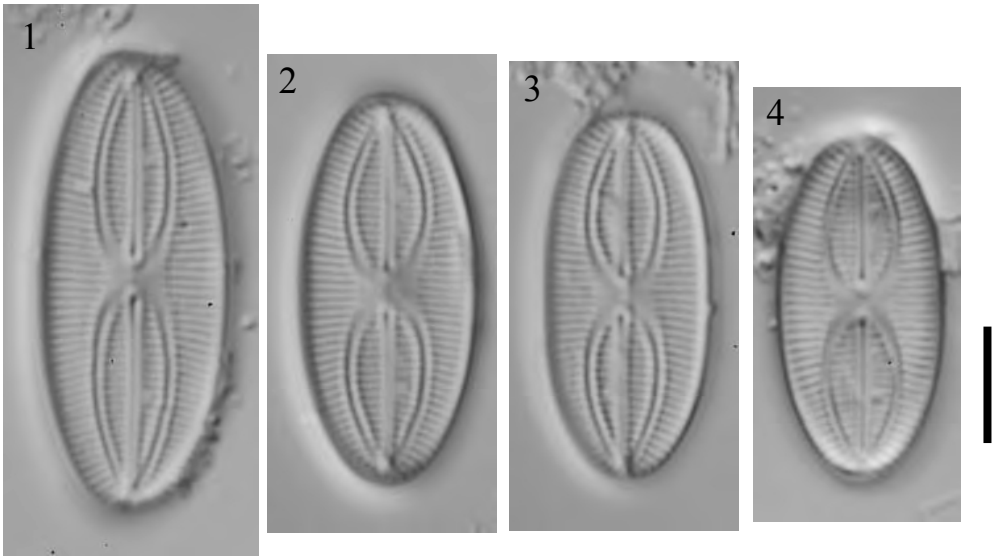

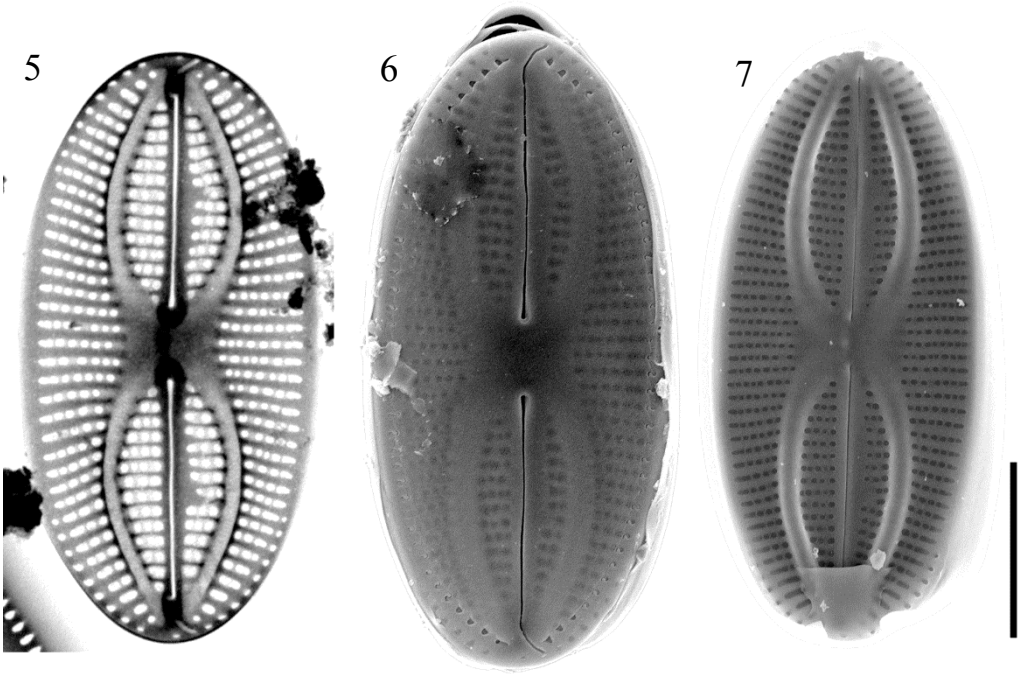

Plate 27. Plain view of valves of *Fallacia decussata* sp. nov. with LM(Figs 1–4), TEM(Fig. 5) and SEM (Figs 6, 7). Scale bars = 5 μm.

Figs 1–4. Light micrographs of cleaned valves.

Fig. 5. Pattern of valve.

Figs 6, 7. External and internal faces of valve.

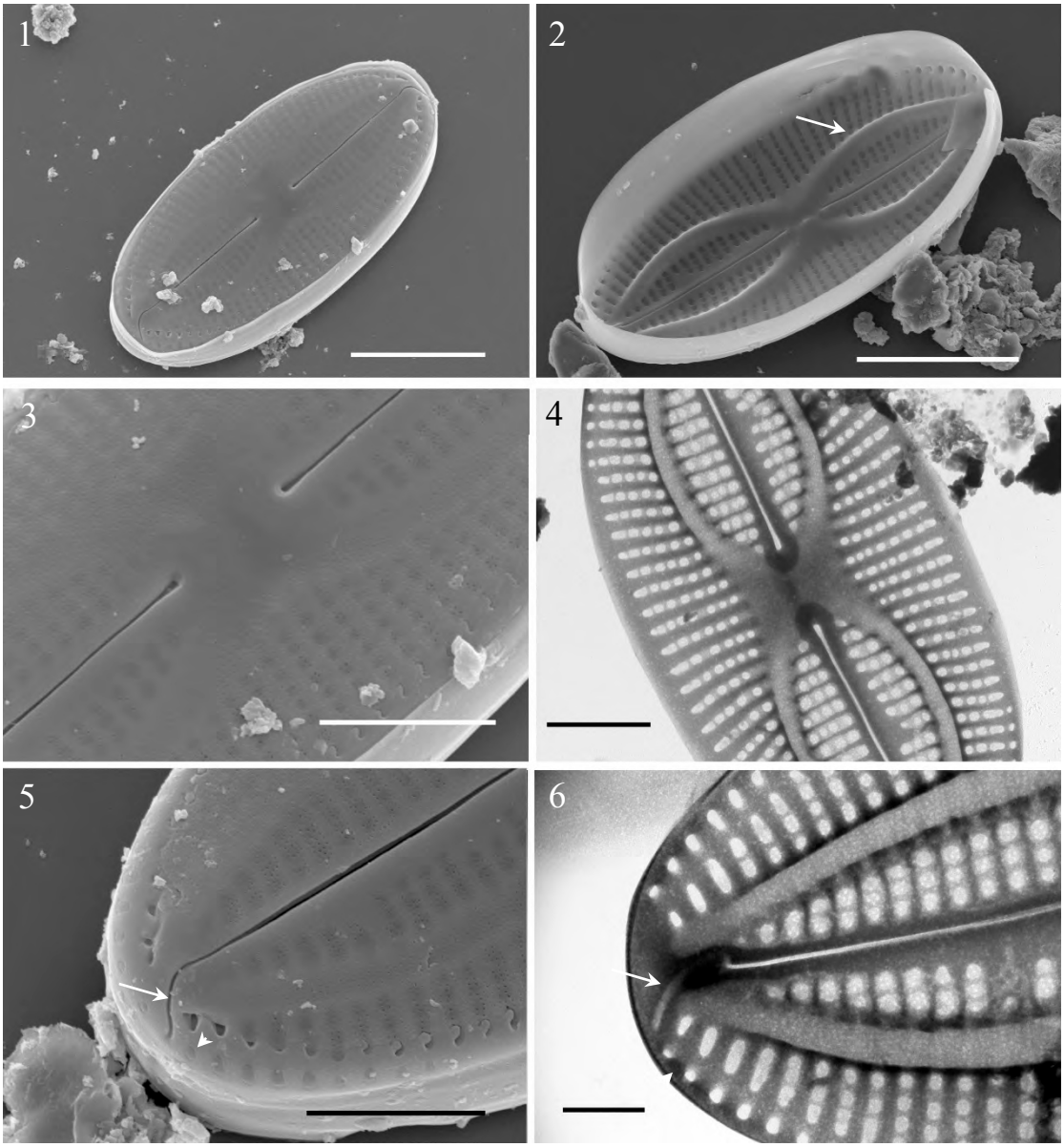

Plate 28. External (Figs 1, 3, 5) and internal (Figs 2, 4, 6) valve view of *Fallacia decussata* sp. nov., Scale bars = 5 µm (Figs 1, 2), 2 µm (Figs 3–6).

Figs 1, 2. Whole valves, showing the remarkable lateral sterna on internal valve face (arrow, Fig. 2).

Figs 3, 4. Central raphe endings.

Figs 5, 6. Poles of valve, showing the hooked terminal fissures (arrows) and areolae (arrow) uncovered by conopea.

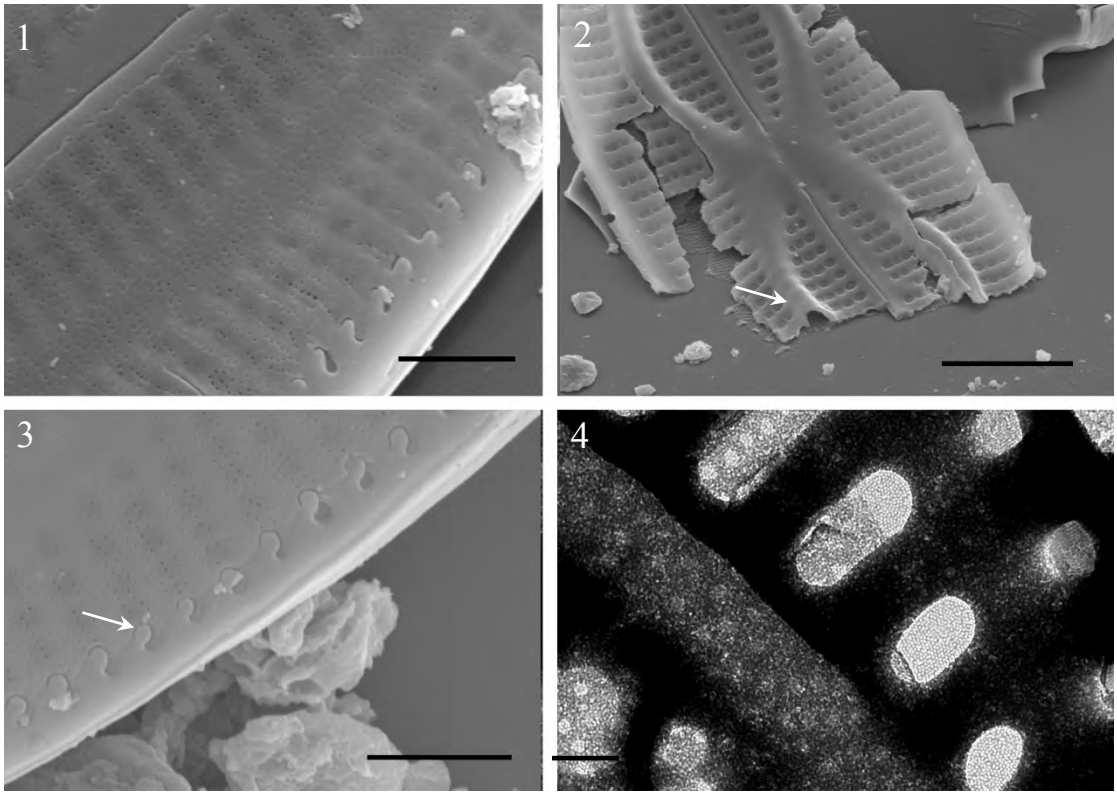

Plate 29. Valve structure *Fallacia decussata* sp. nov., Scale bars = 1 μm (Figs 1, 3), 2.5 μm (Fig. 2), and 200nm (Fig. 4).

Fig. 1. Whole surface was covered by finely porous conopeum.

Fig. 2. Internal view of a broken valve, showing the longitudinal lateral sterna (arrow).

Fig. 3. Pegs (arrows) project from the valve shoulder.

Fig. 4. Areolae occlusion: hymens with hexagonal array perforation.

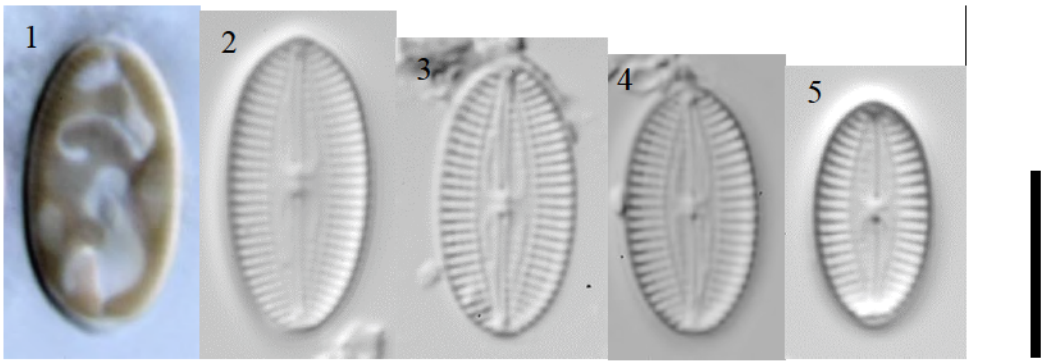

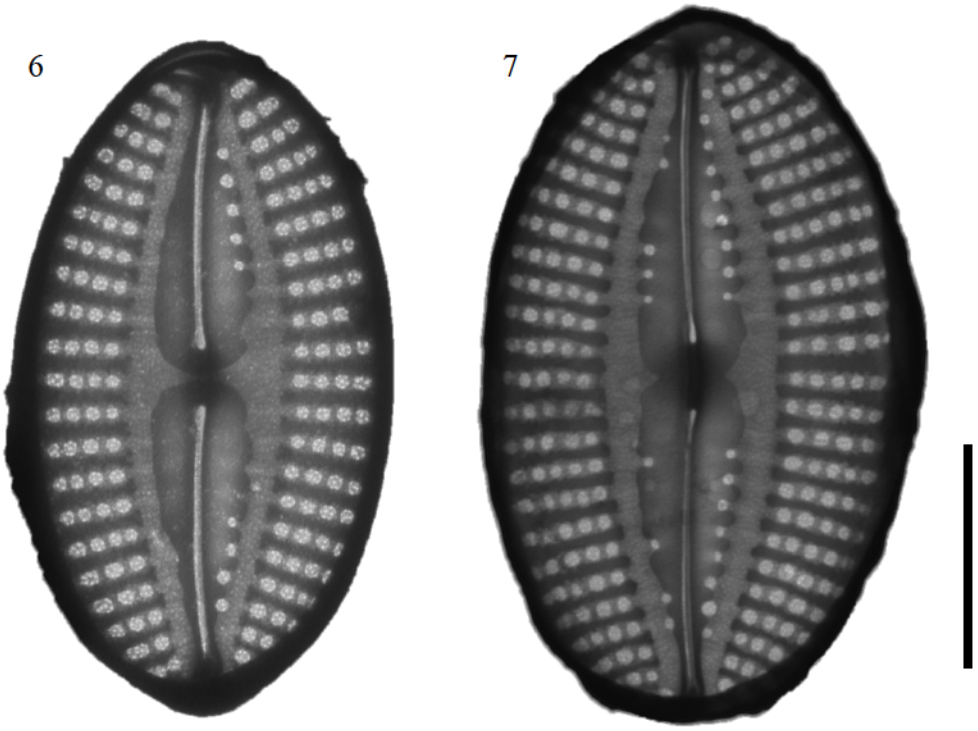

Plate 30. Plain views of vegetative cells and valves of *Fallacia nodulifera* sp. nov. , Scale bars =10 µm (Figs 1–5) and 5 µm (Fig. 6, 7).

Fig. 1. Chloroplast.

Figs 2–5.Cleand valves.

Figs 6, 7. Pattern of valve.

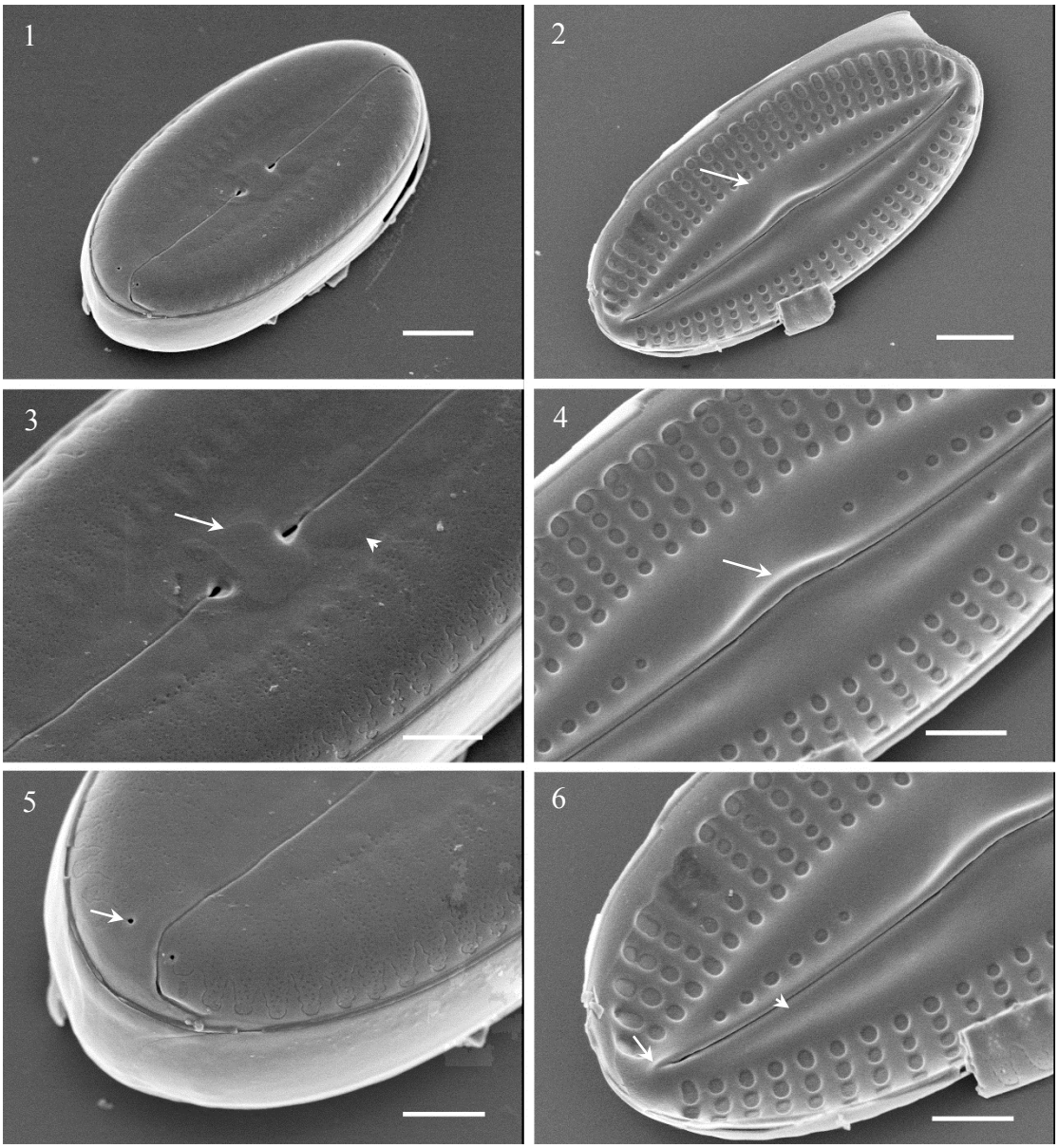

Plate 31. External (Figs 1, 3, 5) and internal (Figs 2, 4, 6) valve views of *Fallacia nodulifera* sp. nov. , Scale bars = 2 μm (Figs 1, 2) and 1 μm (Figs 4–6).

Figs 1, 2. Whole valves. Note the centrally convex lateral sterna (arrow).

Fig. 3. External central raphe endings expanded forming a water drop like pores. Note the siliceous block (arrow) between the central endings and slightly thicken layer (arrowhead) around the raphe branches.

Fig. 4. Central nodule presenting at central area. The central raphe endings hided in this nodule.

Fig. 5. External view of valve pole, showing the tiny pores (arrow), one on both sides of raphe.

Fig. 6. Polar raphe endings forming a small helictoglossa (arrow), Note the missing areolae on one side of raphe (arrowhead).

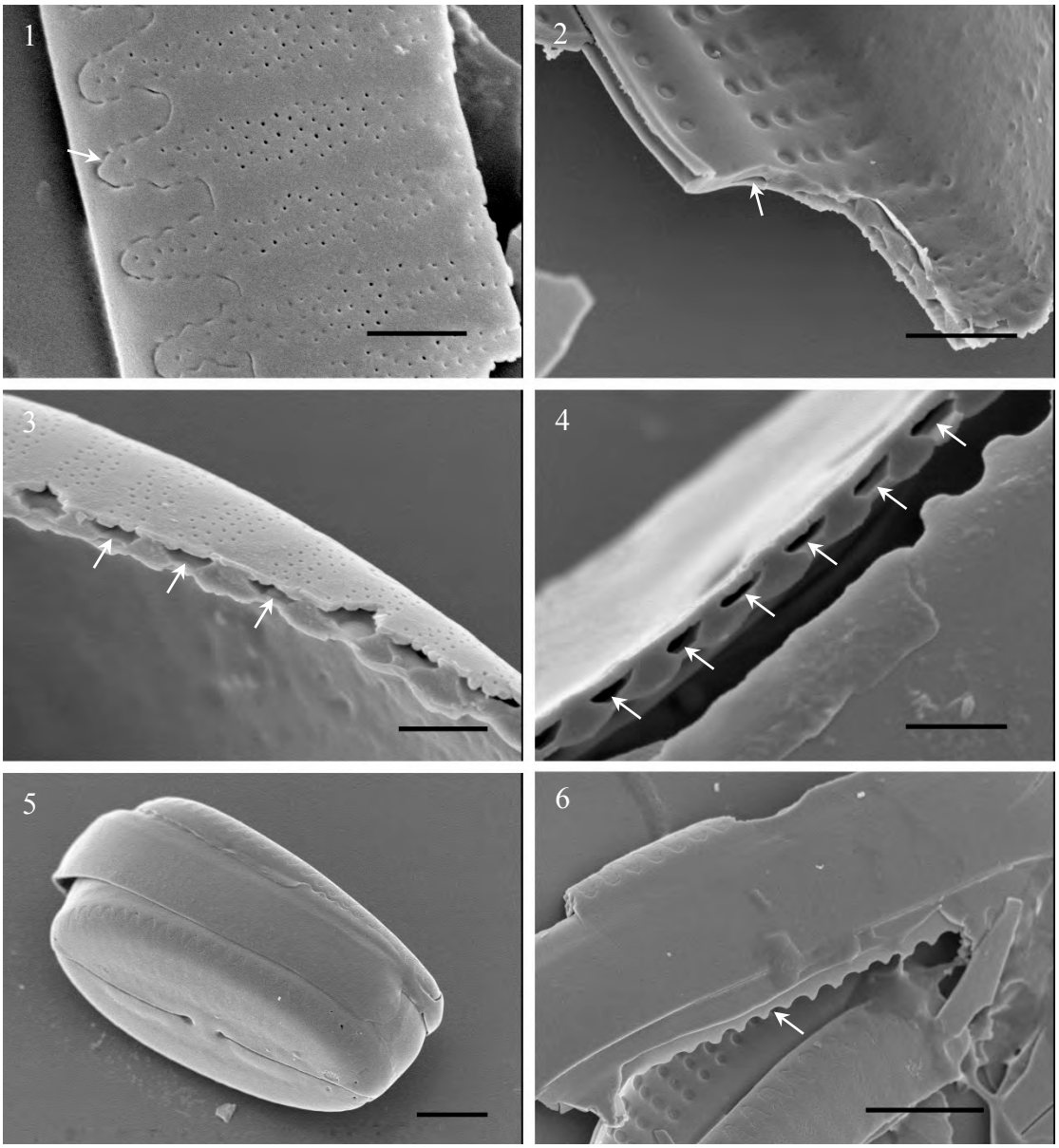

Plate 32. Valve structure of *Fallaica nodulifera* sp. nov. , Scale bars = 500nm (Figs 1, 3, 4), 1 μm (Fig. 2) and 2 μm (Figs 5, 6).

Fig. 1. Finely porous conopeum with finger-liked edge (arrow).

Fig. 2. Lumen (arrow) between sterna and conopeum.

Figs 3, 4. Canals (arrows) between conopeum and primary valve layer.

Figs 5, 6. Valvocopula with a wave-shaped margin (arrow).

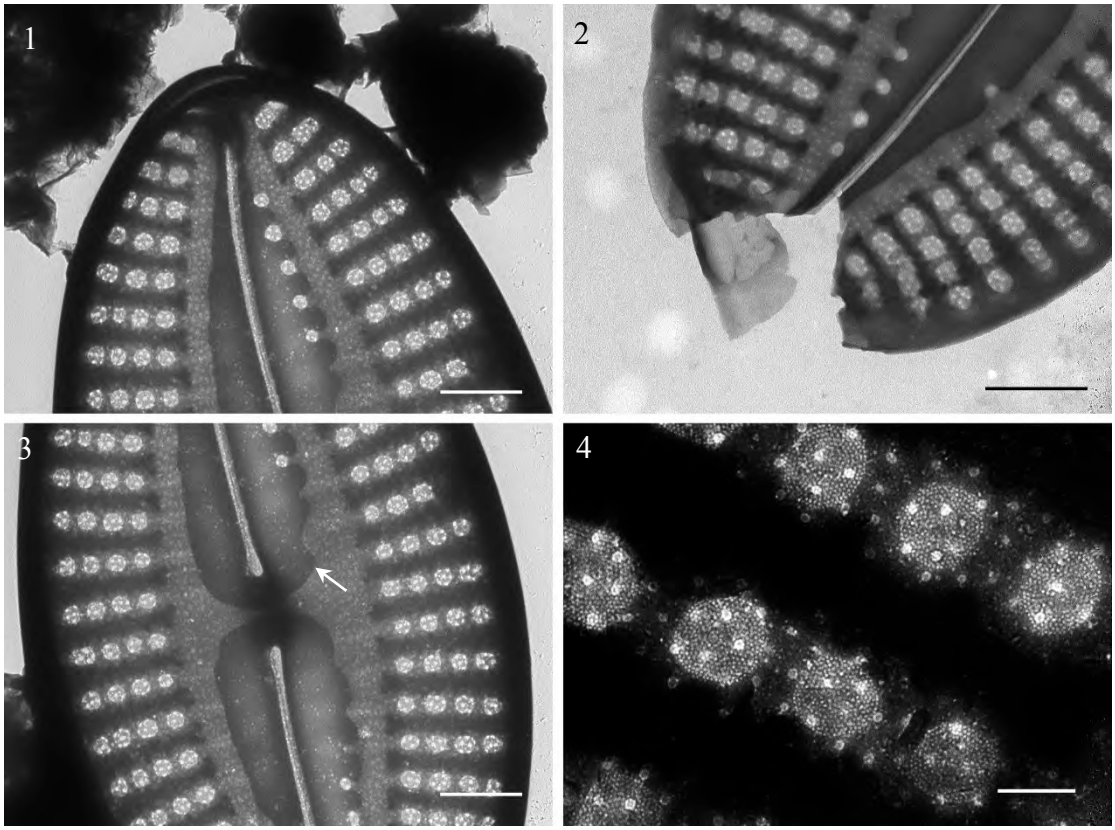

Plate 33. Valve structure of *Fallacia nodulifera* sp. nov. with TEM. Scale bars = 1 μm (Figs 1–3) and 200nm (Fig. 4).

Fig. 1. Asymmetric longitudinal uniseriate areolae adjacent with raphe.

Fig. 2. Broken terminal of valve, showing the two layer of valve.

Fig. 3. Central area of valve, showing the thick siliceous layer (arrow) around the raphe.

Fig. 4. Areolae occluded by hymen with centric arrayed perforations.

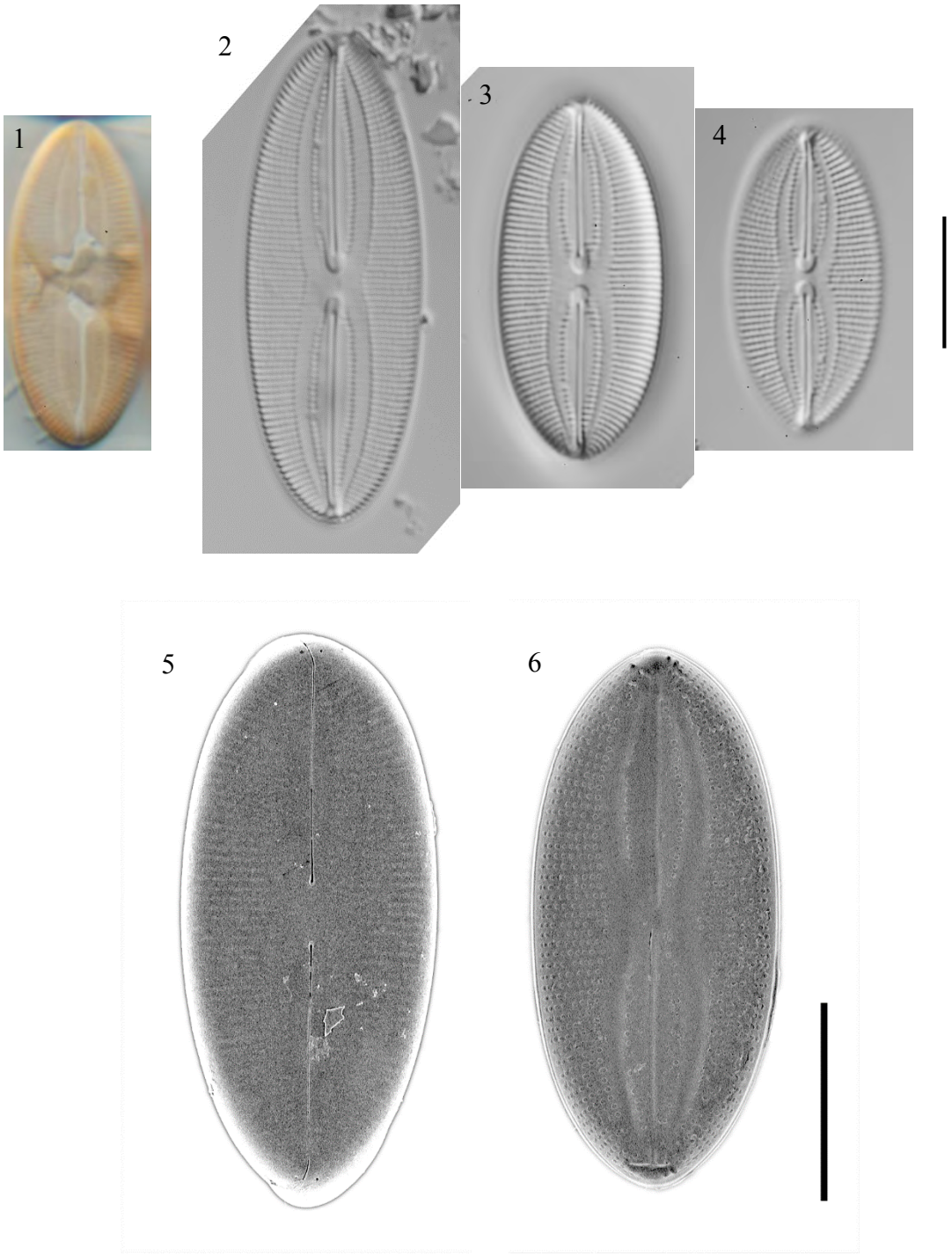

Plate 34. Plain views of vegetative cells and valves of *Fallacia tateyamensis* sp. nov. Scale bars = 10 μm.

Fig. 1. Chloroplasts consisted of two connected plates.

Figs 2–4. Cleaned valves.

Fig. 5. External and internal faces of valve.

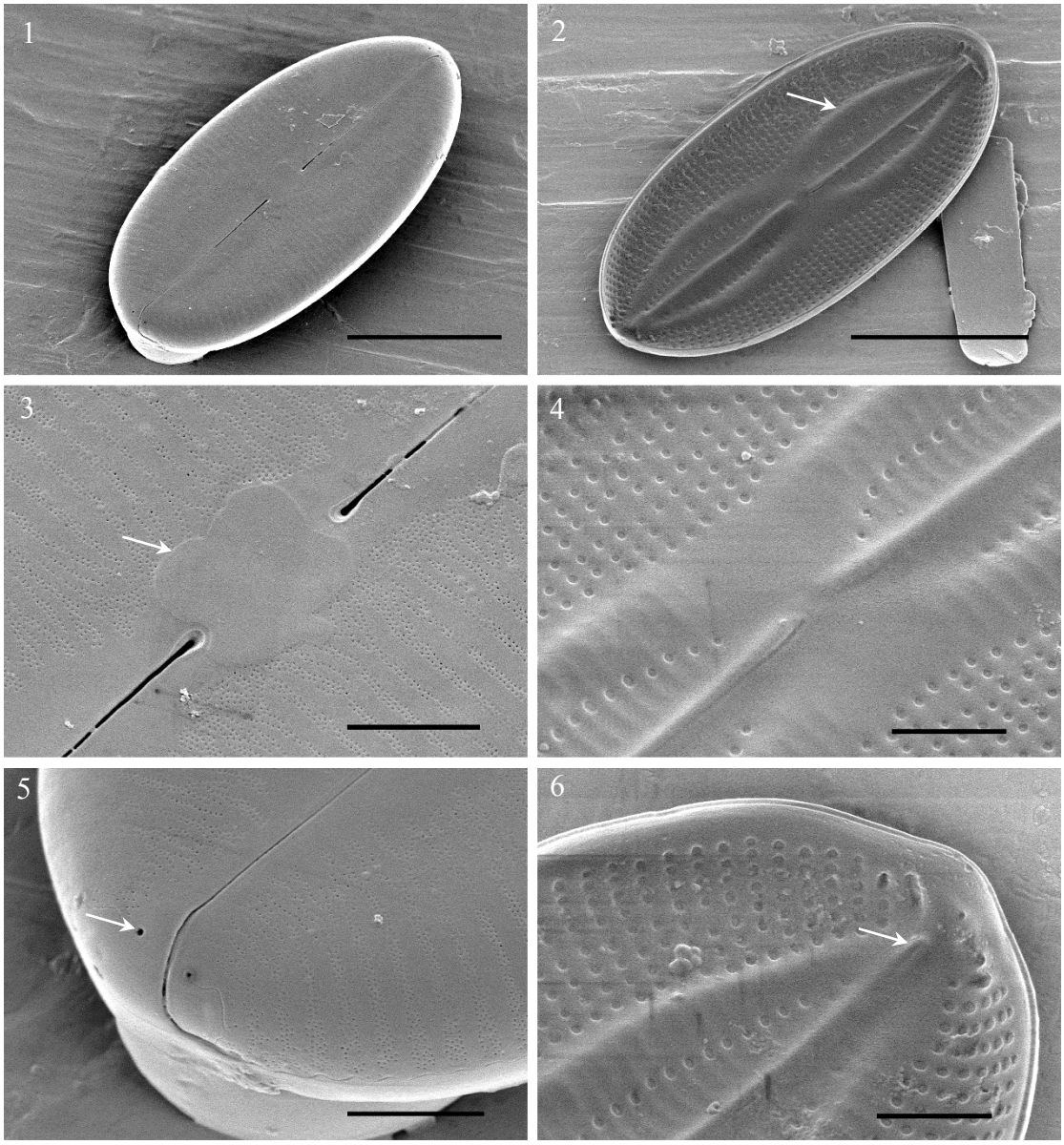

Plate 35. External (Figs 1, 3, 5) and internal (Figs 2, 4, 6) valve views of *Fallacia tateyamensis* sp. nov. , Scale bars = 10 μm (Figs 1, 2) and 2 μm (Figs 3–6).

Figs 1, 2. Whole valves, note the centrally constrict lyre shaped lateral sterna (arrow) on internal valve face.

Figs 3, 4. Central raphe endings, showing the thick siliceous block (arrow).

Fig. 5. Pole of valve, showing the buoyant terminal fissure and two tiny pores (arrow).

Fig. 6. Internal pole raphe ending, showing the small helictoglossa (arrow).

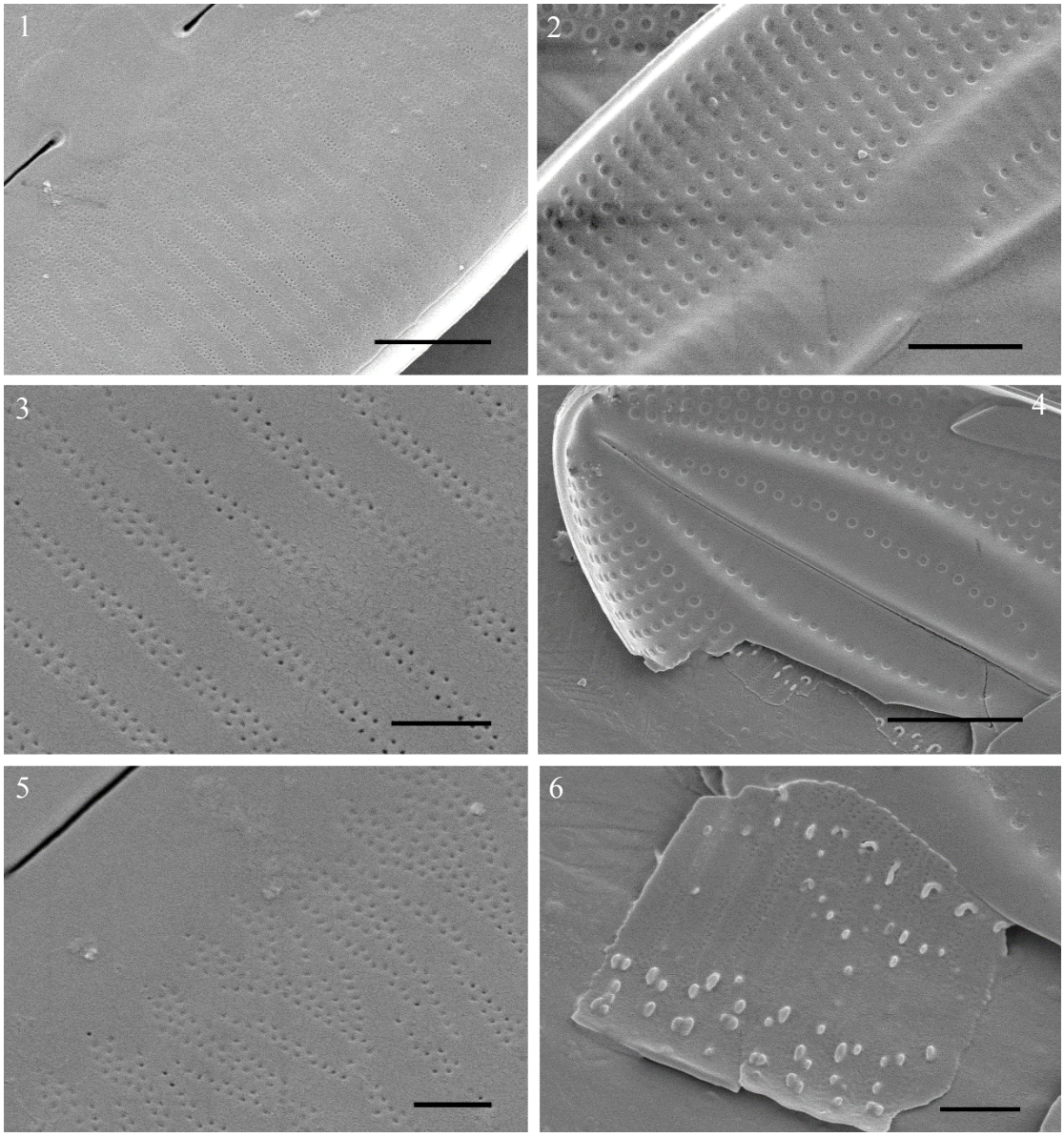

Plate 36. Valve structure of *Fallacia tateyamensis* sp. nov. , Scale bars = 2 μm (Figs 1, 2, 4), 1 μm (Fig. 6) and 500nm (Fig. 3).

Fig. 1. Primary valve layer is covered by finely porous conopeum.

Fig. 2. Uniseriate striae.

Fig. 3, 5. Fine pores on the conopeum are well arranged.

Fig. 4, Lumen between conopeum and primary valve layer.

Fig. 5. Internal face of a piece of conopeum.

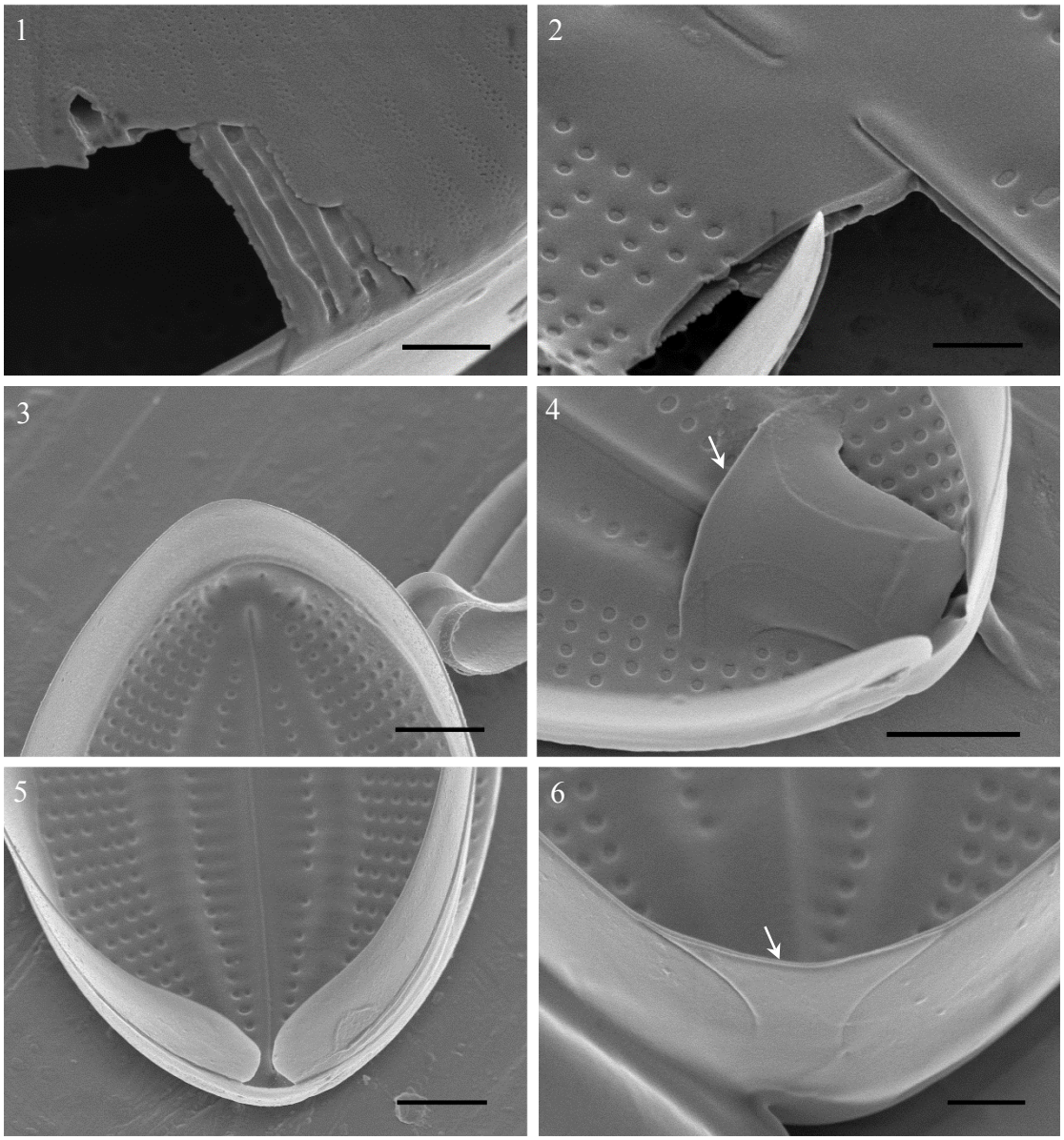

Plate 37. Valve structure and a cingulum of *Fallacia tateyamensis* sp. nov. , Scale bars = 1 μm (Figs1, 2, 6), and 2 μm (Figs 3–5).

Figs 1, 2. Lumen between conopeum and primary valve layer, showing the through-like depression between virgae.

Figs 3–6. Cingulum consisted of a valvocopula and a pleura (arrow, Fig. 4).

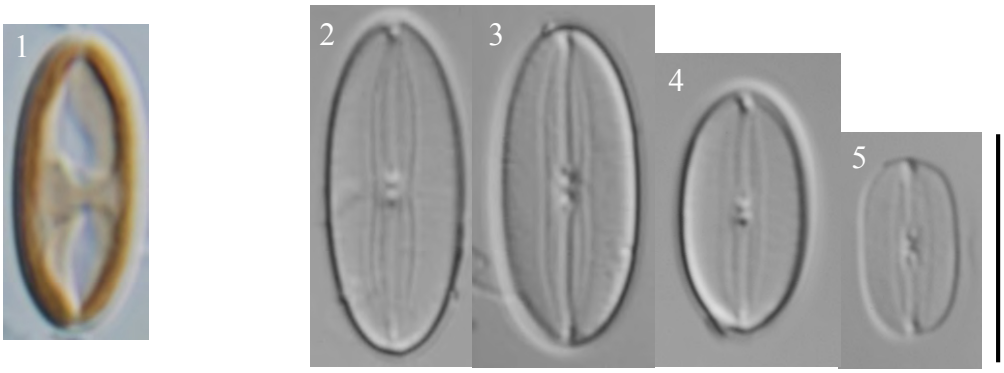

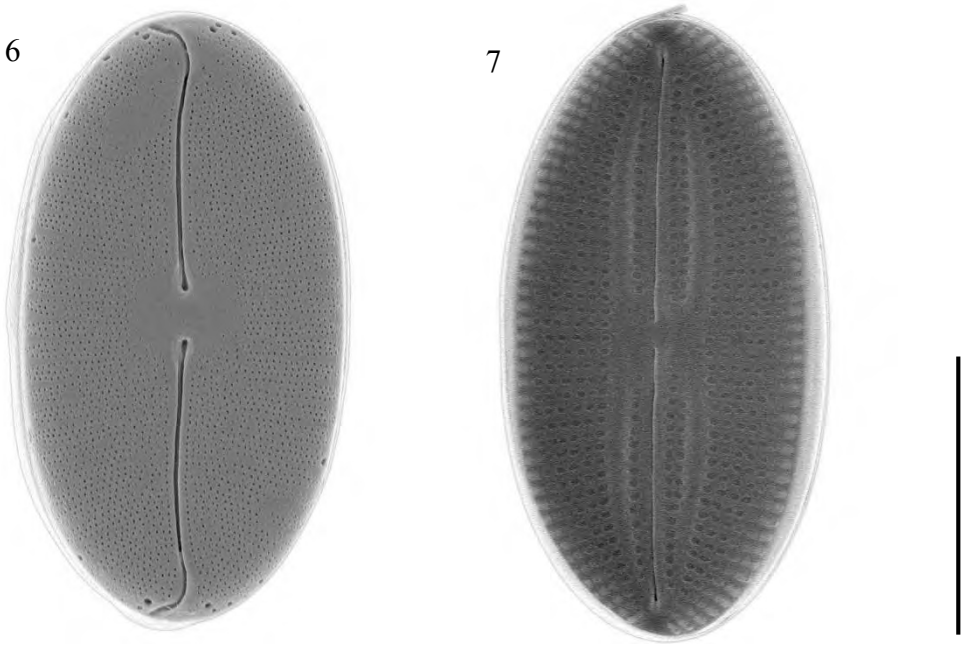

Plate 38. Plain views of vegetative cells and valves of *Fallacia laevis* sp. nov. with LM (Figs 1–5) and SEM (Figs 6, 7). Scale bars = 5 μm.

Fig. 1. A basic H-shaped chloroplast.

Figs 2–5. Cleaned valves.

Figs 6, 7. External and internal valve faces.

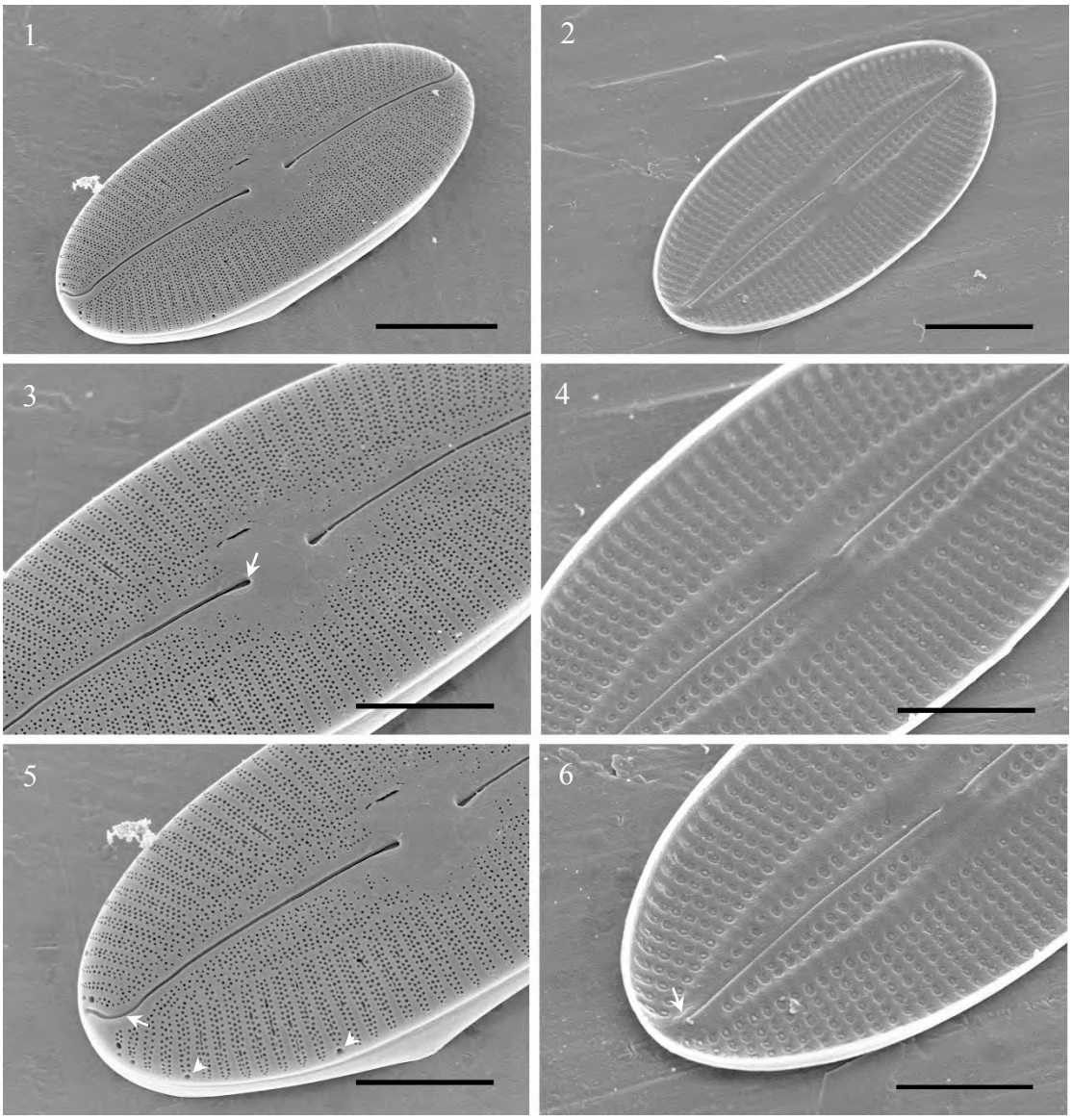

Plate 39. External (Figs 1, 3, 5) and internal (Figs 2, 4, 6) valve views of *Fallacia laevis* sp. nov. . Scale bars = 5 μm (Figs 1, 2) and 2 μm (Figs 3–5).

Figs 1, 2. Whole valves.

Fig. 3. Slightly expanded external central raphe endings (arrow), surround by a sallow circular groove.

Fig. 4. Slightly deflect internal central endings.

Fig. 5. Pole of valve, showing the curved terminal raphe fissure (arrow) and a number of pores (arrowheads) around the valve.

Fig. 6. Polar raphe ending, showings a small helictoglossa (arrow) and laterally asymmetric areolae between raphe and sterna.

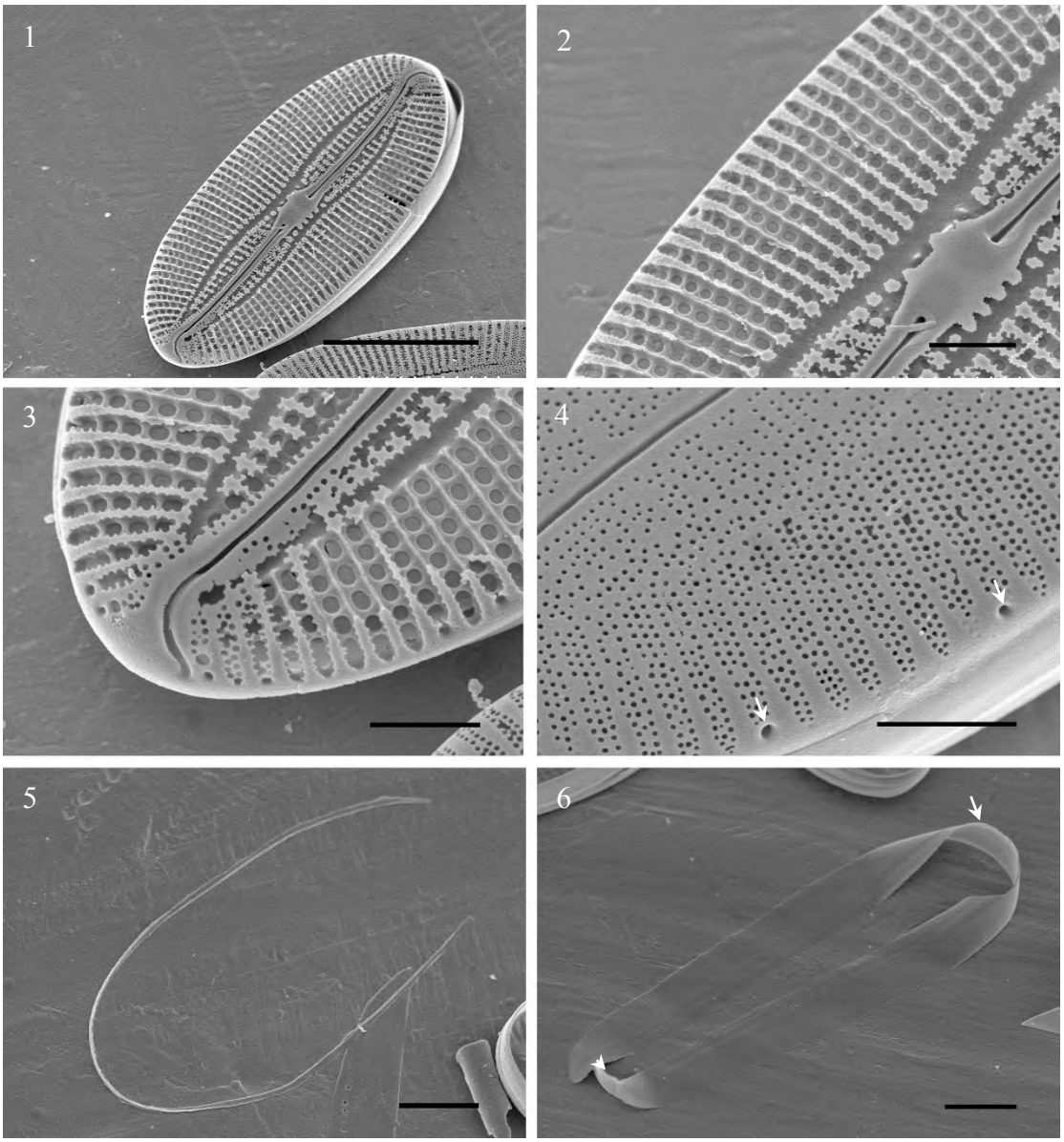

Plate 40. Valve structure of *Fallacia laevis* sp. nov. . Scale bars = 5 μm (Fig. 1) and 1 μm (Figs 2–6).

Fig. 1. A valve with formatting conopeum.

Fig. 2. Uniseriate striae without covering by the conopeum.

Fig. 3. Pole of valve, showing the pore besides the raphe.

Fig. 4. Striae are covered by finely porous conopeum, showing the tiny pores on the shoulder of valve (arrows).

Fig. 5. Thin pleura.

Fig. 6. Open valvocopula (arrow) with a ligula (arrowhead).

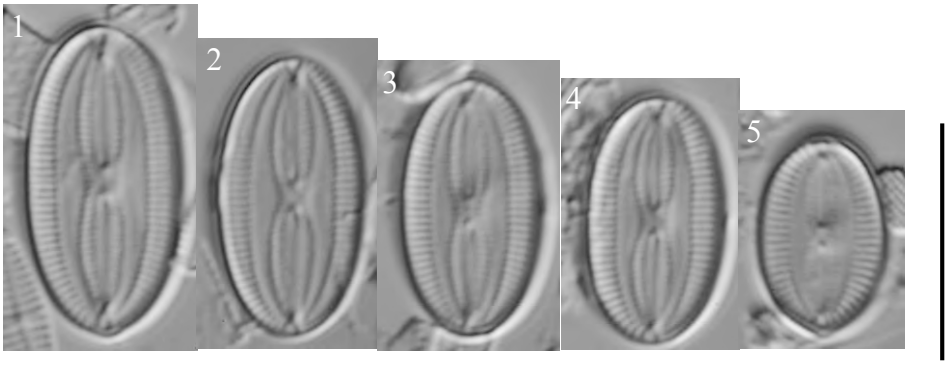

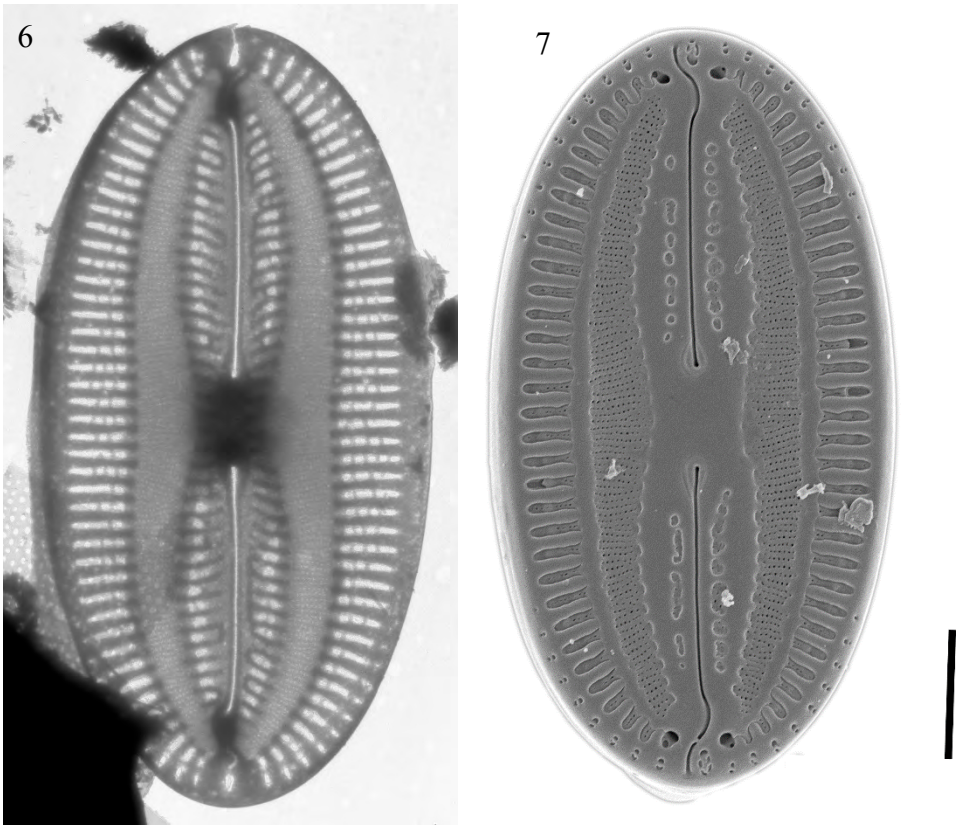

Plate 41. Plain views of valves of *Fallacia oculiformis* var. *miyajimensis* var. nov. with LM (Figs 1–5), TEM (Fig. 6) and SEM (Fig. 7). Scale bars = 10 μm (Figs 1–5) and 2 μm (Figs 6–7).

Figs 1–5. Cleaned valves.

Figs 6, 7. The detailed pattern of valves.

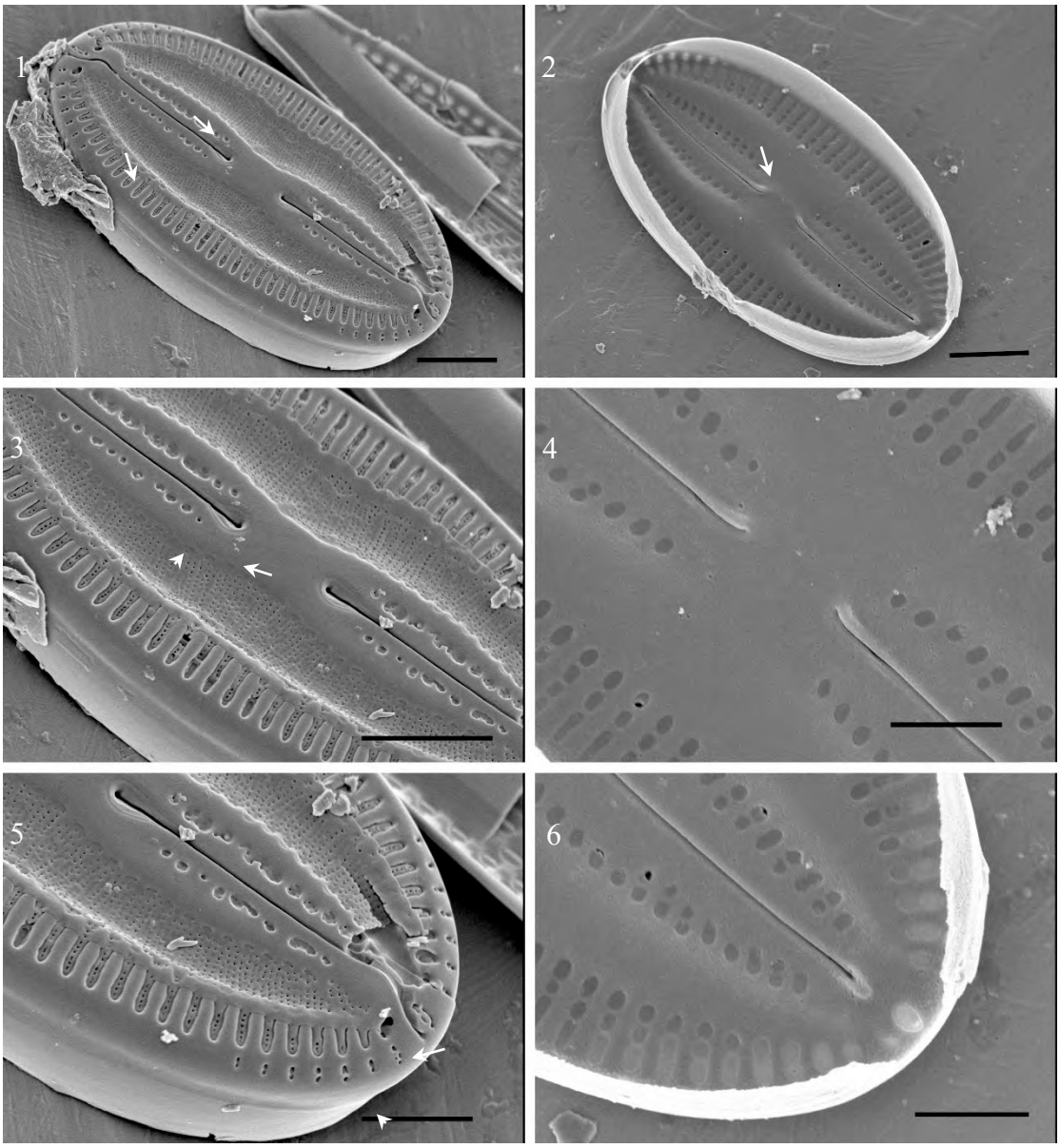

Plate 42. External (Figs 1, 3, 5) and internal (Figs 2, 4, 6) valve view of *Fallacia oculiformis var. miyajimensis* var. nov. . Scale bars = 1 μm (Figs 1–3) and 2 μm (Figs 4–6).

Fig. 1. Whole valve face, showing the lateral depressed finely porous conopea (arrow).

Fig. 2. Whole valve face, showing the relatively wide lateral sterna (arrow).

Fig. 3. Slightly expanded central raphe endings (arrow), surrounding by sallow circular groove. Note the pores beside the raphe branches (arrowhead).

Fig. 4. Deflect central raphe endings.

Fig. 5. Pole of valve, showing the waved terminal fissure of raphe (arrow) and tiny pores (arrowhead) on the valve shoulder.

Fig. 6. Pole raphe endings forming a small helictoglossae (arrow). Note the pole (arrowhead) on top of it.

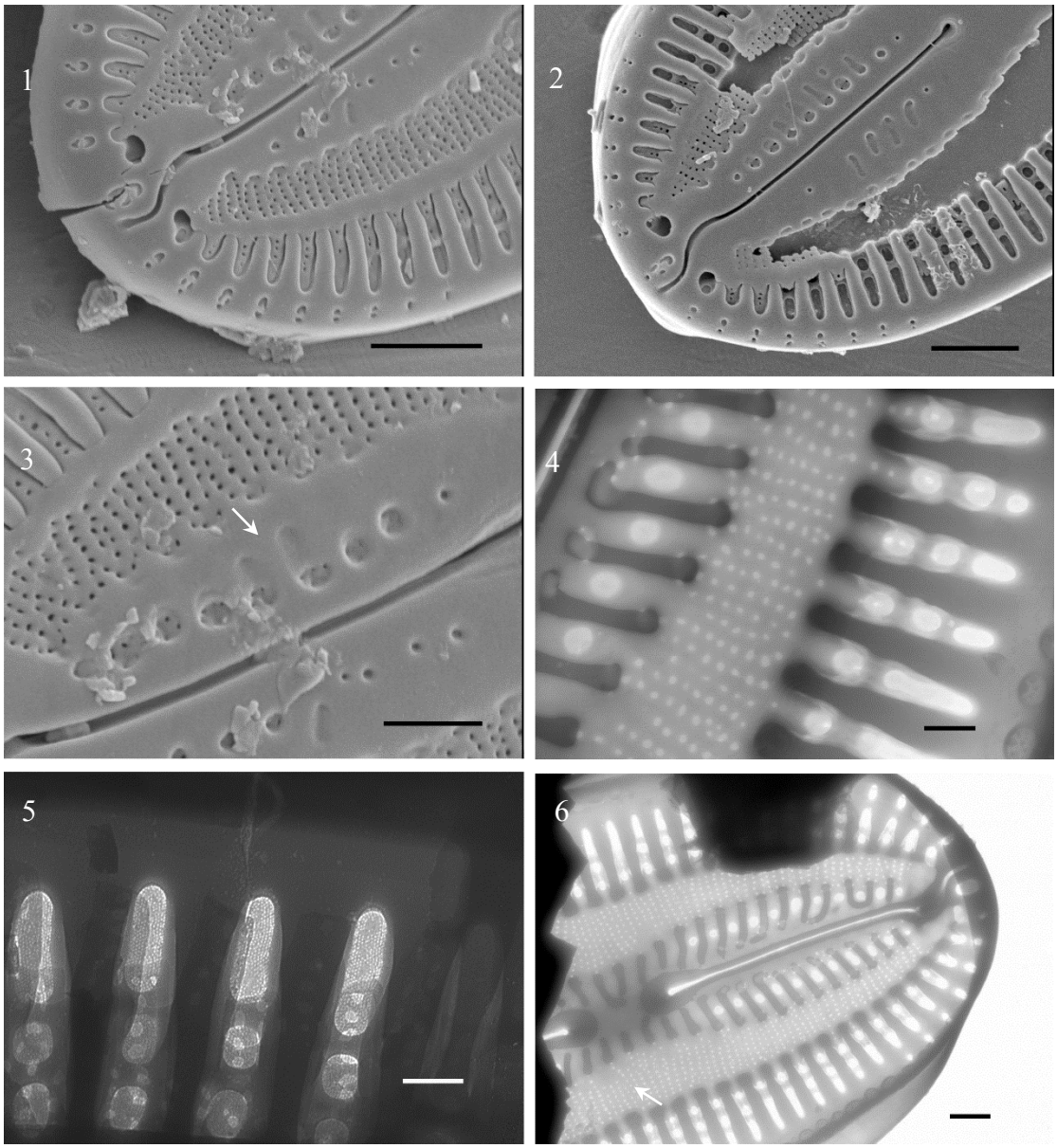

Plate 43. Valve structure of *Fallacia oculiformis* var. *miyajimensis* var. nov. .
Scale bar =1 μm (Figs 1, 2), 500nm (Fig. 3, 6) and 200nm (Fig. 4, 5).

Figs 1, 2. Lateral finely porous conopea and structurs beneath the conopea.

Fig. 3. The thin siliceous layer above the conoepea (arrow).

Fig. 4. The siliceous ribs extending from valve mantle and near the raphe.

Fig. 5. Areolae occluded by hymen with hexagonal arrayed perforations.

Fig. 6. Ribs at axial area and central area (arrow).

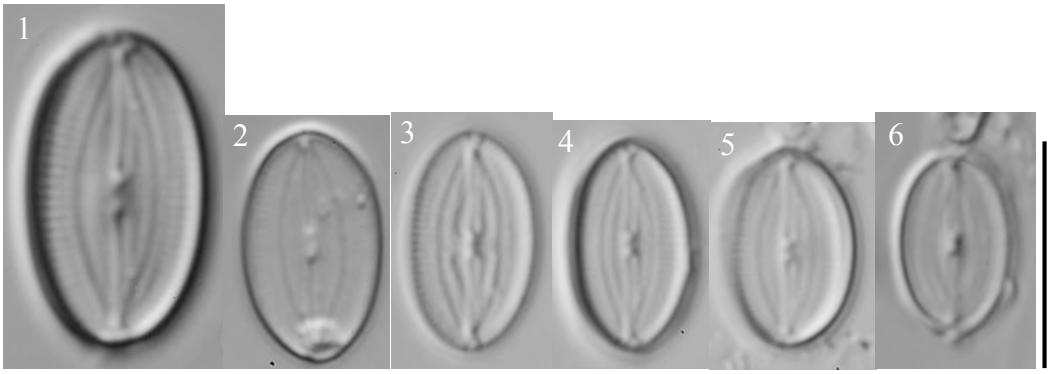

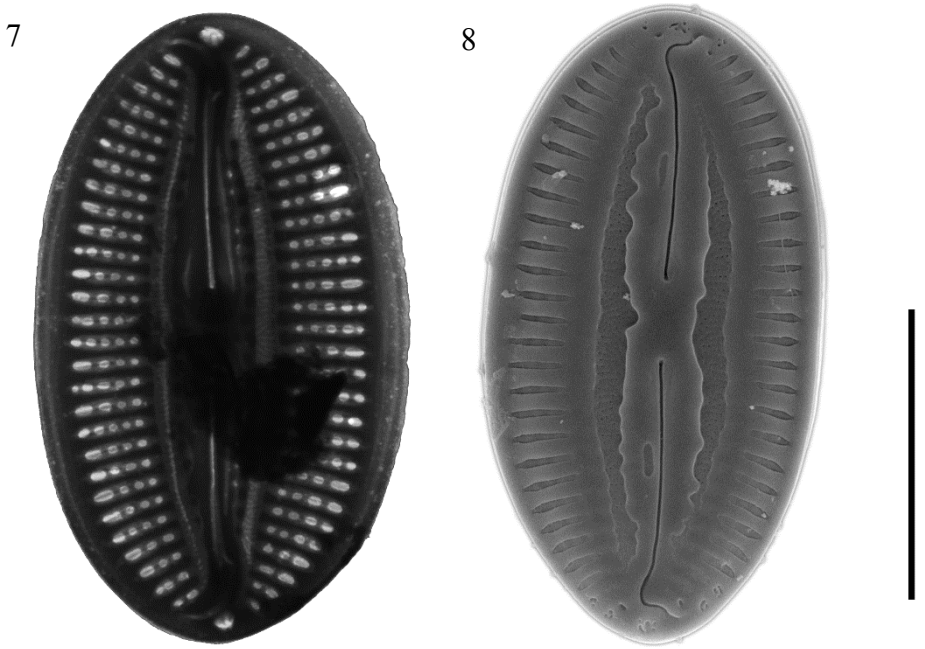

Plate 44. Plain views of valves of *Fallacia florinae* with LM (Figs 1–6), TEM (Fig. 7) and SEM (Fig. 8). Scale bars = 10 μm (Figs 1–6) and 5 μm (Figs 7, 8).

Figs 1–6. Cleaned valves.

Figs 7, 8. Detailed pattern of valve.

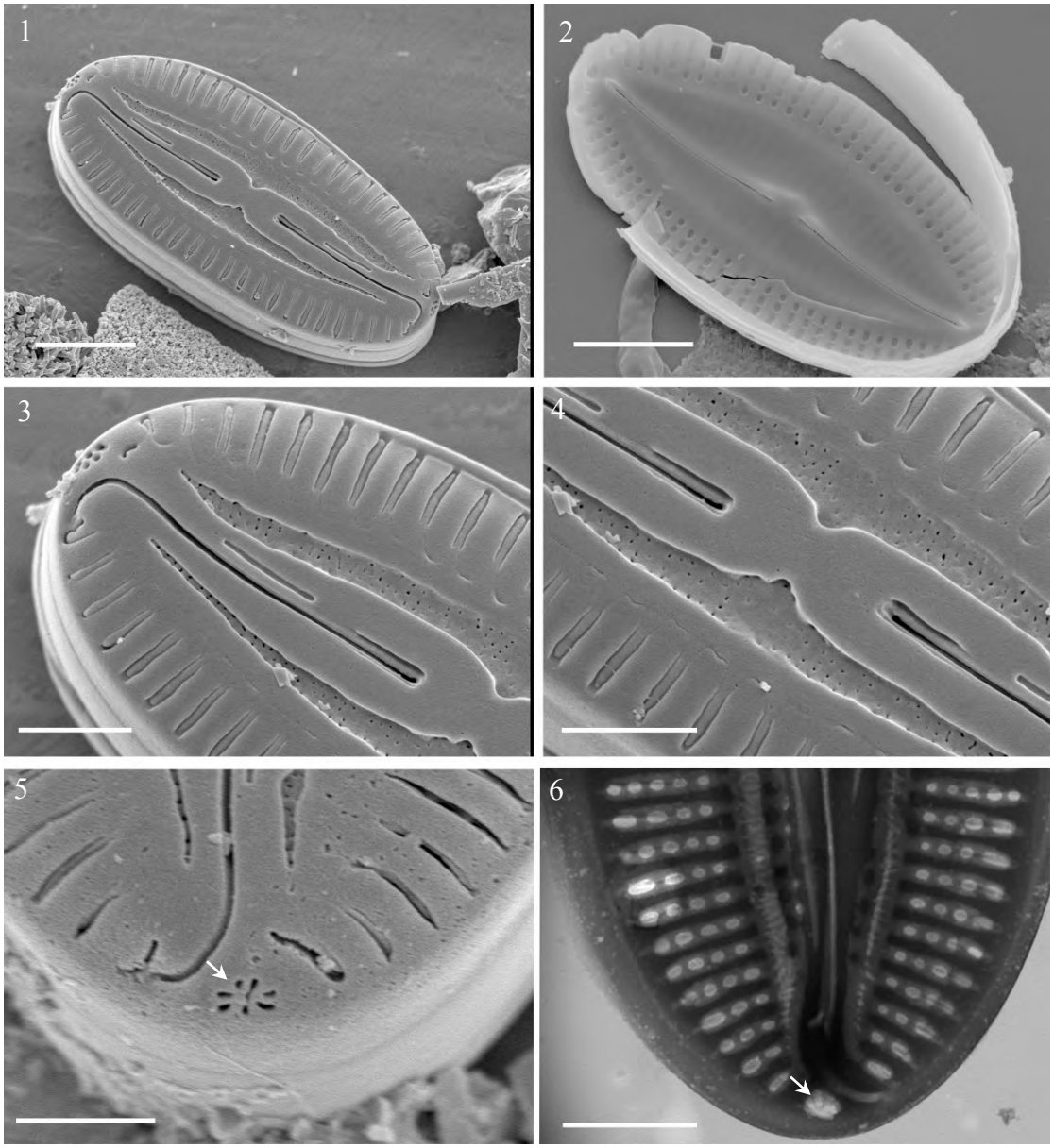

Plate 45. Valve structure of *Fallacia florinae.* Scale bars = 2 μm (Figs 1, 2) and 1 μm (Figs 4–6).

Figs 1, 2. External and internal view of valves.

Figs 3, 4. Axial area with thicken siliceous layer.

Figs 5, 6. Terminal of valve, showing the terminal pore (arrows) composed of radiated short slits.

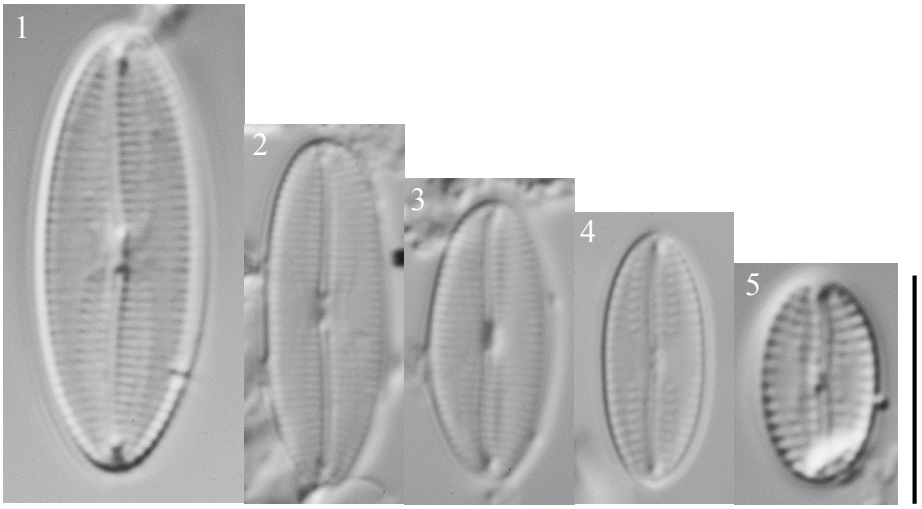

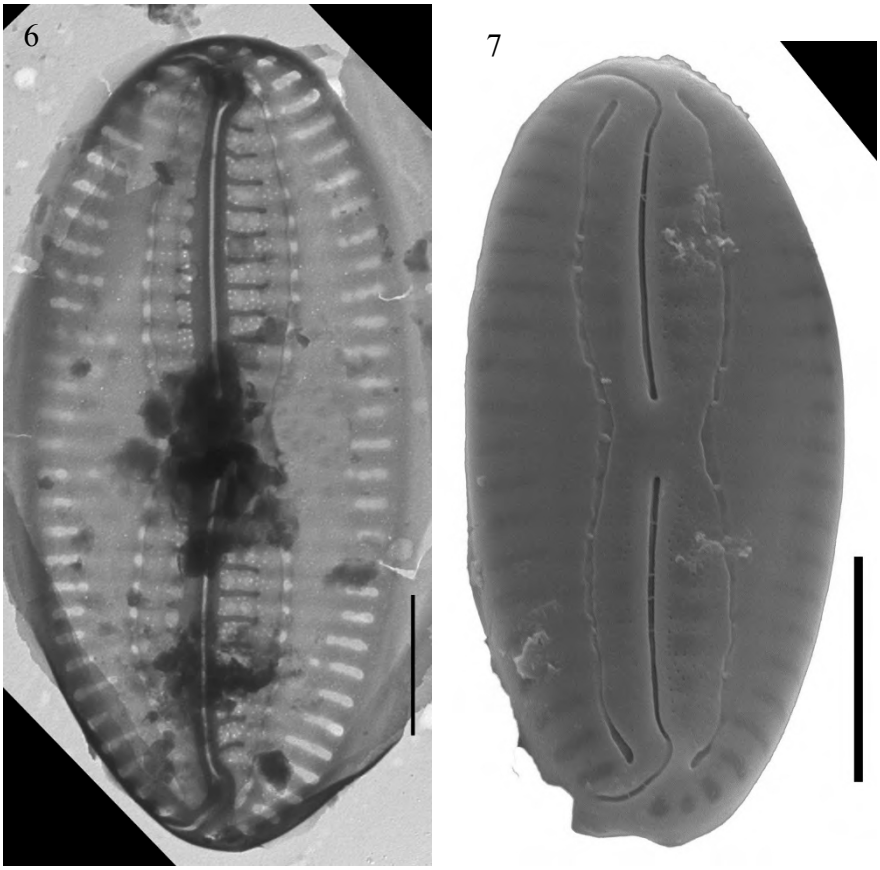

Plate 46. Plain views of valves of *Fallacia teneroides* with LM (Figs 1–5), TEM (Fig. 6) and SEM (Fig. 7). Scale bars = 1 μm (Figs 1–5) and 2 μm (Figs 6, 7).

Figs 1–5. Cleaned valves.

Figs 6, 7. Detailed pattern of valves.

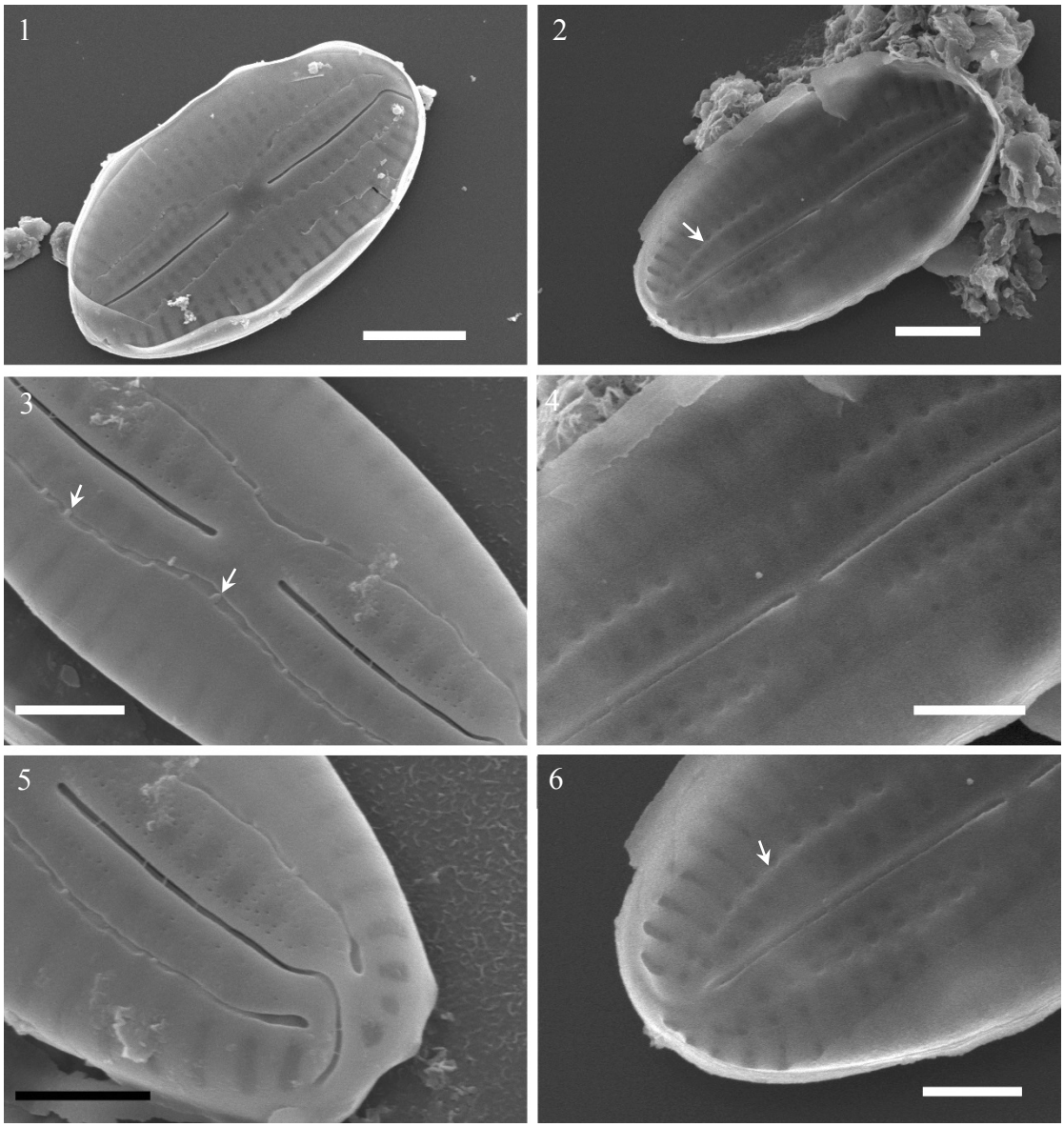

Plate 47. External (Figs 1, 3, 5) and internal (Figs 2, 4, 6) valve view of *Fallacia teneroides*. Scale bars = 2 μm (Figs 1, 2) and 1 μm (Figs 3–6).

Figs 1, 2. Whole valves.

Figs 3, 4. Straight central raphe endings. Note the small "pegs" (arrows).

Fig. 5. Pole of valve, showing the strongly hooked terminal fissures and unfused edge (arrow) of conopea.

Fig. 6. Pole of valve, showing the position of lateral sterna (arrow).

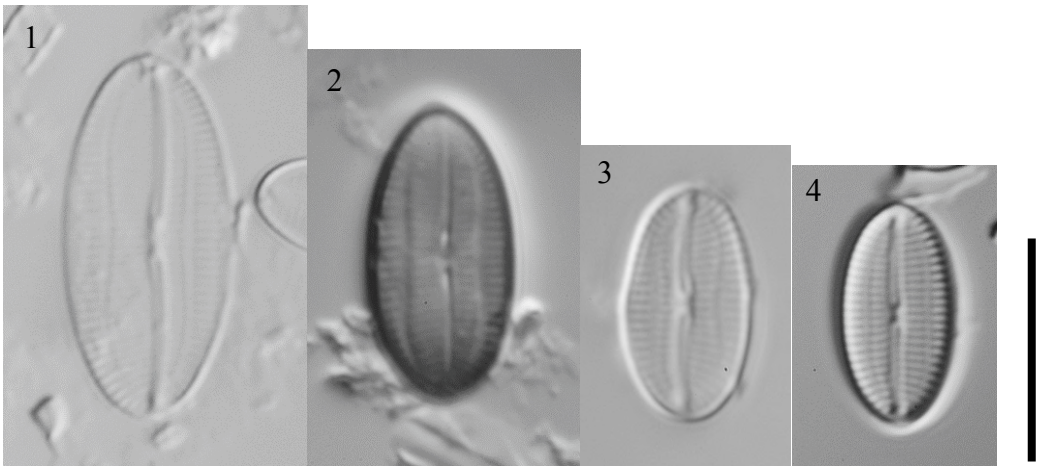

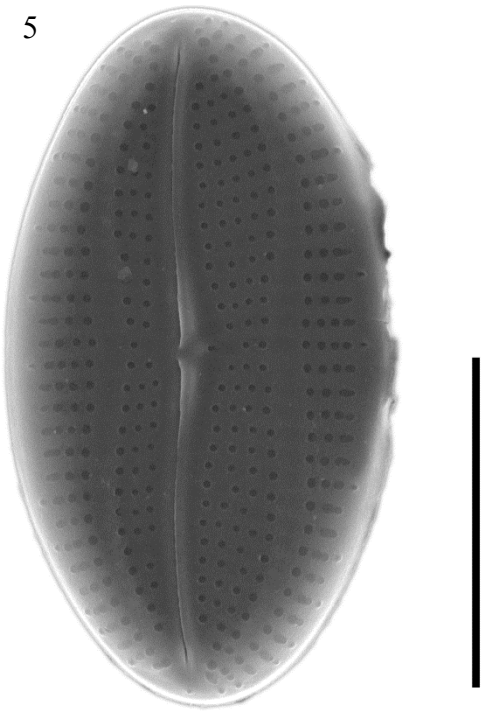

Plate 48. Plain views of valves of *Fallacia inscriptura* with LM (Figs 1–4) and SEM (Fig. 5). Scale bars = 10 µm (Figs 1–4) and 5 µm (Fig. 5).

Figs 1–4. Cleaned valves.

Fig. 5. Internal surface of valve.

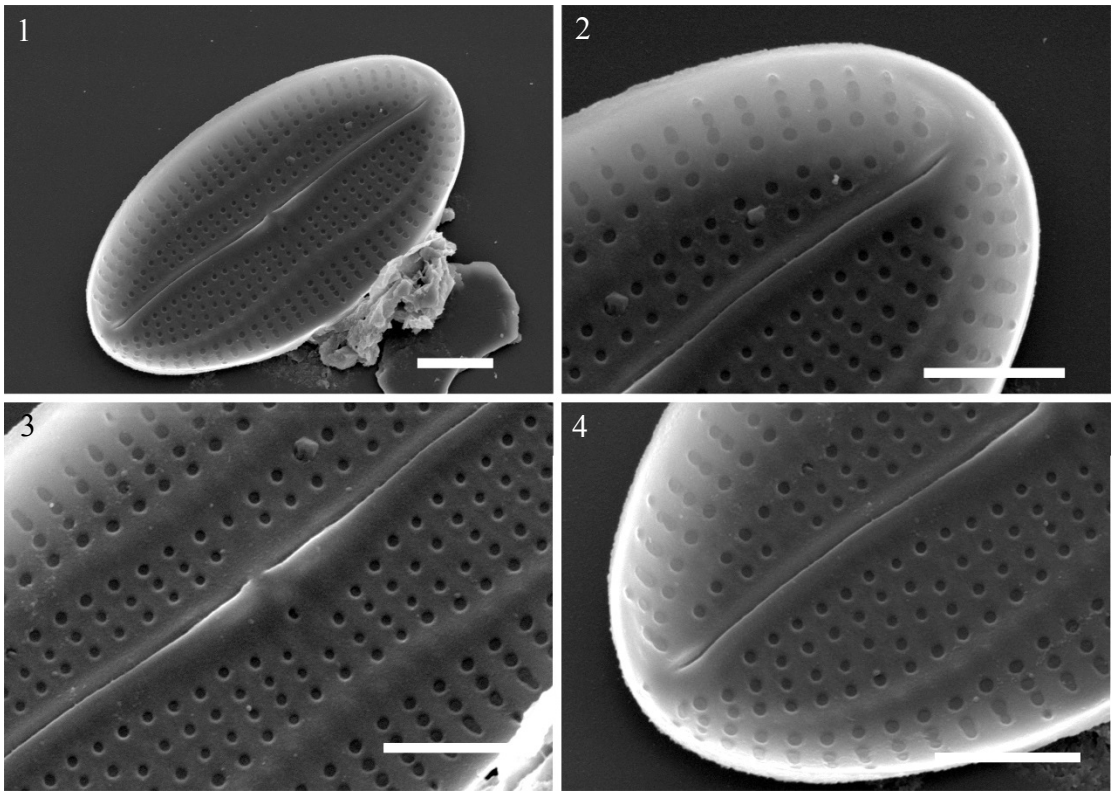

Plate 49. Internal valve of *Fallacia inscriptura* with SEM. Scale bars = 2 μm (Fig. 1) and 1.5 μm (Figs 2–4).

Fig.1 Internal view of a whole valve.

Figs 2, 4. Raphe distal terminal ends by a small helictglossa.

Fig. 3. Internal ending closed.

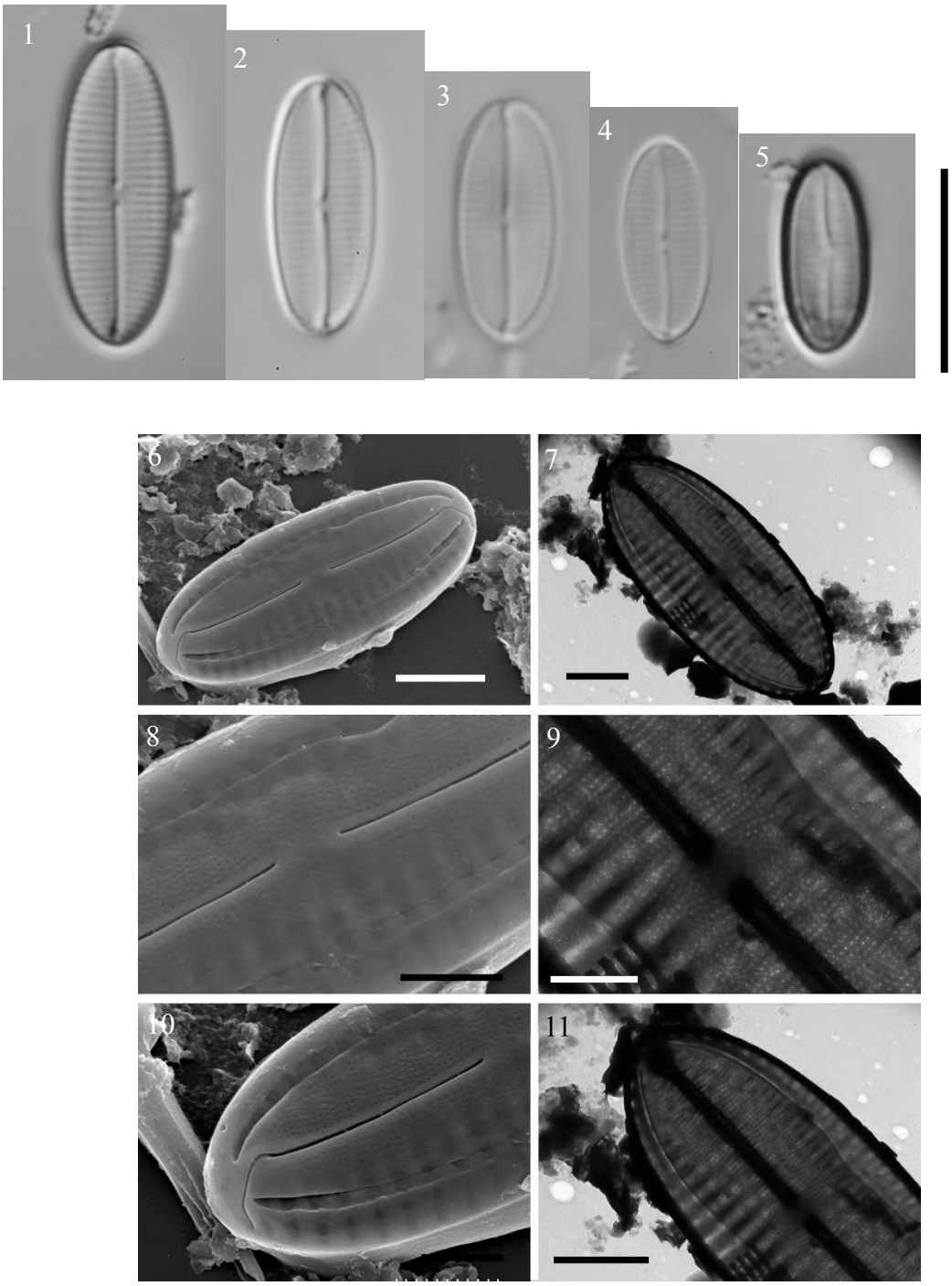

Plate 50. Valve of *Fallacia pulchella* with LM (Figs 1–5), TEM (Figs 7, 9, 11) and SEM (Figs 6, 8, 10).

Figs 1–5. Cleaned valves.

Figs 6, 7. Whole valves.

Figs 8, 9. Straight central raphe endings.

Figs 10, 11. Curved terminal fissures.

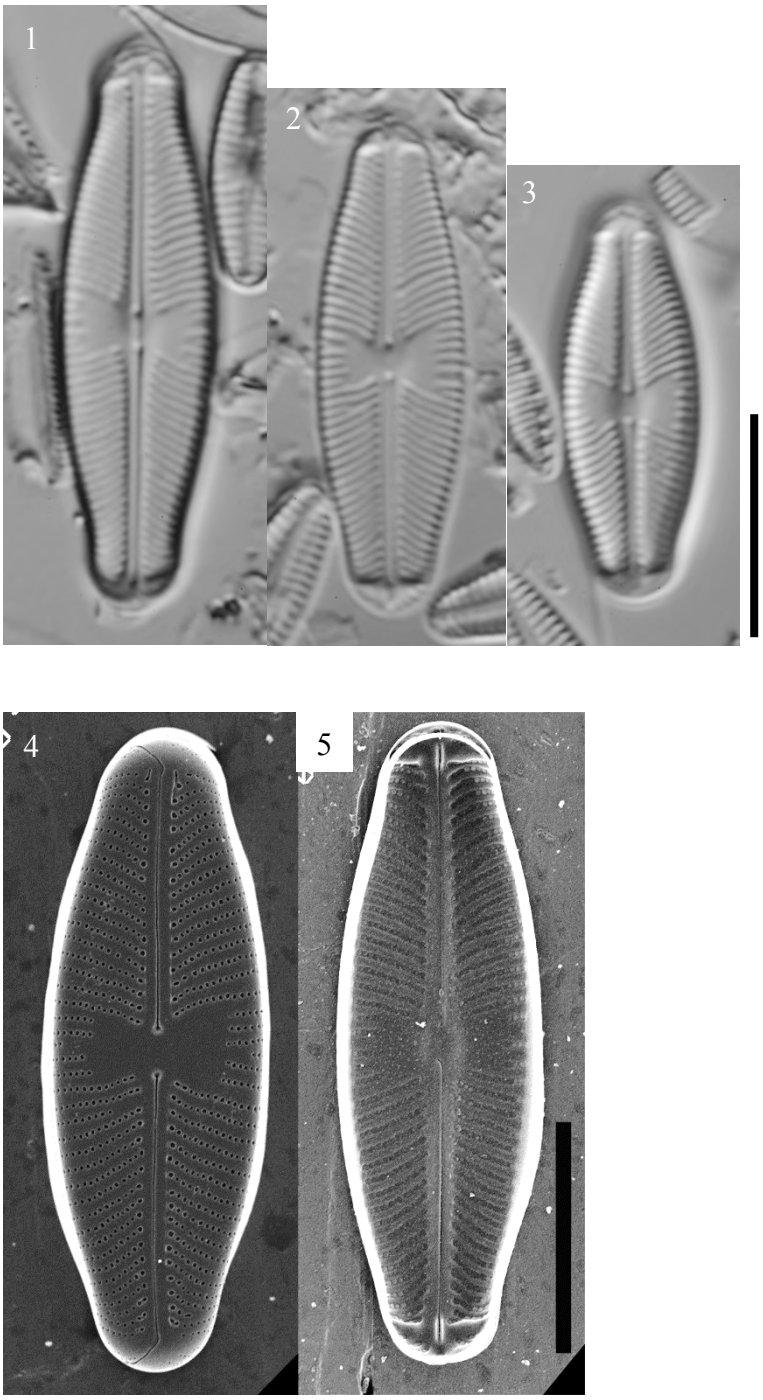

Plate 51. Plain views of valves of *Sellaphora pupula* with LM (Figs 1–3) and SEM (Figs 4, 5). Scale bars = 10 µm (Figs 1–3) and 5 µm (Figs 4, 5).

Figs 1–3. Variation of valves of *S. pupula*.

Figs 4, 5. External and internal valve faces.

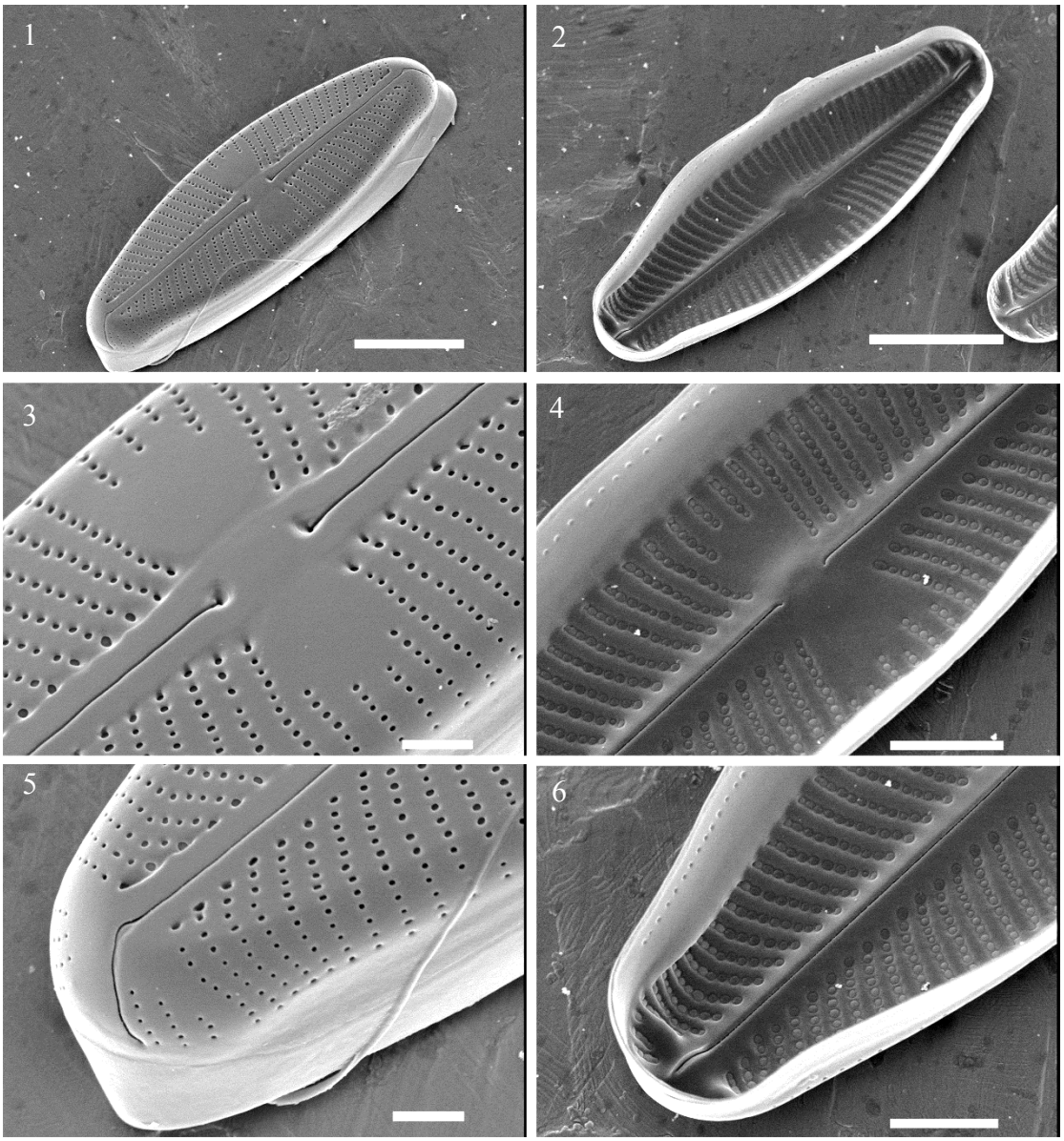

Plate 52. External (Figs 1, 3, 5) and internal (Figs 2, 4, 6) valve views of *Sellaphora pupula*. Scale bars = 5 μm (Figs 1, 2), 1 μm (Figs 3, 4) and 2 μm (Figs 5, 6).

Figs 1, 2. Whole valves.

Figs 3, 4. Central raphe endings.

Figs 5, 6. Poles of valves.

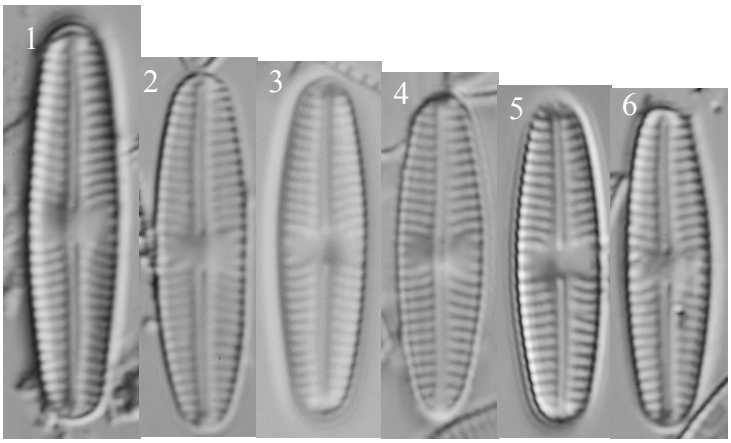

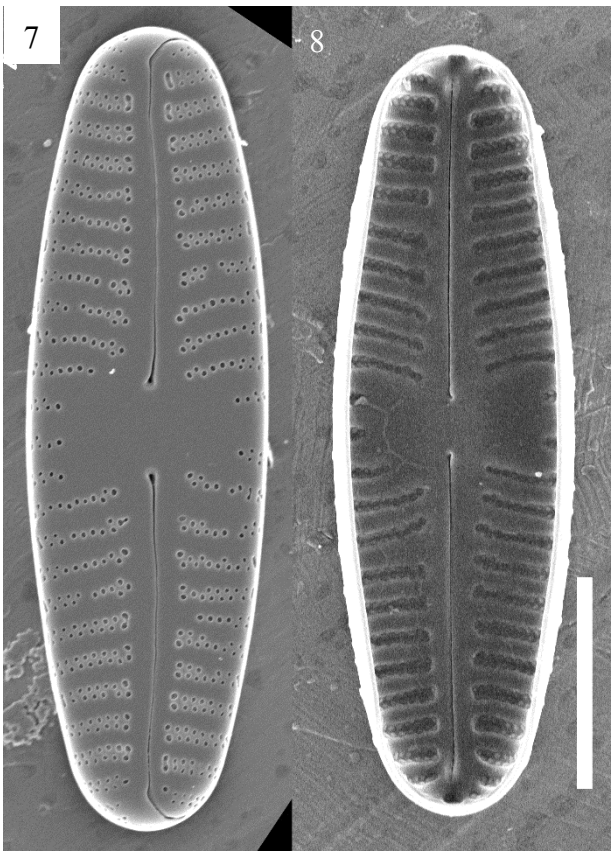

Plate 53. Plain views of valves of *Sellaphora seminulum* with LM (Figs 1–6) and SEM (Figs 7, 8). Scale bars = 10 μm (Figs 1–6) and 5 μm (Figs 7, 8).

Figs 1–6. Cleaned valves.

Figs 7, 8. External and internal valve faces.

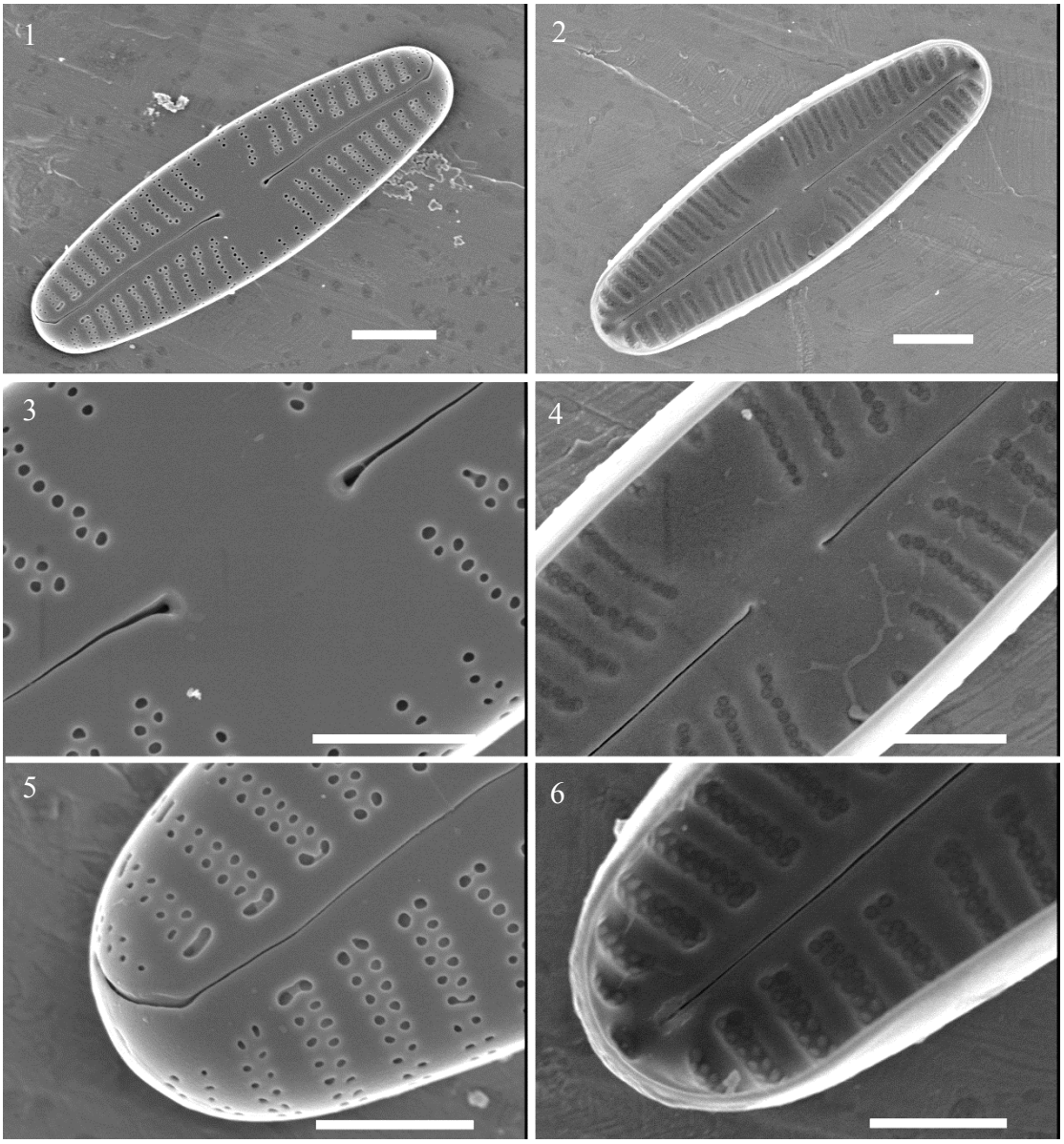

Plate 54. External (Figs 1, 3, 5) and internal (Figs 2, 4, 6) valve views of *Sellaphora seminulum*. Scale bars = 2 μm (Figs 1, 2) and 1 μm (Figs 3–6).

Figs 1, 2. Whole valves.

Figs 3, 4. Central raphe endings.

Figs 5, 6. Terminal raphe fissure and polar raphe ending.

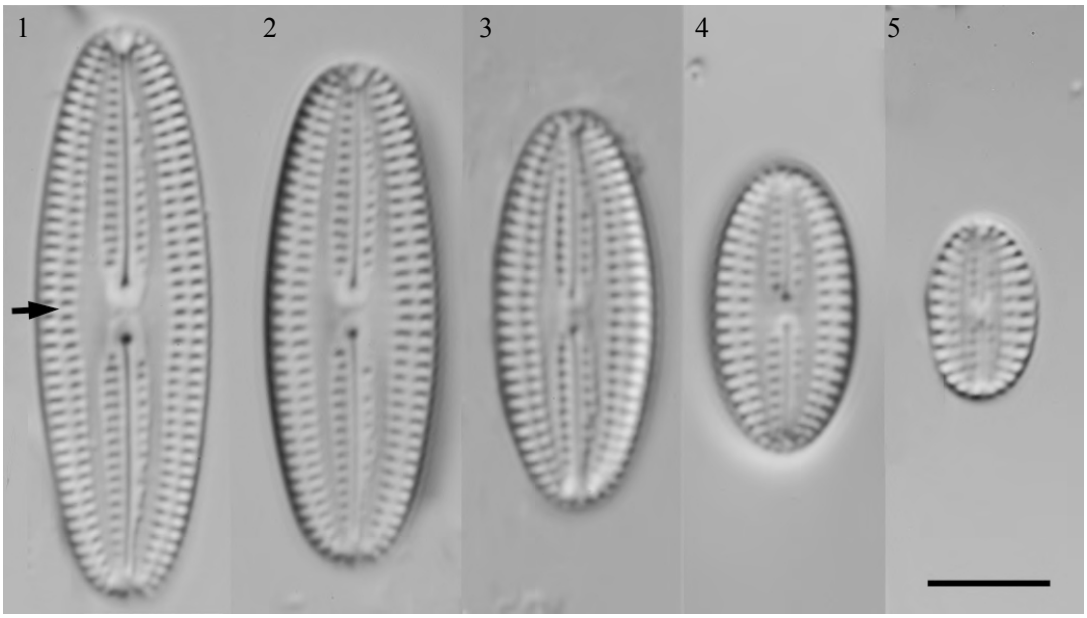

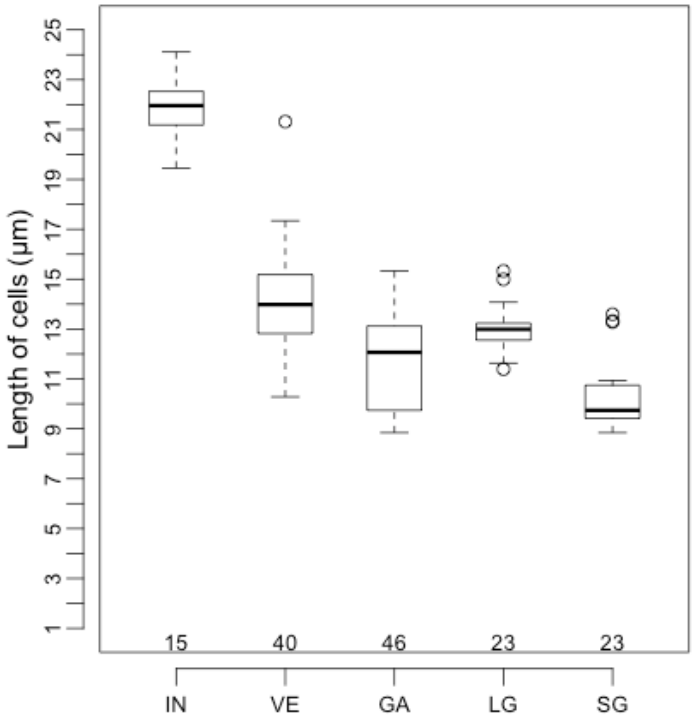

Plate 55. Range of cell length for each life stages of *Fallacia tenera*.

Figs 1–5. Variation of valves with LM. Scale bar = 5µm.

IN: Initial cells, VE: Vegetative cells, GA: Gametangia (paired parental cells), LG: the longer gametangium of the two paired gametangia, SG: the shorter gametangium of the two paired gametangia. The numbers on the horizontal axis are the number of observations.

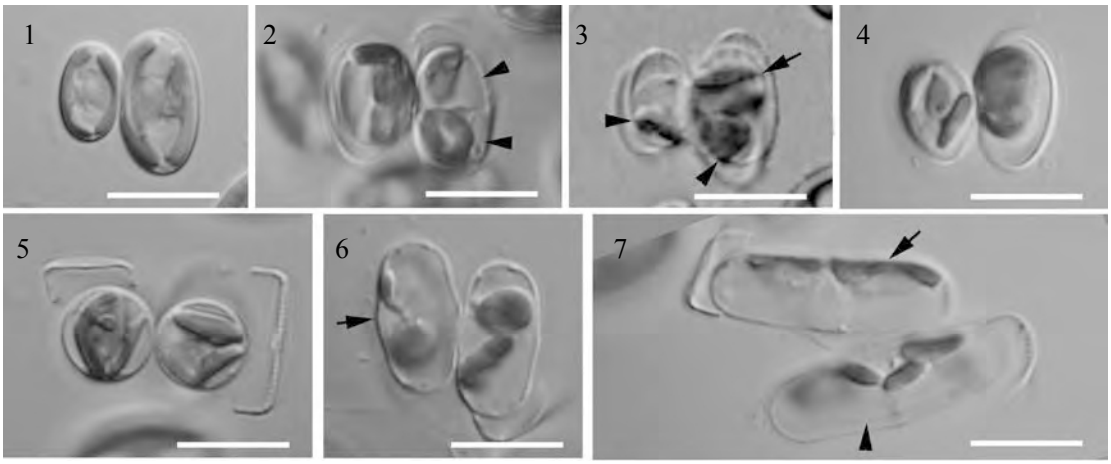

Plate 56. Sexual reproduction, auxospore development and formation of initial cells. Scale bars = 10 μm.

Fig. 1. Two paired cells in different size.

Fig. 2. Two gametes (arrowheads) were formed in one gametangia.

Fig. 3. The trans anisogamy was occurred. One zygote (arrow) was formed in a theca (right) of gametangia and two unfused gametes (arrowheads).

Fig. 4. Two zygotes were formed after the gametes fusing.

Fig. 5. Two zygotes were released from thecae of gametangia.

Fig. 6. Younger auxospores paired more or less parallel to each other. Note the slightly convex centre (arrow).

Fig. 7. Mature auxospores. Two chloroplasts (arrow) were pressed to the wall of auxospore. The longitudinal bands also could been found (arrowhead).

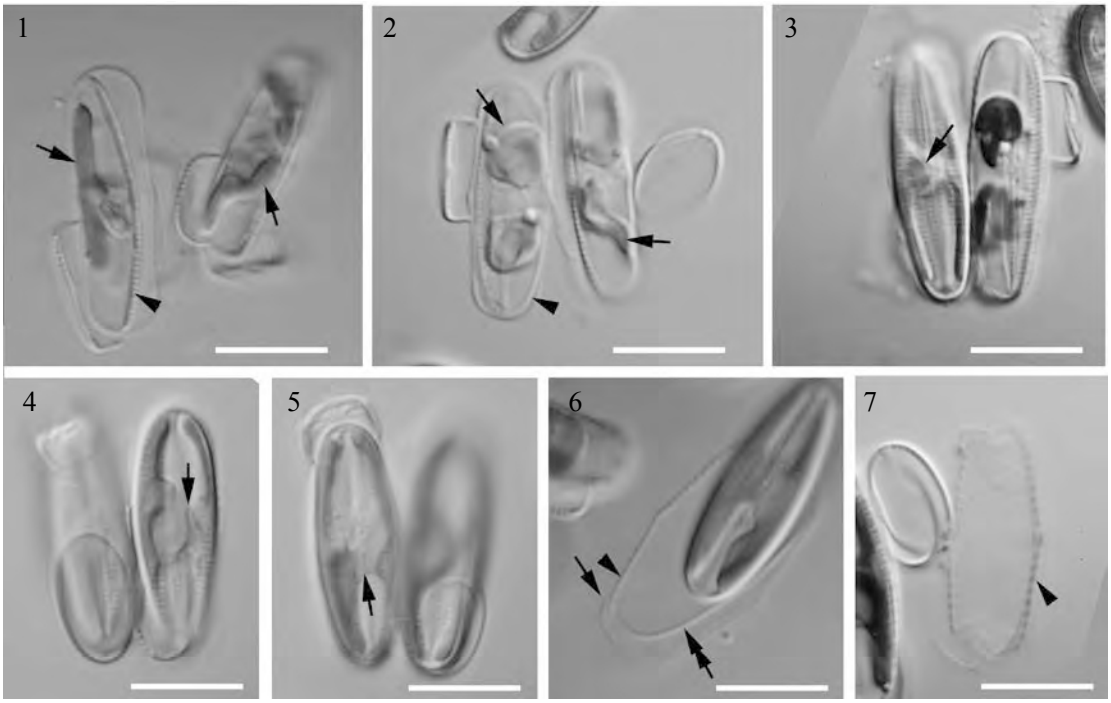

Plate 57. Sexual reproduction, auxospore development and formation of initial cells. Scale bars = 10 μm.

Figs 1–2. Formation of initial cells. A theca was present in the left auxospore (arrowhead) in Fig. 3. During the formation of initial cells, the two chloroplasts show strongly contraction (arrows).

Fig. 3. In new formed initial cells, two elongate chloroplasts pressed to the girdle. One chloroplast projects to another one along the hyaline connection between them (arrow).

Figs 4, 5. The initial cells formed complete in the two auxospore. The two chloroplasts nearly fused (arrow) in the right initial cell (fig. 5). The H-shaped chloroplast (arrow) already formed in the left initial cell (fig. 6).

Fig. 6. The initial cell were escaping from perizonium. Note the transverse perizonial bands (arrowhead), cape (=incunabular cap, arrow) and probably longitudinal band (double arrows).

Fig. 7. The empty perizonium with two broken poles. Note the primary transverse perizonial band and seven to nine secondary perizonial bands on each side of it.

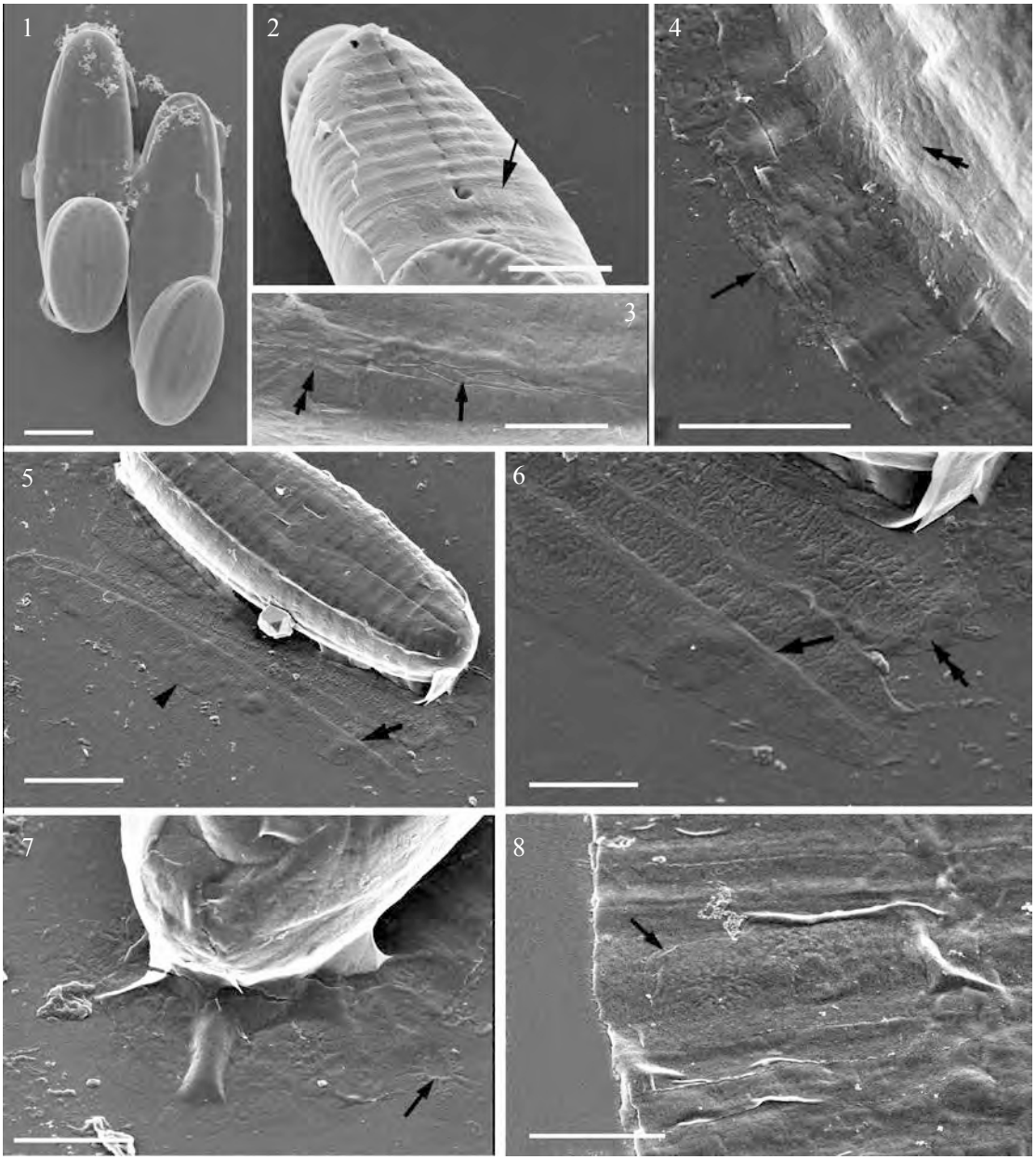

Plate 58. Incunabula and perizonium of *Fallacia tenera.* Scale bars = 2 μm (Figs 2, 3, 6), 5 μm (Figs 1, 4, 5).

Fig. 1. Paring of two auxospores with two parental cells valves in different size.

Fig. 2. Perizonium investing the initial cell, note the primary transverse band (arrow).

Fig. 3. "Suture" of secondary transverse perizonial bands (arrow) and closed primary band (double arrows).

Fig. 4. Detial of primary transverse band (arrow) with incunabular scale (double arrows) on the surface.

Fig. 5. The longitudinal series of perizonial bands. Note the semilanceolate secondary bands (arrow) with a slightly convex outline in the centre (arrowhead).

Fig. 6. The detail of fig. 5. Showing the one side fimbriate margin of secondary longitudinal bands and lanceolate primary longitudinal band (double arrows).

Figs 7, 8. Incunabular scale (arrow) on the terminal and on the primary transverse band.

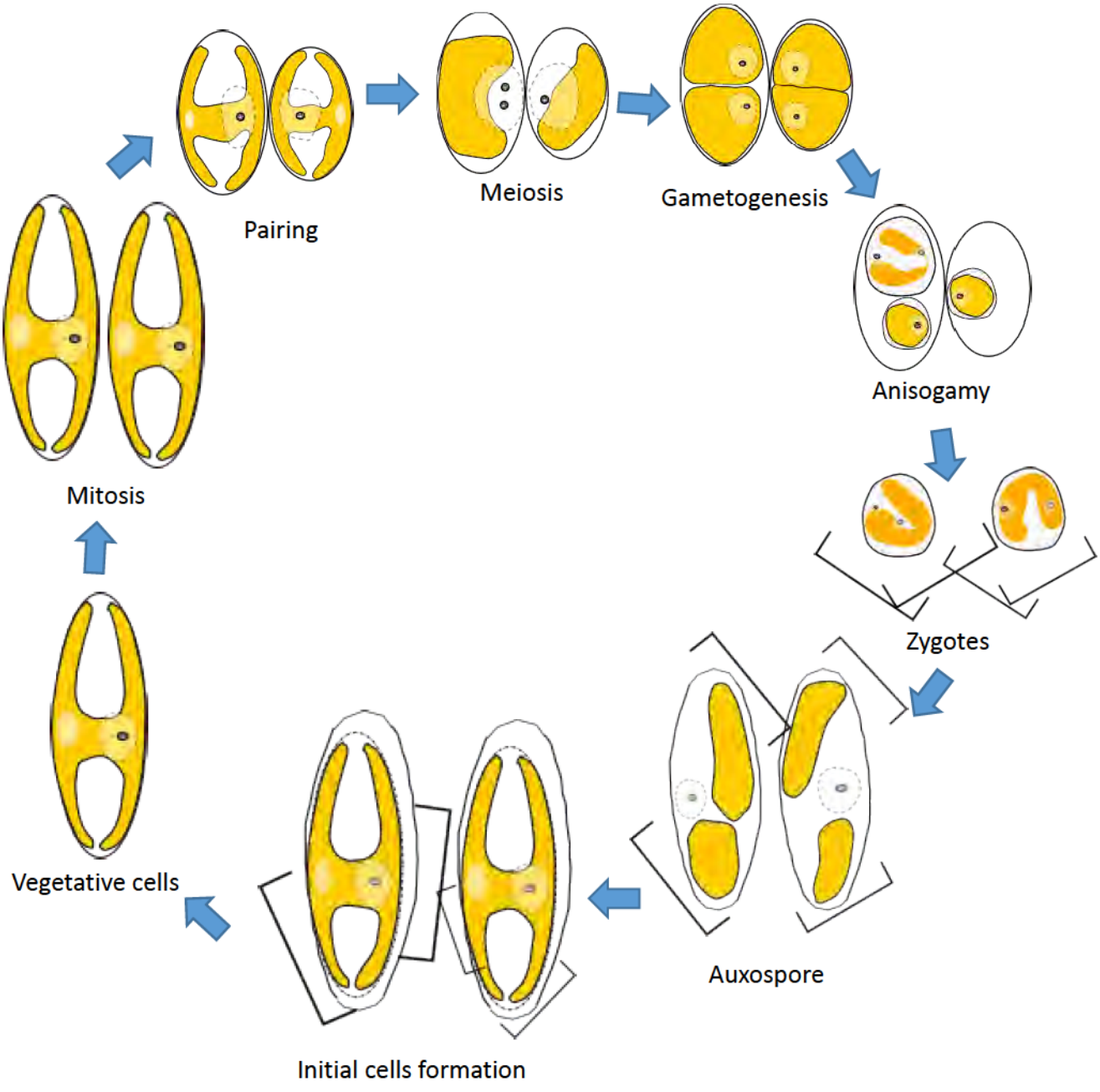

Plate 59. Life cycle of *Fallacia tenera*.

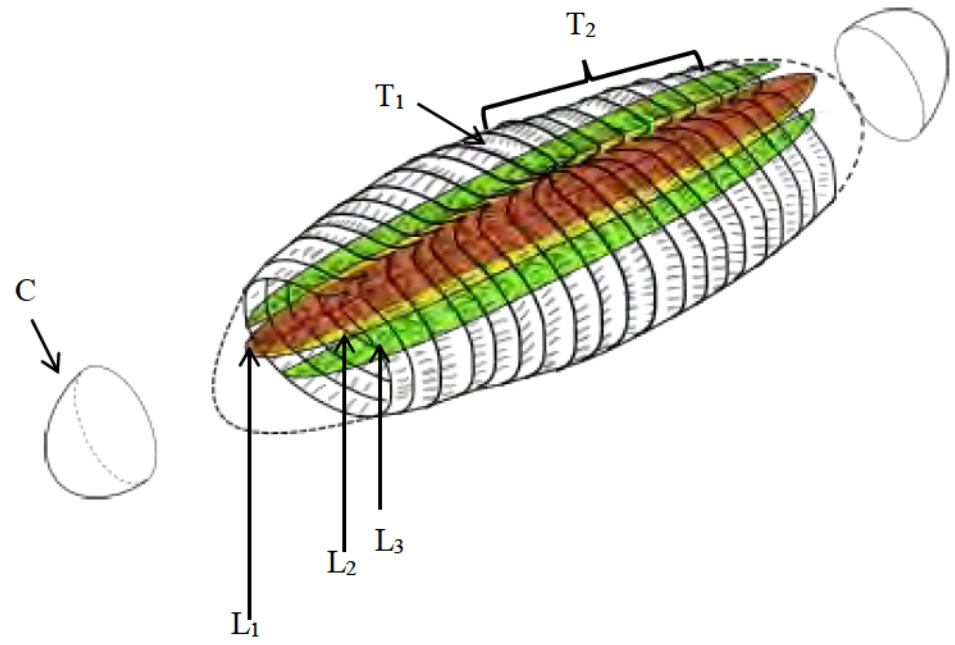

Plate 60. Pattern diagram of matured auxospore with incunabular cap in *Fallacia tenera.*

T_1: Primary transverse band; T_2: Secondary transverse bands; L_1: Primary longitudinal band; L_2: Secondary longitudinal band; L_3: Tertiary longitudinal band; C: Incunabular cap.

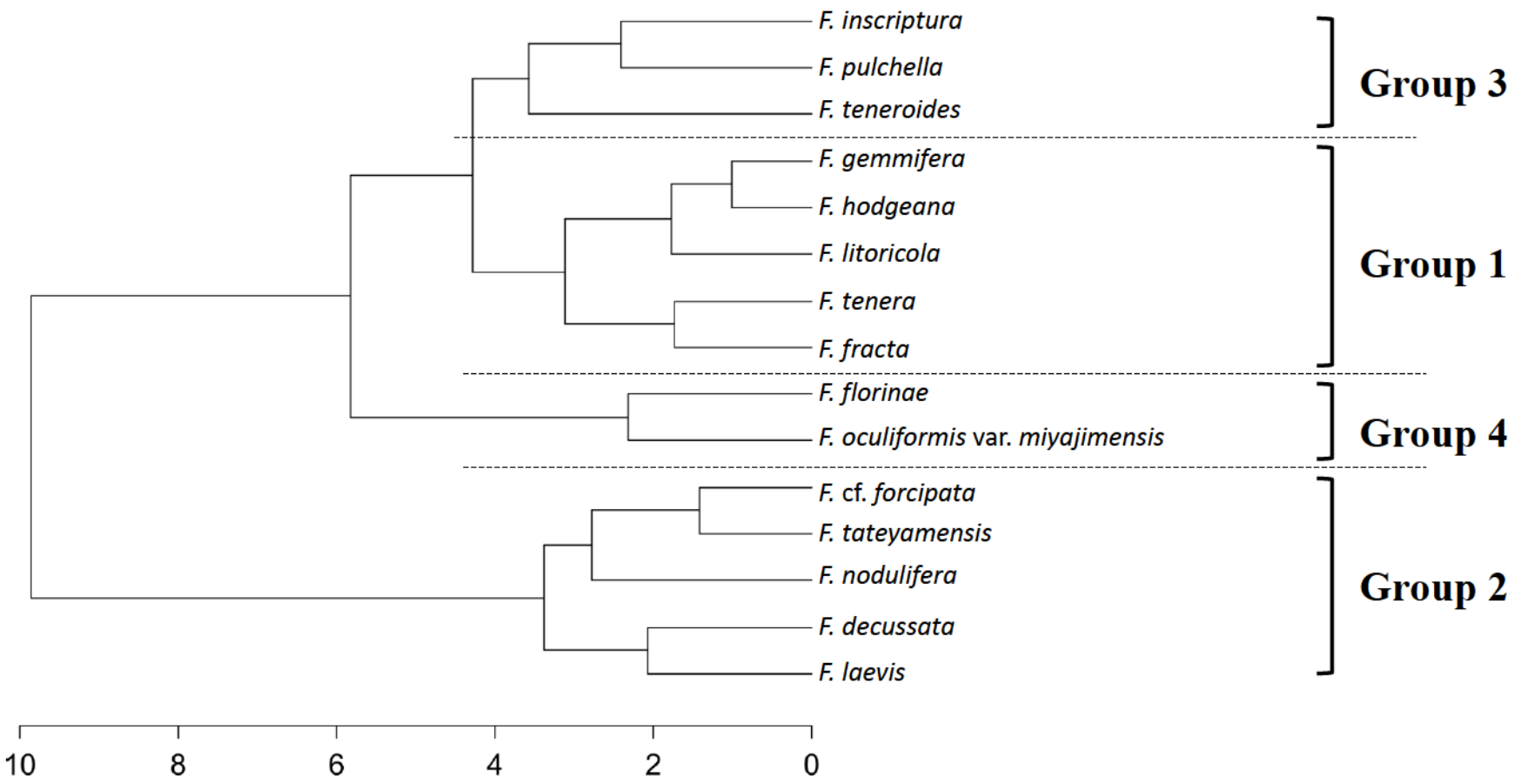

Plate 61. Dendrogram of 15 *Fallacia* species derived from morphological features.

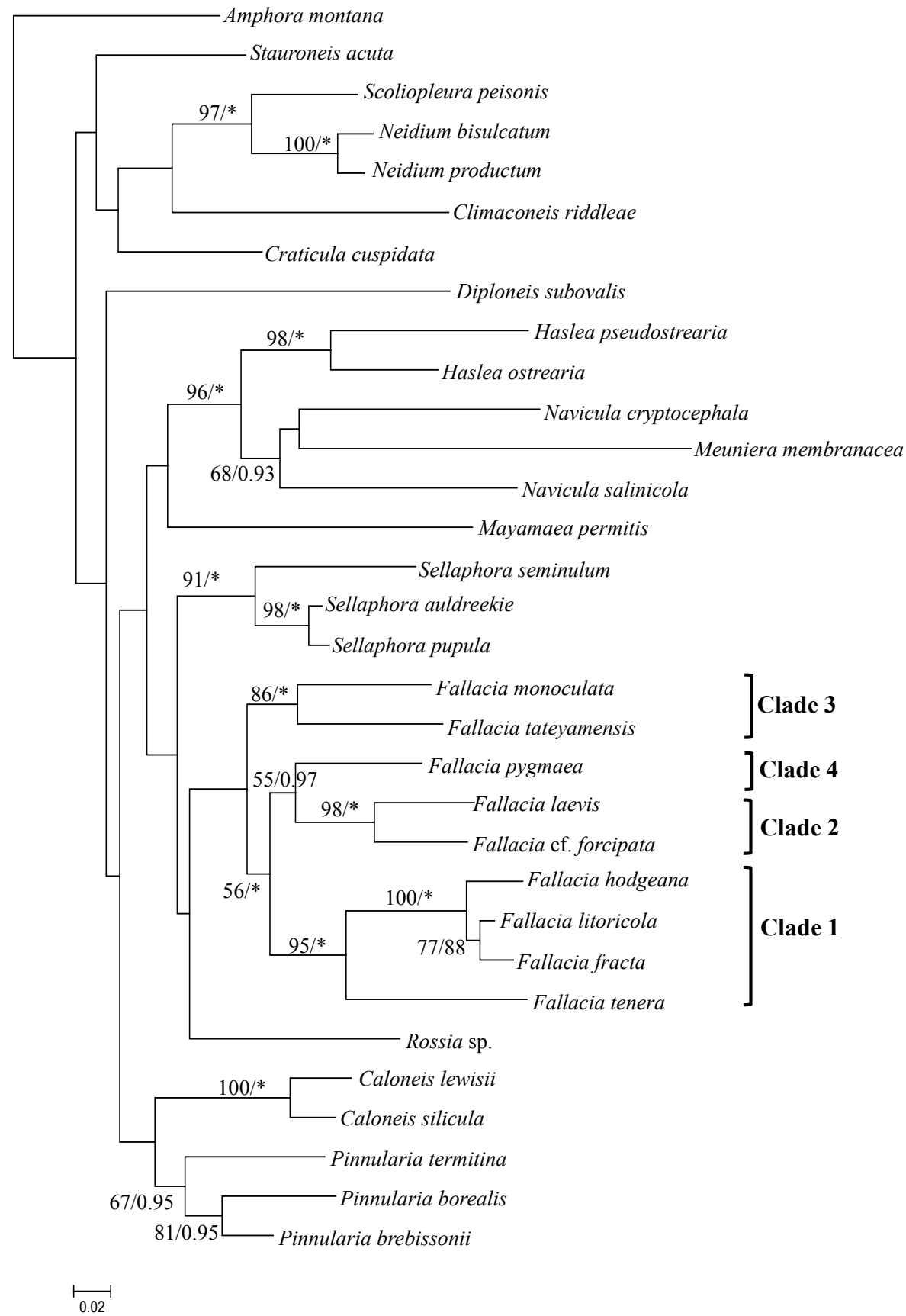

Plate 62. Maximum likelihood (ML) tree inferred from *rbc*L gene using GTR+G+I model. Branch support is summarized above branches as ML bootstrap (BS) value/Bayesian posterior probabilities that BS≥ 50. Support of 100% are shown as an asterisk (*).